National Library of Canada
Canadian Theses Service
Ottawa, Canada
K1A 0N4

Bibliothèque nationale du Canada
Services des thèses canadiennes

CANADIAN THESES

THÈSES CANADIENNES

NOTICE

The quality of this microfiche is heavily dependent upon the quality of the original thesis submitted for microfilming. Every effort has been made to ensure the highest quality of reproduction possible.

If pages are missing, contact the university which granted the degree.

Some pages may have indistinct print especially if the original pages were typed with a poor typewriter ribbon or if the university sent us an inferior photocopy.

Previously copyrighted materials (journal articles, published tests, etc.) are not filmed.

Reproduction in full or in part of this film is governed by the Canadian Copyright Act, R.S.C. 1970, c. C-30.

AVIS

La qualité de cette microfiche dépend grandement de la qualité de la thèse soumise au microfilmage. Nous avons tout fait pour assurer une qualité supérieure de reproduction.

S'il manque des pages, veuillez communiquer avec l'université qui a conféré le grade.

La qualité d'impression de certaines pages peut laisser à désirer, surtout si les pages originales ont été dactylographiées à l'aide d'un ruban usé ou si l'université nous a fait parvenir une photocopie de qualité inférieure.

Les documents qui font déjà l'objet d'un droit d'auteur (articles de revue, examens publiés, etc.) ne sont pas microfilmés.

La reproduction, même partielle, de ce microfilm est soumise à la Loi canadienne sur le droit d'auteur, SRC 1970, c. C-30.

THIS DISSERTATION HAS BEEN MICROFILMED EXACTLY AS RECEIVED

LA THÈSE A ÉTÉ MICROFILMÉE TELLE QUE NOUS L'AVONS REÇUE

NL-339 (r. 86/06)

Canada

THE UNIVERSITY OF ALBERTA

DIAGENESIS OF FINE-GRAINED UPPER CRETACEOUS AND TERTIARY CLASTIC ROCKS FROM THE NOVA SCOTIA SHELF AND SLOPE

by

STEVEN D. BURTCH

A THESIS

SUBMITTED TO THE FACULTY OF GRADUATE STUDIES AND RESEARCH

IN PARTIAL FULFILMENT OF THE REQUIREMENTS FOR THE DEGREE

OF MASTER OF SCIENCE

DEPARTMENT OF GEOLOGY

EDMONTON, ALBERTA

SPRING 1986

Permission has been granted to the National Library of Canada to microfilm this thesis and to lend or sell copies of the film.

The author (copyright owner) has reserved other publication rights, and neither the thesis nor extensive extracts from it may be printed or otherwise reproduced without his/her written permission.

L'autorisation a été accordée à la Bibliothèque nationale du Canada de microfilmer cette thèse et de prêter ou de vendre des exemplaires du film.

L'auteur (titulaire du droit d'auteur) se réserve les autres droits de publication; ni la thèse ni de longs extraits de celle-ci ne doivent être imprimés ou autrement reproduits sans son autorisation écrite.

ISBN 0-315-30142-2

THE UNIVERSITY OF ALBERTA

RELEASE FORM

NAME OF AUTHOR STEVEN D. BURTCH

TITLE OF THESIS DIAGENESIS OF FINE-GRAINED UPPER CRETACEOUS AND TERTIARY CLASTIC ROCKS FROM THE NOVA SCOTIA SHELF AND SLOPE

DEGREE FOR WHICH THESIS WAS PRESENTED MASTER OF SCIENCE

YEAR THIS DEGREE GRANTED SPRING 1986

Permission is hereby granted to THE UNIVERSITY OF ALBERTA LIBRARY to reproduce single copies of this thesis and to lend or sell such copies for private, scholarly or scientific research purposes only.

The author reserves other publication rights, and neither the thesis nor extensive extracts from it may be printed or otherwise reproduced without the author's written permission.

(SIGNED) Steve Burtch

PERMANENT ADDRESS:

22 Greenwood Trail

Brantford, Ontario

N3R 6G5

DATED March 25 1986

THE UNIVERSITY OF ALBERTA

FACULTY OF GRADUATE STUDIES AND RESEARCH

The undersigned certify that they have read, and recommend to the Faculty of Graduate Studies and Research, for acceptance, a thesis entitled DIAGENESIS OF FINE-GRAINED UPPER CRETACEOUS AND TERTIARY CLASTIC ROCKS FROM THE NOVA SCOTIA SHELF AND SLOPE submitted by STEVEN D. BURTCH in partial fulfilment of the requirements for the degree of MASTER OF SCIENCE.

Fred J. Longstaffe
Supervisor

Frank W. Schwartz

Fujii Dondoh

J. Lindstrom

Date March 13, 1986

DEDICATION

The research contained in this thesis is dedicated to my family and close friends whose consideration has made this work possible. Especially, this effort is dedicated to my wife, Kathryn Ann; my parents, Marion and Norman Burtch and my inlaws, Ann and Ernie Booth.

Thanks for the memories.

ABSTRACT

The style of compaction and chemical diagenesis has been investigated in fine-grained clastic rocks from four exploratory drillholes along the Nova Scotia shelf and slope. The diagenesis of these fine-grained rocks was modelled in the context of this margin's tectonic and stratigraphic histories.

Petrophysical and petrographic work have indicated that these sections exhibit an immature style of compaction, despite present burial depths exceeding 2000 meters at temperatures greater than 60°C. Immature compaction has resulted in: (i) the occurrence of appreciable undercompaction and (ii) low burial temperatures throughout many intervals. Mineralogical and geochemical investigations (x-ray diffraction, thin section and scanning electron microscopy, energy dispersive x-ray microanalysis, inductively coupled, plasma emission spectrography and stable isotopes of carbonate minerals) reveal that chemical diagenesis is at an early stage. For example, early pyrite, early calcite and detrital minerals exist at significant depths without evidence of corrosion or alteration. As well, the transformation of smectitic minerals to illitic phases was recognised only in two sequences (Shubenacadie and Glenelg) and is not far advanced.

Only at Glenelg is a greater degree of mineralogic alteration observed: incipient feldspar dissolution, depotassification of very fine 10 Å clay and the absence of early calcite, except in calcareous Wyandot mudstones. Glenelg's anomalous character is further indicated by petrophysical and isotopic data suggesting that the upper section of this sequence has experienced erosion (>300 m).

The style of diagenesis along the Nova Scotia margin closely resembles that of fine-grained clastic rocks from the North Sea. Low burial temperatures and minimal fluid circulation, resulting largely from undercompaction, can inhibit physical and chemical diagenesis in fine-grained sediments. This behaviour contrasts with that reported in classic, diagenetic studies of fine-grained rocks. For example, the progressive transformation of smectite to illite with depth was recognised in the U.S. Gulf Coast (Tertiary); in this sequence, illitization was controlled primarily by temperature and whole rock mineralogy.

ACKNOWLEDGEMENTS

Throughout the course of this study, many individuals have assisted my progress. Foremost, I wish to express my gratitude to Dr. Fred Longstaffe, my advisor, for his encouragement and criticism. As well, I wish to acknowledge the substantial contribution made by Shell Canada Resources Ltd. and Shell Canada Ltd.'s, Calgary Research Centre, for permitting access to geological specimens from "the offshore" and research facilities, respectively. Special thanks are extended to Jon McGovern, Mark Thomas, Mary Given and Charlie Bruce, of Shell.

Discussions with Allan Crowe and Dr. Avner Ayalon were greatly appreciated. I also thank Kathryn Burtch and Diane Caird for their assistance with various parts of the laboratory work.

Generous financial support was provided by a Province of Alberta Graduate Scholarship and a Natural Sciences and Engineering Research Council of Canada, Postgraduate Scholarship. Major analytical costs were borne by Dr. Fred Longstaffe and Shell Canada Ltd.

Table of Contents

Chapter — Page

DEDICATION iv

ABSTRACT v

ACKNOWLEDGEMENTS vi

LIST OF TABLES x

LIST OF FIGURES xi

LIST OF PLATES xii

LIST OF SYMBOLS, NOMENCLATURE AND ABBREVIATIONS xiii

I. INTRODUCTION AND REGIONAL SETTING 1

A. INTRODUCTION 1

PREVIOUS WORK 1

OBJECTIVES 1

STUDY AREA 2

B. REGIONAL SETTING 2

TECTONIC AND GEOTHERMAL HISTORIES 2

STRATIGRAPHY 7

CONTROLS ON DETRITAL CLAY OCCURRENCE AND DISTRIBUTION 9

C. SUMMARY OF REGIONAL GEOLOGY 11

D. BIBLIOGRAPHY 12

II. PETROGRAPHY, FABRIC AND PETROPHYSICS 14

A. INTRODUCTION 14

B. METHODOLOGY 14

COMPACTION ANALYSIS - PETROPHYSICAL TECHNIQUES 14

DETERMINATION OF GEOTHERMAL GRADIENTS 19

PETROGRAPHIC ANALYSIS - TECHNIQUES 21

C. OBSERVATIONS 22

PETROPHYSICAL DATA 22

PETROPHYSICAL CHARACTER - SHUBENACADIE 23

PETROPHYSICAL CHARACTER - ACADIA 26

PETROPHYSICAL CHARACTER - GLENELG 29

GEOTHERMAL GRADIENT OBSERVATIONS 31
PETROGRAPHIC INFORMATION 33
PETROGRAPHY - OUTER SHELF 33
PETROGRAPHY - LOWER SLOPE 42
D. DISCUSSION OF COMPACTIONAL STYLE 46
E. SUMMARY OF COMPACTION AND FABRIC STUDY 51
F. BIBLIOGRAPHY 53
III. MINERALOGY AND GEOCHEMISTRY 55
A. INTRODUCTION 55
B. METHODOLOGY 55
PETROGRAPHIC EXAMINATION 55
XRD ANALYSIS 55
TECHNIQUES FOR XRD DATA EVALUATION 59
CHEMICAL INVESTIGATION 60
STABLE ISOTOPE ANALYSIS 62
C. OBSERVATIONS 62
WHOLE ROCK XRD DATA 62
PETROGRAPHY 65
0.2 - 2.0 μm XRD DATA 68
<0.2 μm XRD DATA 74
OBSERVATIONS FROM ELEMENTAL ANALYSIS 79
CLAY ELEMENTAL DATA 79
WHOLE ROCK ELEMENTAL DATA 86
CARBONATE ELEMENTAL DATA 86
STABLE ISOTOPE DATA FOR CARBONATE MINERALS 89
D. DISCUSSION OF CHEMICAL DIAGENESIS 95
E. SUMMARY OF MINERALOGICAL AND GEOCHEMICAL STUDY 102
F. BIBLIOGRAPHY 104
IV. GENERAL DISCUSSION AND CONCLUSIONS 107
A. INTRODUCTION 107

B. MODEL OF THE DIAGENESIS OF FINE-GRAINED CLASTIC ROCKS IN OFFSHORE-NOVA SCOTIA 107

C. DIAGENESIS OF FINE-GRAINED CLASTIC ROCKS IN OTHER BASINS 110

D. EVALUATION OF NOVA SCOTIA MODEL 114

E. BIBLIOGRAPHY 117

LIST OF TABLES

Table	Description	Page
2.1	Seismic Velocities of Typical Shaly Constituents	16
2.2	Offshore-Nova Scotia Geothermal Gradients	32
3.1	Samples Investigated	56
3.1	Continued	57
3.2	Whole Rock XRD Summary	63
3.2	Continued	64
3.3	0.2 - 2.0 μm XRD Data	71
3.4	Fine Size-Fraction XRD Data	75
3.4	Continued	76
3.5	Elemental Analyses of Standards	82
3.6	Normalized <0.1 μm Elemental Analyses: Shubenacadie	84
3.7	Normalized Whole Rock Elemental Analyses: Shubenacadie	88
3.8	Stable Isotope Data for Carbonate Minerals	91
3.8	Continued	92

LIST OF FIGURES

Figure	Description	Page
1.1	Location Map of Offshore-Nova Scotia	3
1.2	Schematic Stratigraphic Section Across Central Nova Scotia Shelf and Slope	4
1.3	Interpretive Crustal Profile Across Central Nova Scotia Shelf and Slope	5
1.4	Generalized Stratigraphic Column, Offshore-Nova Scotia	10
2.1	Technique for Determining Compaction Trends	18
2.2	Flow Equations	20
2.3	Sonic Travel Time vs. Depth, Shubenacadie H-100	24
2.4	Synthetic Seismographs from BHC Sonic Logs	27
2.5	Sonic Travel Time vs. Depth, Acadia K-62	28
2.6	Sonic Travel Time vs. Depth, Glenelg J-48	30
3.1	Smectite:Illite Ratio of 0.2 - 2.0 μm Clay	73
3.2	Apparent %Smectite in Very Fine 10 and 17 Å Clay from the Shelf	77
3.3	Apparent %Smectite in Very Fine 10 and 17 Å Clay from the Slope	80
3.4	<0.1 μm, Ca^{2+} Glycerin Diffractograms from Shubenacadie	81
3.5	Elemental Trends in <0.1 μm Clay from Shubenacadie H-100	85
3.6	Elemental Trends in <0.1 μm Clay from Shubenacadie H-100	87
3.7	Major Cation Distributions in Secondary Carbonates	90
3.8	$\delta^{18}O$ vs. Present Burial Depth for Calcite	94

LIST OF PLATES

Plate	Description	Page
2.1a	Thin Section Micrograph of Lithoclastic Facies from Outer Shelf	34
2.1b	Thin Section Micrograph of Graywacke Containing Glauconite	34
2.1c	Thin Section Micrograph of Fossiliferous Mudstone	34
2.1d	Thin Section Micrograph of Calcareous, Fossiliferous Mudstone	34
2.2a	Backscattered Electron Micrograph of Glauconite Grains	37
2.2b	Backscattered Electron Micrograph of Subparallel Fabric in Mudrock	37
2.2c	Backscattered Electron Micrograph of Calcareous Mudstone	37
2.2d	Backscattered Electron Micrograph of Microfossil Tests	37
2.3a	Secondary Electron Micrograph of Subparallel Compaction Fabric	40
2.3b	Secondary Electron Micrograph Close-up of Compacted Clay	40
2.3c	Secondary Electron Micrograph of Unbroken Fossil Debris	40
2.3d	Secondary Electron Micrograph of Degraded Fossil Debris	40
2.3e	Secondary Electron Micrograph of Poorly Compacted Mudstone	40
2.3f	Secondary Electron Micrograph of Compacted Mudstone	40
2.4a	Thin Section Micrograph of Fossiliferous Mudstone	44
2.4b	Thin Section Micrograph of Partly Filled Intraskeletal Porosity	44
2.4c	Thin Section Micrograph of Open Intraskeletal Porosity	44
3.1a	Secondary Electron Micrograph of Corrosion on Detrital K-Feldspar	66
3.1b	Secondary Electron Micrograph of Corrosion on Detrital Plagioclase	66
3.1c	Secondary Electron Micrograph of Euhedral Pyrite Grain Adjacent to Secondary Calcite	66
3.1d	Secondary Electron Micrograph of Euhedral Pyrite Grain	66
3.1e	Secondary Electron Micrograph of Secondary Calcite Infilling Early Micro-porosity	66
3.2a	Thin Section Micrograph of Mudstone	69

LIST OF SYMBOLS, NOMENCLATURE AND ABBREVIATIONS

The abbreviations listed below are used in Tables, Figures and Text:

ROCK TYPES

Qw= Graywacke (15% to 75% matrix consisting of <30 μm size grains)

Sl= Siltstone (>67% silt; indurated, non-fissile)

Md= Mudstone (<67% silt; indurated, non-fissile)

clc= Calcareous

MINERALOGY

Q= Quartz

K-spar= Potassium Feldspar

Ca= Calcite

Py= Pyrite

I= Illite

K= Kaolinite

Cl= Chlorite

Sm= Smectite

Mnt= Montmorillonite

Bd= Beidellite

ABUNDANCE OF MINERALS

na = Not Analyzed

nd = Not Detected

t = Trace (<2%)

mt = Minor or Trace (2-5%)

m = Minor (5-10%)

mM = Moderate (10-35%)

M = Major (>35%)

ABBREVIATIONS

RANDOM = Randomly Interstratified

TD = Total Depth

SF = Sea Floor

UNITS OF MEASUREMENT

μm = micrometer (1×10^{-6} m)

μs/m = microsecond (1×10^{-6} s)/meter

Å = angstrom (1×10^{-10} m)

mbmsl = meters below mean sea level

I. INTRODUCTION AND REGIONAL SETTING

A. INTRODUCTION

PREVIOUS WORK

The style of diagenesis in fine-grained clastic rocks from passively subsiding, sedimentary basins has been investigated for many years. This research is of interest because: (i) the diagenesis of these rocks is a tool for assessing the tectonic maturity of a uniformly subsiding basin, (ii) post-depositional changes in fine-grained rocks may influence diagenesis in adjacent permeable units and (iii) pore-fluids from fine-grained rocks may influence hydrocarbon migration.

Most work has focused on land-based wells from the Gulf Coast of the United States (Burst, 1969; Perry and Hower, 1971; Hower et al., 1976; Morton, 1985). However, as other sedimentary basins are explored, new information is being added to our knowledge of diagenetic styles in fine-grained clastic rocks. Locations for such studies include: (i) the North Sea (Dypvik, 1983), (ii) the Niger Delta (Bruce, 1984), (iii) the Bay of Bengal (Dilli and Rao, 1982) and (iv) the northern Labrador Shelf (Hiscott, 1984).

With the exception of Hiscott (1984), the diagenesis of fine-grained rocks along much of the Atlantic margin of North America has not been investigated. Recent exploration off Nova Scotia has provided shaly sections previously unavailable for analysis. This study will present a model for the diagenesis observed in these fine-grained clastic sequences.

OBJECTIVES

Most research into the diagenesis of fine-grained clastic rocks has focused upon particular mineral transformations observed from deep sequences along the U.S. Gulf Coast. This study will attempt a broader view of the diagenesis of this rock type by considering other information in addition to mineralogy. Also, this research will focus upon diagenesis observed in four deep water, rather than on-land, drillholes.

The principal objective of this research is to develop an *integrated* model describing the diagenetic style observed in fine-grained clastic rocks. This model will account for: (i) observed physical and geochemical alteration of constituent phases and (ii) the relationship of diagenesis

to tectonic and geothermal setting. The model will then be compared to diagenetic models from other passive margins to determine whether sequences from Nova Scotia exhibit a typical diagenetic style.

STUDY AREA

Four sequences of fine-grained clastic rocks from two outer shelf wells (Glenelg J-48 and Triumph P-50) and two slope wells (Acadia K-62 and Shubenacadie H-100) were examined (Figure 1.1). In general, each well penetrates a substantial thickness (>1800 m) of fine-grained, Upper Cretaceous and Tertiary rocks (Figure 1.2). Triumph and Acadia were drilled and abandoned in 1971 and 1977 respectively. Shubenacadie and Glenelg were drilled most recently and have been sampled since 1983.

B. REGIONAL SETTING

TECTONIC AND GEOTHERMAL HISTORIES

The Nova Scotia shelf and slope lie along the passive margin off eastern North America. This margin formed during Triassic to Jurassic time with the onset of tensional tectonism which established the modern Atlantic Ocean some 180 million years ago (Royden and Keen, 1980). Understanding tectonic and geothermal styles off Nova Scotia is necessary when evaluating controls on compaction and chemical diagenesis.

The evolution of the Atlantic continental margin has been characterized by appreciable subsidence in response to: (i) crustal thinning through continental extension (Sawyer et al., 1982) and (ii) sediment loading (Steckler and Watts, 1978). Uchupi and Austin (1979) have described the evolution of this margin in terms of a rift/drift tectonic model.

At the onset of tensional tectonism, the rift phase began with brittle extension of continental crust separating North America from Europe during the opening of the modern Atlantic Ocean (Steckler and Watts, 1978). During Early Jurassic time, tectonic subsidence was manifested by downfaulting along numerous half grabens (Figure 1.3), resulting in the formation of several subbasins (McIver, 1972). Sawyer et al. (1982) claimed that approximately 40% of total tectonic subsidence occurred during initial crustal extension.

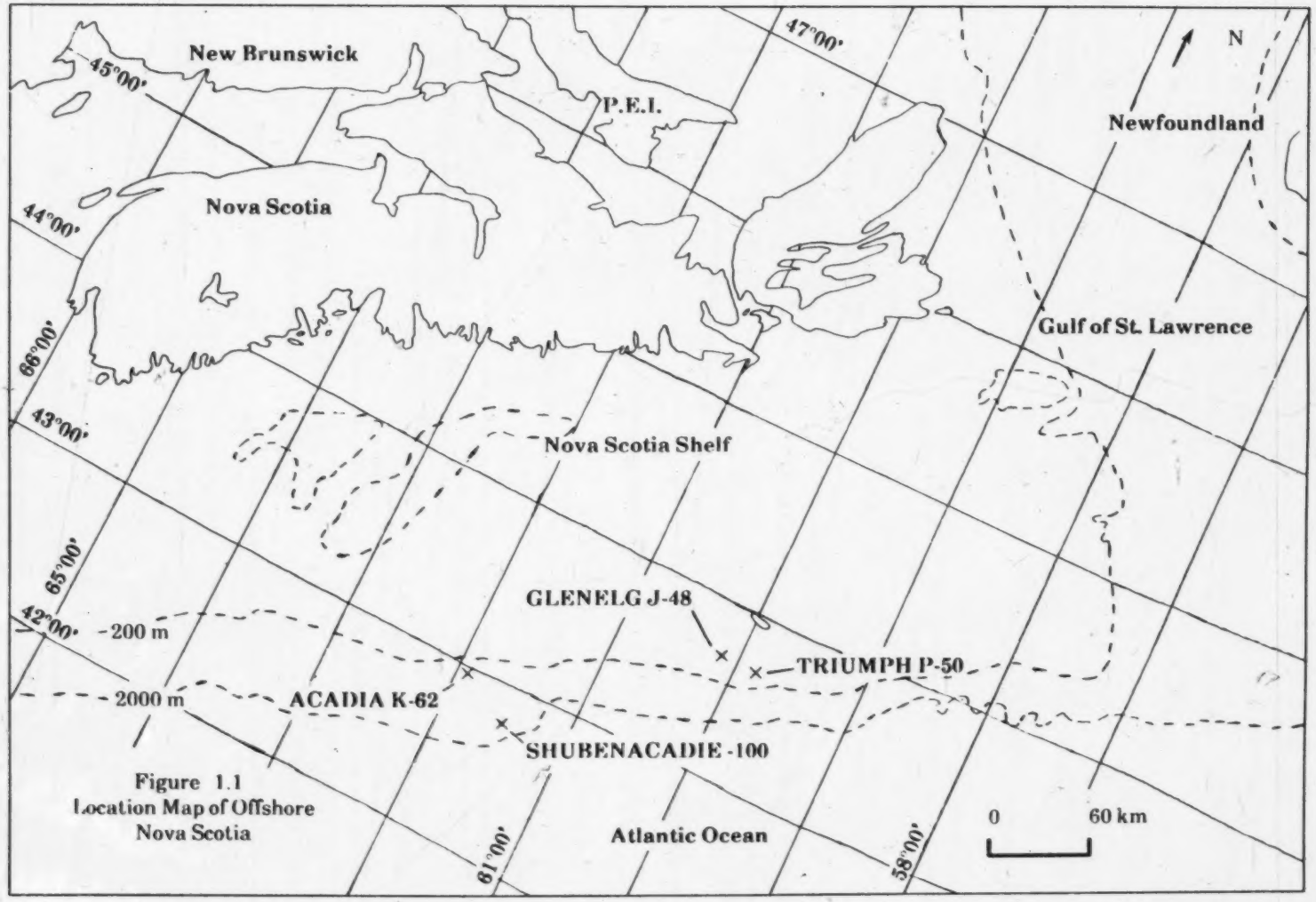

Figure 1.1
Location Map of Offshore
Nova Scotia

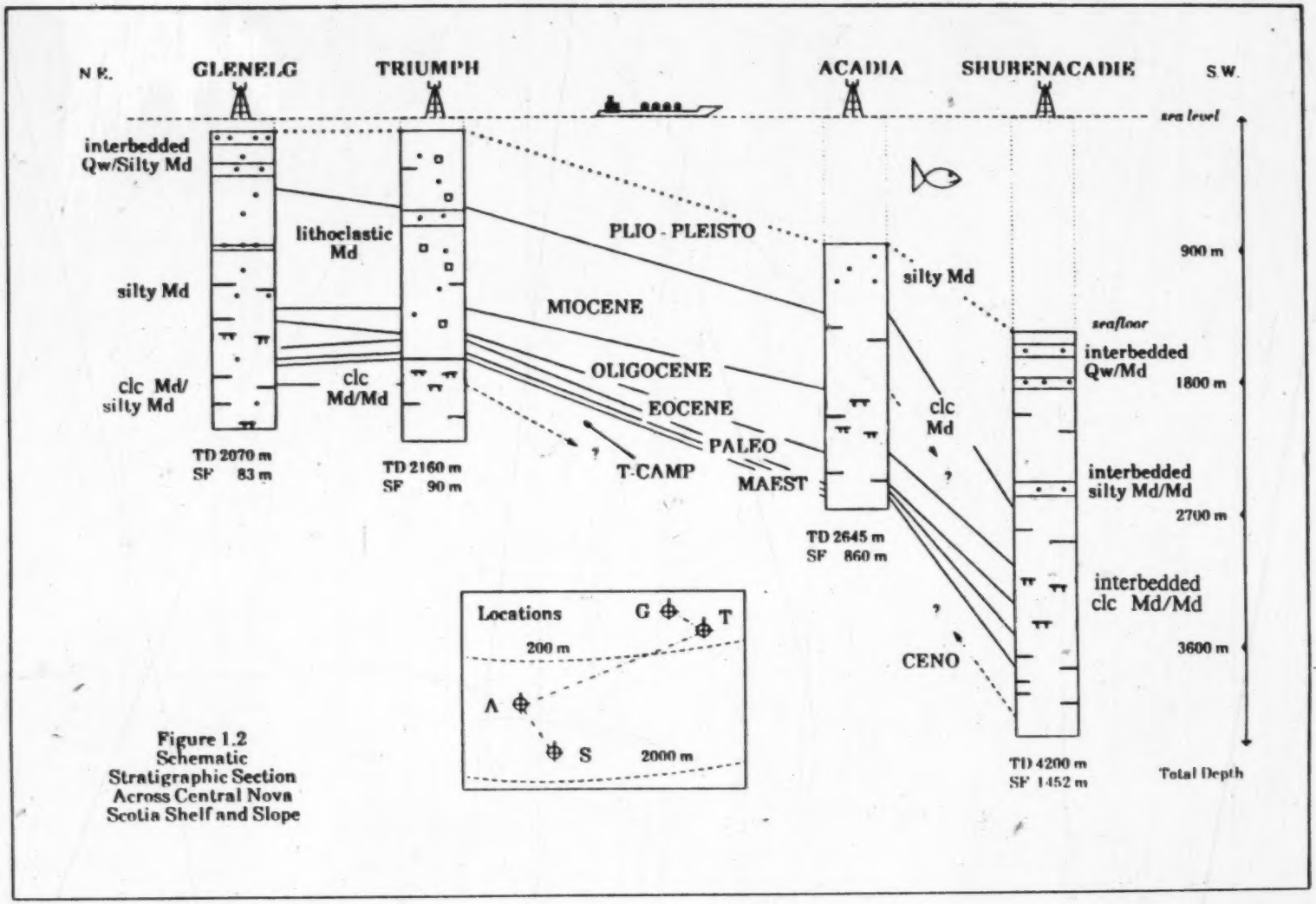

Figure 1.2
Schematic
Stratigraphic Section
Across Central Nova
Scotia Shelf and Slope

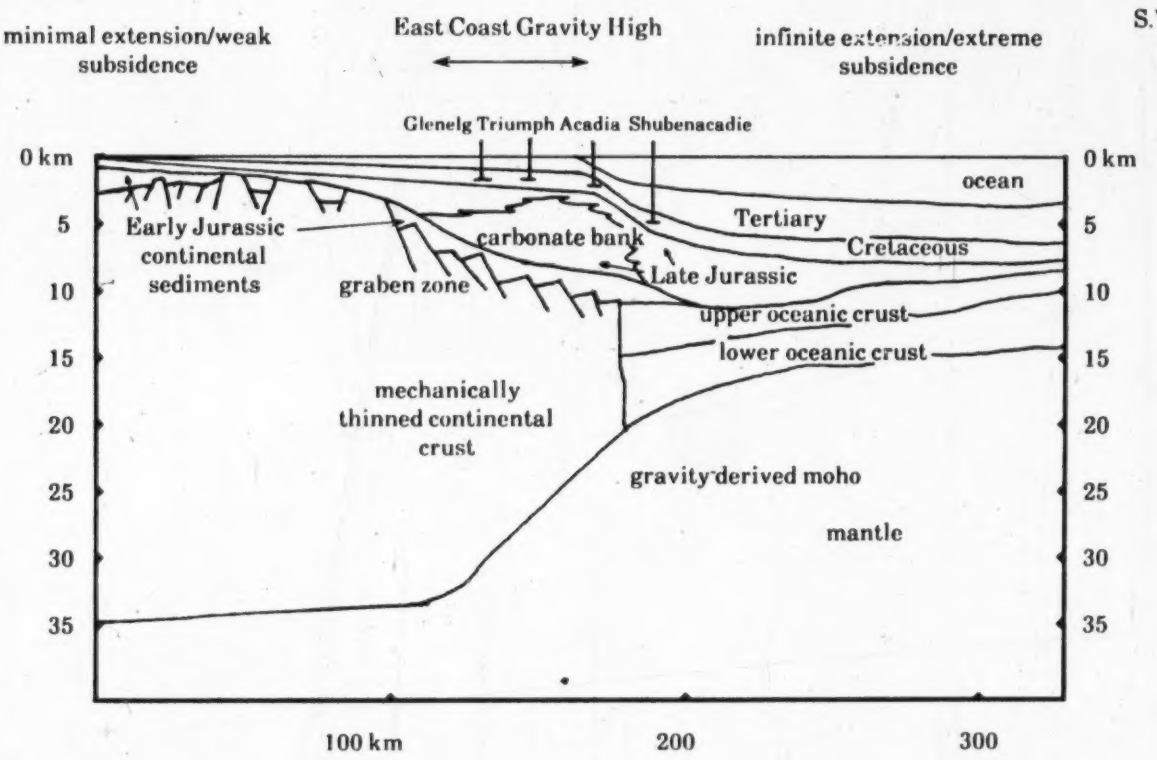

Figure 1.3
Interpretive Crustal Profile
Across Central Nova Scotia
Shelf and Slope

after Sawyer et al. (1982) and
Shell Canada Resources

The timing of initial subsidence is variously cited as Late Triassic for the continental margin off New England (Uchupi and Austin, 1979) to Early Jurassic for offshore-Nova Scotia (Royden and Keen, 1980). As mechanical deformation lasted only some 20 million years, the stratigraphic sections examined likely did not experience the effects of initial subsidence.

The drift phase followed initial subsidence upon full separation of the North American and European continental masses in mid-Jurassic time (Royden and Keen, 1980). As a result, thermal subsidence replaced mechanical subsidence upon completion of crustal thinning (Steckler and Watts, 1978; Royden and Keen, 1980; Sawyer et al., 1982).

According to Sawyer et al. (1982), thermal subsidence occurred as mechanically thinned continental crust was underplated by ultramafic rock, passively upwelled from the mantle (i.e., peridotites). Through time, elevated heat levels within underplated crust dissipated permitting cooling and subsequent increase in density of thinned crust. Thermal subsidence followed in response to density settling of mechanically thinned, continental crust. During this period, the sequences examined in this study were deposited.

Along the Atlantic passive margin, Sawyer et al. (1982) attributed approximately 60% of total tectonic subsidence to thermally induced subsidence. However other forces contribute to passive margin subsidence. Steckler and Watts (1978) considered sediment loading to be an important influence. Once appreciable sediment accumulated during the onset of thermal subsidence, sediment loading effects became more significant with time. Accordingly, their studies attribute between 40% and 60% of total subsidence to loading. Combining diminishing thermal subsidence and increasing sediment loading, the greatest net subsidence apparently occurred during the early drift phase (Early Cretaceous).

To evaluate subsidence trends in the region of the sequences of interest, Uchupi and Austin (1978) classified crust underlying the outer margin during the late drift phase as: (i) continental, (ii) transitional and (iii) oceanic. As transitional crust corresponds with thinned, continental crust along the East Coast Gravity High (i.e., suggesting crustal underplating), Royden and Keen (1980) predicted increasing crustal thinning oceanward. Good agreement between crustal thicknesses estimated from mechanical/thermal modelling and refraction seismic and gravity surveys across the shelf and slope confirms Royden and Keen's (1980) model. Refraction surveys indicate that mid to outer shelf regions are underlain by 25 km and 16 - 18 km of continental crust, respectively (prethinning estimate = 40 km). Relection seismic

estimates of crustal thickness by Steckler and Watts (1978) and Sawyer et al. (1982) corroborate these findings.

As the quantity of underplated material is proportional to the degree of crustal thinning at any location, greater net subsidence is expected oceanward. This subsidence trend resulted in: (i) greater net sediment accumulation and (ii) potentially greater water depth during deposition farther oceanward (Figure 1.3).

Royden and Keen (1980) placed the continent/ocean transition under the mid to outer continental shelf. If so, Glenelg and Triumph are situated over transitional crust. However Acadia and Shubenacadie are underlain by either extremely thin continental or true oceanic crust. These findings suggest that the outer shelf and slope have undergone considerable subsidence since Jurassic time (Keen and Cordsden, 1981).

Thermal subsidence diminished during Late Cretaceous time. In agreement, Brocher (1983) has reported minimal seaward thickening of post-Early Cretaceous sediment deposited along the continental shelf.

Passive margin evolution has exercised considerable influence on the thermal history of the Nova Scotia shelf and slope. During initial rifting, passive upwelling of mantle-derived ultramafic rocks increased heat flow through the shelf and slope area. Although mantle upwelling may have established higher geothermal gradients, Royden and Keen (1980) and Keen and Cordsden (1981) suggested that shelf and slope gradients have declined in response to heat dissipation through the crust since initial underplating. They suggested that heat flow and subsidence have diminished to a uniformly low level since Late Cretaceous time. However Reiter and Jessop (1985) measured the southwestern Nova Scotia shelf and slope to be relatively warm compared to other parts of the Atlantic margin.

STRATIGRAPHY

The Nova Scotia shelf and slope developed as part of the Atlantic passive margin. However, detailed study of their stratigraphy and sedimentology has not yet been completed.

On the Atlantic margin, Uchupi and Austin (1979) and Royden and Keen (1980) have placed the thickest sedimentary accumulations above the continent/ocean transition near the present continental margin. They claimed that this location, situated at the site of initial rifting, has been subjected to sedimentary accumulations longer than anywhere else. The presence of

shallow water sediments immediately above the rift site (evaporites, lagoonal limestones) grading upsection into deeper water sediments (mudstones, siltstones, calcareous mudstones) suggests appreciable subsidence.

Brocher (1983) described the post-rift sequence as a series of onlapping reflectors which progressively diverge seaward toward the shelf edge and thin again farther offshore toward the continental rise. Brocher's (1983) results suggested that progressive continental flooding was initiated at the site of initial rifting along the continental margin.

Seismic profiles shot across the shelf reveal shallow subparallel reflectors. The upper boundaries of these reflectors may exhibit truncation markers due to channel erosion or growth faulting (Marlowe, 1969). Seismic reflectors thicken slightly seaward in agreement with studies by Uchupi and Austin (1978). These results confirm a model of calm, onlapping deposition in a slowly subsiding basin during Late Cretaceous time.

Much sedimentological research on the shelf and slope has involved analysis of sediment cores from sea bottom taken along the continental slope and rise (Stow, 1976; Piper and Slatt, 1977). Recent sediments consist of interbedded fine-grained sands and silts from the slope and rise respectively, and muds. These clastic units preserve numerous Bouma cycles which decrease in grain size away from recognised deep sea channels.

Stow (1976), in describing sediment cores from the continental slope and rise, considered most sediments to consist of deep water clastics (gravels and fine sands) and hemipelagic muds. He attributed deep water clastics on the slope and rise to either classical turbidity currents or deep water contourites.

Marlowe (1969) described results of a dredging program along a submarine canyon known as "The Gully" lying southeast of Sable Island. The samples consisted primarily of flaggy mudstones with minor siltstones, sandy mudstones and sandy siltstones, all of Oligocene to Miocene age. Authigenic pyrite was present, an indication of reducing conditions in the sediment.

Due to the recent exploration history (circa 1967) and inaccessability of offshore-Nova Scotia, published stratigraphic studies are rare (McIver, 1972). Stratigraphic information used in this study was obtained from Shell Canada Resources well files.

McIver (1972) presented a stratigraphic classification based on numerous shelf drillholes. According to his scheme, each section examined in this study contains sediments

from the upper Nova Scotia Group (Logan Canyon Formation) and The Gully Group, as well as Quaternary material (Figure 1.4). Due to a lack of well control in the region considered, detailed lithostratigraphic nomenclature is not available for stratigraphic correlation. Paleontological and palynological age divisions were used to correlate rock intervals, rather than lithostratigraphic nomenclature.

CONTROLS ON DETRITAL CLAY OCCURRENCE AND DISTRIBUTION

Variations in the distribution of seabottom clays were discussed by Powers (1957), Nelson (1960) and recently by Gibbs (1977). In considering clay-mineral distribution on a shelf setting, Gibbs (1977) examined the continental shelf downcurrent from the mouth of an Amazon River distributary. Across the Amazon shelf, smectite tends to be preferentially concentrated in distal, outer shelf sites; detrital kaolinite and illite occur nearer to the distributary. Gibbs (1977) observed that smectite (average diameter=0.4μm) is much finer-grained than detrital kaolinite (1-2μm) or detrital illite (2-4μm), and proposed that trends in the distribution of shallowly buried clays were controlled by partical size. Flocculation and mineral alteration were not significant influences on clay distribution. If Gibbs (1977) is correct, consideration of clay distibution must be given when interpreting the diagenetic evolution of sediments from outer shelf and slope regions.

As well, clay-mineral composition can vary widely between depositional basins. Hein and Longstaffe (1985) described the clay composition of fine-grained sediments from Baffin Island fiords as being primarily illitic. Illitic composition may be a response to an ambient source terrain which has not undergone extensive chemical weathering (i.e., arctic). In contrast to a composition indicative of arctic weathering, sections through the Niger Delta are kaolinite-rich (Bruce, 1984). An abundance of detrital kaolinite suggests greater weathering in adjacent source terrains.

Between the extreme environments of tropical and arctic weathering, the composition and distribution of sea-bottom clays from the Nova Scotia margin have been examined. Piper and Slatt (1977) determined that the Nova Scotia margin contains significant quantities of kaolinite and smectite. They attributed the source of smectite present in these rocks to material weathered from Triassic redbeds, with a minor contribution from Paleozoic ashes. As well, the Nova Scotia margin is characterized by a predominance of detrital quartz with little feldspar or

GROUP	FORMATION	MEMBER
QUATERNARY	SABLE ISLAND	
	LA HAVE	
	SAMBRO	
	EMERALD	
	SCOTIAN SHELF	
THE GULLY GROUP (UPPER CRETACEOUS)	BANQUEREAU	
	WYANDOT	
	DAWSON CANYON	
NOVA SCOTIA GROUP (LOWER CRETACEOUS)	LOGAN CANYON	SABLE SHALE
	NASKAPI (*not examined*)	

Figure 1.4
Generalized Stratigraphic Column, Offshore-Nova Scotia

after McIver (1972) and Shell Canada Resources

amphibole.

C. SUMMARY OF REGIONAL GEOLOGY

1. Fine-grained Upper Cretaceous and Tertiary clastic rocks, deposited along Nova Scotia's passive margin, have undergone continuous subsidence in a marine environment.
2. Along the Nova Scotia margin, the greatest subsidence has occurred near the outer shelf/slope break during the drift stage (Early Cretaceous). As a result, the sections examined in this study contain the greatest thickness of fine-grained Upper Cretaceous and Tertiary rocks found along this margin.
3. Off Nova Scotia, heat flow has decreased since the Late Cretaceous, but is still high relative to other parts of this margin.
4. Seismic profiles along the outer shelf and slope suggest that deposition has been calm and continuous, as indicated by onlapping reflectors without significant truncations.
5. Recent sediments cored along the outer shelf and slope consist of very fine sands and silts which are quartz-rich (i.e., low feldspar and mafic mineral content). Bouma cycles suggest the occurrence of turbidites implying that these sediments are of deep water origin.
6. The composition of detrital clays occurring in any sedimentary basin is primarily a response to weathering conditions in their source regions. Detrital clays from offshore-Nova Scotia generally are illite and smectite-rich.

D. BIBLIOGRAPHY

Brocher, T.M., 1983, Shallow crustal structure of the continental margin off Nova Scotia: Can. Jour. Earth Sciences, v. 20, p. 1657-1672.

Bruce, C.H., 1984, Smectite dehydration, its relation to structural development and hydrocarbon accumulation in northern Gulf of Mexico basin: Am. Assoc. Petroleum Geologists Bull., v. 68, p. 673-683.

Burst, J.F., 1969, Diagenesis of Gulf Coast clayey sediments and its possible relation to petroleum migration: Am. Assoc. Petroleum Geologists Bull., v. 53, p. 73-93.

Dilli, K. and Rao, C.N., 1982, A note on the burial diagenesis of clay minerals in the Bengal Fan: Jour. Geol. Soc. India, v. 23, p. 561-566.

Dypvik, H., 1983, Clay mineral transformations in Tertiary and Mesozoic sediments from the North Sea: Am. Assoc. Petroleum Geologists Bull., v. 67, p. 160-165.

Gibbs, R.J., 1977, Clay mineral segragation in the marine environment: Jour. Sedimentary Petrology, v. 47, p. 237-243.

Hein, F.J. and Longstaffe, F.J., 1985, Sedimentologic, mineralogic, and geotechnical descriptions of fine-grained slope and basin deposits, Baffin Island fiords: Geo-Marine Letters, v. 5, p. 11-16.

Hiscott, R.N., 1984, Clay mineralogy and clay mineral provenance of Cretaceous and Paleogene strata, Labrador and Baffin shelves: Bull. Can. Petroleum Geology, v. 32, p. 272-280.

Hower, J., Eslinger, E.V., Hower, M.E. and Perry, E.A., 1976, Mechanism of burial metamorphism of argillaceous sediment: 1. mineralogical and chemical evidence: Geol. Soc. Am. Bull., v. 87, p. 725-737.

Keen, C.E. and Cordsden, A., 1981, Crustal structure, seismic stratigraphy, and rift processes of the continental margin of eastern Canada: ocean bottom seismic refraction results off Nova Scotia: Can. Jour. Earth Sciences, v. 18, p. 1523-1538.

McIver, N.L., 1972, Cenozoic and Mesozoic stratigraphy of the Nova Scotian shelf: Can. Jour. Earth Sciences, v. 9, p. 54-70.

Marlowe, J.I., 1969, A succession of Tertiary strata off Nova Scotia, as determined by dredging: Can. Jour. Earth Sciences, v. 6, p. 1077-1094.

Morton, J.P., 1985, Rb-Sr evidence for punctuated illite/smectite diagenesis in the Oligocene Frio Formation, Texas Gulf Coast: Geol. Soc. Am. Bull., v. 96, p. 114-122.

Nelson, B.W., 1960, Clay minerals of the bottom sediments, Rappahannock River, Virginia: Clays and Clay Minerals, v. 7, p. 135-147.

Perry, E.A. and Hower, J., 1970, Burial diagenesis of Gulf Coast pelitic sediments: Clays and Clay Minerals, v. 18, p. 165-177.

Piper, D.J.W. and Slatt, R.M., 1977, Late Quaternary clay mineral distribution on the eastern margin of Canada: Geol. Soc. Am. Bull., v. 88, p. 267-272.

Powers, M.C., 1957, Adjustment of land derived clays to the marine environment: Jour. Sedimentary Petrology, v. 27, p. 355-372.

Reiter, M. and Jessop, A.M., 1985, Estimates of terrestrial heat flow in offshore eastern Canada: Can. Jour. Earth Science, v. 22, p. 1503 1517.

Royden, L. and Keen, C.E., 1980, Rifting process and thermal evolution of the continental margin of eastern Canada determined from subsidence curves: Earth and Planetary Science Letters, v. 51, p. 343-361.

Sawyer, D.S., Swift, B.A., Sclater, J.G. and Toksöz, M.N., 1982, Extensional model for the subsidence of the northern United States Atlantic continental margin: Geology, v. 10, p. 134-140.

Steckler, M.S. and Watts, A.B., 1978, Subsidence of Atlantic-type continental margin off New York: Earth and Planetary Science Letters. v. 41, p. 1-13.

Stow, D.A.V., 1976, Deep water sands and silts on the Nova Scotian continental margin: Maritime Sediments, v. 12, p. 81-90.

Uchupi, E. and Austin, J.A., Jr., 1979, The geological history of the passive margin off New England and the Canadian Maritime Provinces: Tectonophysics, v. 59, p. 53-69.

II. PETROGRAPHY, FABRIC AND PETROPHYSICS

A. INTRODUCTION

The diagenesis of fine-grained rocks is characterized by two processes: compaction (i.e., physical diagenesis) and chemical diagenesis. Petrophysical, petrographic and geothermal observations relating to the compaction history of fine-grained, Upper Cretaceous and Tertiary rocks from offshore-Nova Scotia are presented in this chapter.

Petrophysical and petrographic observations provide information on the style of compaction and the nature of fabric development in the rock sequences of interest. For fine-grained rocks, this information is especially important because it could help to determine: (i) the degree to which constituent minerals have evolved in response to burial, (ii) the degree of pore-fluid mobility within fine-grained systems, and (iii) whether pore-fluids have changed compositionally in response to mixing and burial.

Geothermal gradients through these sequences can be estimated using petrophysical methods (i.e., compensated, logging-run temperatures). Evaluation of compaction data together with geothermal data can determine the accuracy of geothermal gradient estimates because fluid content in rock is inversely proportional to geothermal gradient (Zierfuss, 1969). Once geothermal gradients are satisfactorily determined, they can provide temperature constraints on diagenetic processes.

B. METHODOLOGY

COMPACTION ANALYSIS - PETROPHYSICAL TECHNIQUES

Petrographic characterization of porosity distribution in fine-grained clastic rocks is difficult, due to their grain size. However, understanding the nature of porosity reduction with burial is crucial when evaluating the effects of compaction on the diagenesis of these rocks. In this chapter, first consideration will be given to petrophysical evaluation of *relative changes* in the porosity of fine-grained rocks with burial.

Fine-grained clastic rocks from the Nova Scotia shelf and slope are composed primarily of mudstones and graywackes, with minor occurrences of calcareous mudstone. Graywackes and mudstones both contain abundant mud and silt-size material. To determine the matrix

velocities of these rock types, Press (1966) has suggested that highly compacted graywackes and slates have similar sonic velocities when measured over a range of high pressure conditions (Table 2.1). Equivalent sonic velocities are expected as each rock type has a similar type of matrix.

Generally, mudrocks have matrix velocities which are slower than other rock types (e.g., carbonates, igneous rocks) (Press, 1966). Presuming that matrix velocities of various fine-grained clastic rocks do not change appreciably, significant reductions in rock velocity can be attributed to: (i) the presence of pore-filling fluids (Nafe and Drake, 1957), and (ii) random particle orientation (Kaarsberg, 1959). In this way, most shaly rock types can be used for sonically-based, compaction (i.e., porosity) evaluations, with the exception of fine-grained rocks bearing high-velocity matrix materials, such as carbonate in calcareous mudstones.

To estimate the initial fluid composition in these sequences, micropaleontological and palynological studies have determined that most of these fine-grained sediments were deposited under open marine conditions (pers. comm., F. Brillo, Shell Canada Resources). Original *in situ* fluids infilling porosity were likely seawater. Press (1966) has presented velocities for standard seawater at various pressure and temperature conditions (Table 2.1). Despite variable conditions, brines still have characteristic velocities consistently much less than highly consolidated, fine-grained rocks (i.e., matrix materials); variations in the sonic velocity of fine-grained clastic rocks may be attributed to the amount of fluid-filled porosity present in the rocks of interest (Wyllie et al., 1956; Nafe and Drake, 1957).

The concept of ***exponential porosity-reduction*** with increasing pressure is long established (Athy, 1930; Hedberg, 1936). Meade (1966) generalized the concept to exponential porosity-reduction with ***burial*** over shallow depth ranges of several thousand meters. As sonic velocity is inversely proportional to the porosity of fine-grained clastic rocks, it should increase exponentially with depth. In this way, sonic velocity can provide a qualitative means for measuring variations in the compaction of fine-grained clastic rocks with burial (Magara, 1976b), as fluid velocity is ***effectively constant*** relative to matrix velocity over the range of depths examined (Press, 1966).

Variations in porosity of fine-grained rocks during burial are important; undercompaction can occur if pore-fluids under load are prevented from escaping porous rocks. As Magara (1976a) considers vertical fluid flow to dominate in fine-grained,

TABLE 2.1. SEISMIC VELOCITIES OF TYPICAL SHALY CONSTITUENTS

MUDROCK MATRIX VELOCITIES

PRESSURE (kg/cm^2)	DENSITY (g/cm^3)	VELOCITY (km/s)	TRANSIT TIME ($\mu s/m$)
	Graywacke (Quebéc)		
10.2	2.705	5.40	185
1020.0	2.705	5.92	167
2040.0	2.705	6.04	166
	Graywacke (New Zealand)		
10.2	2.679	5.40	185
1020.0	2.679	5.76	174
2040.0	2.679	5.87	170
	Slate (Massachusetts)		
10.2	2.734	5.49	182
1020.0	2.734	5.79	173
2040.0	2.734	5.91	169

SEAWATER VELOCITIES

PRESSURE (kg/cm^2)	DEPTH (@ 1.1 g/cm^3)	VELOCITY (km/s)	TRANSIT TIME ($\mu s/m$)
	measured at ambient water temperature		
22	200	1.522	657
94.6	860	1.506	664
159.5	1450	1.492	670
	measured at 15°C		
22	200	1.510	662
94.6	860	1.520	658
159.5	1450	1.530	654

after Press (1966)

lithologically homogeneous sequences lacking numerous sandstone conduits, weak undercompaction may be common if vertical barriers inhibit upward migration of fluids. As trapped pore-fluids and matrix are loaded with overburden, fluid pressure can rise as pore-fluids begin to support lithostatic load. In this way, undercompacted units associated with high fluid pressure may be characterized by long sonic transit times (Δt) corresponding to: (i) slow sonic velocities and (ii) low bulk densities compared to a "normal" compaction trend (Magara, 1976b); sonic transit time ($\Delta t = \mu s/m$) is a *colloquial* expression equivalent to the inverse of velocity.

Having defined a qualitative technique for tracing compaction with burial, this tool can be used on wells which have been sonically surveyed over the stratigraphic intervals of interest. Using a borehole-compensated sonic log or a long-spaced sonic log, the sonic signal generally was sampled approximately every 20 meters in fine-grained rocks where no wash-out was observed (Figure 2.1). These points were plotted semi-logarithmically in order to define a linear trend of sonic travel time with depth. Linear regression lines were fit to those parts of the curve demonstrating visibly similar, linear decreases in travel time with depth, resulting in trends of normal compaction. Deviations of less than 10 $\mu s/m$ from normal compaction trends are attributed to system noise. Trends of normal compaction provide a statistical scale with which to determine whether a particular interval is relatively undercompacted or normally compacted.

As well as determining compaction trends (Δt versus depth), relative differences in compaction can be measured by synthetic seismographs. Intervals containing lenses that are compacted to varying degrees are characterized by the development of seismicity. By convolving a digitized sonic log with a digitized density log over the same interval, a synthetic seismic impedence time-series can be defined. If a reliable density log is not available, an impedence time-series can be defined solely on velocity contrast. Such synthetic seismographs have been prepared for Acadia, Glenelg and Shubenacadie.

Using various frequency bandwidths (i.e., 10-70 Hz), seismic wavelets can be compressed into thin markers which define possible reflectors. Aside from seismicity development in response to density and velocity contrasts within the matrix of fine-grained clastic rocks, the occurrence of seismicity suggests that variations in compaction exist, implying that normal compaction is incomplete.

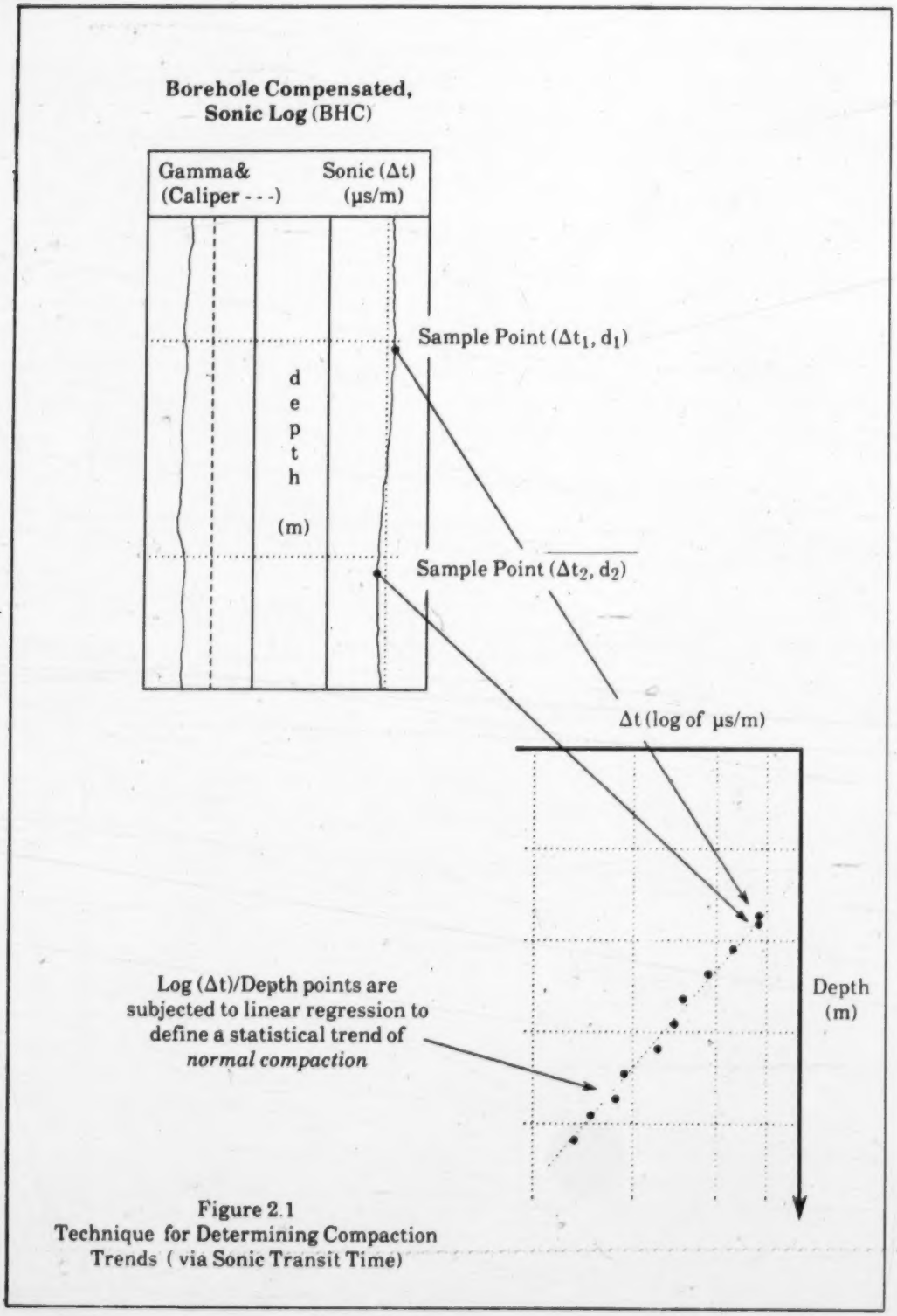

Figure 2.1
Technique for Determining Compaction
Trends (via Sonic Transit Time)

Synthetic seismographs aid identification and classification of potential zones of undercompaction and soft overpressuring. Caution was exercised to evaluate the reliability of wireline logs with respect to hole conditions. In general, only those logs which were recorded under stable hole conditions have been considered. However, although unreliable logs may generate spurious reflectors and/or obscure important markers, "wash-out" zones serve to identify those parts of each section which are poorly consolidated.

DETERMINATION OF GEOTHERMAL GRADIENTS

Geothermal gradients were determined for the outer shelf, upper slope and lower slope using compensated, logging-run temperatures. This technique provides information regarding the character of each well's geothermal gradient by downhole temperature measurement.

In order to estimate the geothermal gradient of any section using log-run temperatures, recorded temperatures must be compensated for heat loss associated with circulation of drilling fluids over the period of operation. Several logging runs must be recorded at various depths for each well considered. A greater number of temperature measurements often results in greater reliability of the final extrapolated temperature at each depth. From each logging run, specific information is required including: (i) the depth at which the temperature measurement was taken, (ii) the time over which drilling fluid was circulated downhole, (iii) the time since cessation of circulation and (iv) the formation temperature measured during that recording (pers. comm., E. Bogoslowski).

With this information, a modified version of Theis's equation (Hackbarth, 1978) was used, considering heat flow into a circular borehole, to obtain an estimate of true formation temperature at a time measured long after fluid circulation (Figure 2.2). Reliable temperatures measured at every depth during each logging run were extrapolated to infinite time after circulation cessation to estimate true formation temperatures.

Once compensated (temperature/depth) pairs have been determined, they constitute raw data which can be subjected to linear regression in order to determine the geothermal gradients best fitting gross, qualitative trends in the data. In certain instances, gradients were defined which contain several linear components.

As with the hydrologic Theis equation, certain assumptions are inherent in this discussion. For the modified Theis equation to be valid for our case, the sequence of

Figure 2.2 Flow Equations

$$P_F = P_o - \frac{q\mu}{4\pi kh} \ln \frac{t_o + \Delta t}{\Delta t}$$ (FORMATION PRESSURE)

P_F = true formation pressure
P_o = initial formation pressure
q = pumping rate during flow period
μ = viscosity of fluid
t_o = time of pumping
Δt = time since end of pumping
k = hydraulic conductivity
h = saturated thickness

$$T_F = T_o - \frac{CQ}{\lambda} \log \frac{t_o + \Delta t}{\Delta t}$$ (FORMATION TEMPERATURE)

T_F = true formation temperature
T_o = initial formation temperature
C = calibration constant
Q = rate of heat flow into borehole
t_o = time of circulation
Δt = time since end of circulation
λ = thermal conductivity

Hydraulic information from Hackbarth (1978).

fine-grained clastic rocks must be confined with respect to heat flow. Considering heat conduction in these thick sequences, this is likely true. As well, the conducting unit must possess homogeneous heat conductivity. Again, for a lithologically similar section, this is a good approximation.

In terms of spatial dimension, the borehole must be much narrower than the formation being examined. This too is a very good approximation as these fine-grained clastic rocks are thought to be laterally homogeneous for tens' of kilometers (Figure 1.2).

PETROGRAPHIC ANALYSIS - TECHNIQUES

Sidewall core (SWC) and ditch-cutting subsamples from Glenelg and Shubenacadie, and ditch-cutting subsamples from Triumph, were selected throughout each section for petrographic examination of the outer shelf and lower slope. Petrographic evaluation of fine, Upper Cretaceous and Tertiary clastics from Acadia was not possible because ditch cuttings were finely ground during drilling.

Covered thin sections were prepared from epoxy impregnated samples from Glenelg, Shubenacadie and Triumph. Thin sections were examined using a polarizing, transmitted light microscope. As cited by Nuhfer et al. (1982), conventional microscopy is useful in these types of rocks for examination of preferred orientation in clay and non-clay minerals, and deformation fabrics.

Secondary electron imaging by scanning electron microscope (SEM) was also performed on SWC subsamples from Glenelg and Shubenacadie. It generates information regarding: (i) localized microfabric elements and (ii) the nature of coarser grains within a clay matrix (O'Brien, 1970). Subsamples of rough topography were separated from host SWC approximately perpendicular to bedding plane by fracturing (Gillott, 1969). Broken chips were affixed to aluminum stubs using silver-bearing adhesive, with bedding planes oriented away from the holder. Once mounted, samples were sputter-coated with gold to ensure sample conductivity during analysis. The resulting low-energy gold peak obscures detection of sulphur due to overlapping characteristic energies.

An excitation potential of 20 KeV was used to excite secondary electrons from the sample surface. Qualitative estimates of the elemental composition of particular phases were obtained using a Kevex® energy dispersive, x-ray microanalyser (EDA) mounted onto a

Cambridge 250 Stereoscan SEM. Quantitative elemental analyses by this technique can be difficult because of: (i) widely variable detector/sample orientation, (ii) matrix absorbtion and (iii) fluorescence effects (pers. comm., J. McGovern).

To provide a broader perspective of fabric, additional SWC subsamples from Glenelg and Shubenacadie were chosen for backscattered electron imagery by SEM. SWC samples were vacuum-impregnated with quick drying epoxy and mounted perpendicular to bedding plane onto glass slides. Samples were then cut and polished as uncovered thin sections to approximately 30 - 50 μm thickness. Polished thin sections were made conductive by evaporative coating to approximately 25 Å thickness with high purity carbon.

Samples were examined in a Cambridge 250 Stereoscan SEM at an excitation potential of 20 KeV in secondary and backscattered electron mode. An annular, semiconductor type backscatter detector, similar to the type recommended by Hall and Lloyd (1981), was used to generate images of uniform brightness.

Examination by combined secondary and backscattered SEM imagery accentuates various mineral grains, as both topographic relief and mean atomic number contrast are employed (Krinsley et al., 1983). This technique is useful for rapid analysis of fine-grained clastic fabrics (Pye and Krinsley, 1984; White et al., 1984).

Qualitative elemental microanalysis from a Link Systems® EDA was used to verify mineralogical identifications. To perform reliable, qualitative x-ray microanalysis, flatly polished samples were tilted at 45° to a stationary energy dispersive x-ray detector at a working distance of 27 mm. Spectra for each sample were collected for 100 seconds at count rates of approximately 4000 counts/second with 25% deadtime. Elemental microanalyses of polished samples are considerably more accurate than for rough samples; one indication of this improvement is the development of classical Bremsstrahlung levels (i.e., smooth, continuous background)(Heinrich, 1981).

C. OBSERVATIONS

PETROPHYSICAL DATA

Compaction curves and synthetic seismographs through fine-grained clastic sequences were prepared for wells from the outer shelf and upper/lower slope to: (i) evaluate their style

of compaction with depth and between wells, and (ii) to determine whether undercompaction exists. Evaluation of compaction trends is important when determining whether abnormally high fluid pressures exist in certain parts of each section.

Compaction trends from Shubenacadie, Acadia and Glenelg were determined. A compaction curve could not be constructed for Triumph because downhole petrophysical surveys were not conducted through most of the Upper Cretaceous and Tertiary section.

PETROPHYSICAL CHARACTER - SHUBENACADIE

The lower slope section at Shubenacadie is characterized by two distinct compaction trends which meet at roughly 3000 - 3100 mbmsl in Upper Eocene mudrocks (Figure 2.3). To determine the thickness of uncompacted sediment lying below seafloor at Shubenacadie, compaction trends were extrapolated to a depth at which the sonic velocity of a sediment/fluid mixture is approximately that of seawater (Nafe and Drake, 1957). The sonic velocity of an uncompacted mixture can be estimated by either: (i) extrapolation to the observed sonic travel time at which mudrocks cease to follow compaction trends for other wells on the East Coast ($\Delta t = 600\ \mu s/m$) or (ii) extrapolation to the sonic travel time for sound propagation through water at 1450 meters and the appropriate water temperature at burial (Table 2.1). Both extrapolations place constraints on the deepest level at which uncompacted sediment can occur.

To evaluate the thickness of uncompacted sediment at Shubenacadie, extrapolation to the characteristic Δt for other East Coast wells was considered first. At Shubenacadie, both trends extrapolate to this travel time, corresponding to uncompacted material, at 2060-2090 mbmsl (i.e., within 30 m). This result suggests that essentially no erosion has taken place at the Miocene-Eocene marker separating the two trends. As no Oligocene fauna were identified, this marker may represent a period of very slow deposition. Also, up to 650 meters of uncompacted sediment may lie below seafloor at Shubenacadie.

Alternatively, by presuming that uncompacted sediments are characterized by a sonic travel time equal to seawater (i.e., $\Delta t = 635\ \mu s/m$ at roughly 20°C), upper and lower compaction trends from Shubenacadie extrapolate to 1930 and 1845 mbmsl respectively. This extrapolation implies that: (i) the Miocene-Eocene marker separating each trend has not experienced significant erosion and (ii) roughly 480 meters of uncompacted sediments lie below seafloor. A sonic travel time of 600 $\mu s/m$ was used here because: (i) it represents a velocity consistent with other East Coast wells before compaction is observed to occur, (ii) it avoids complications of

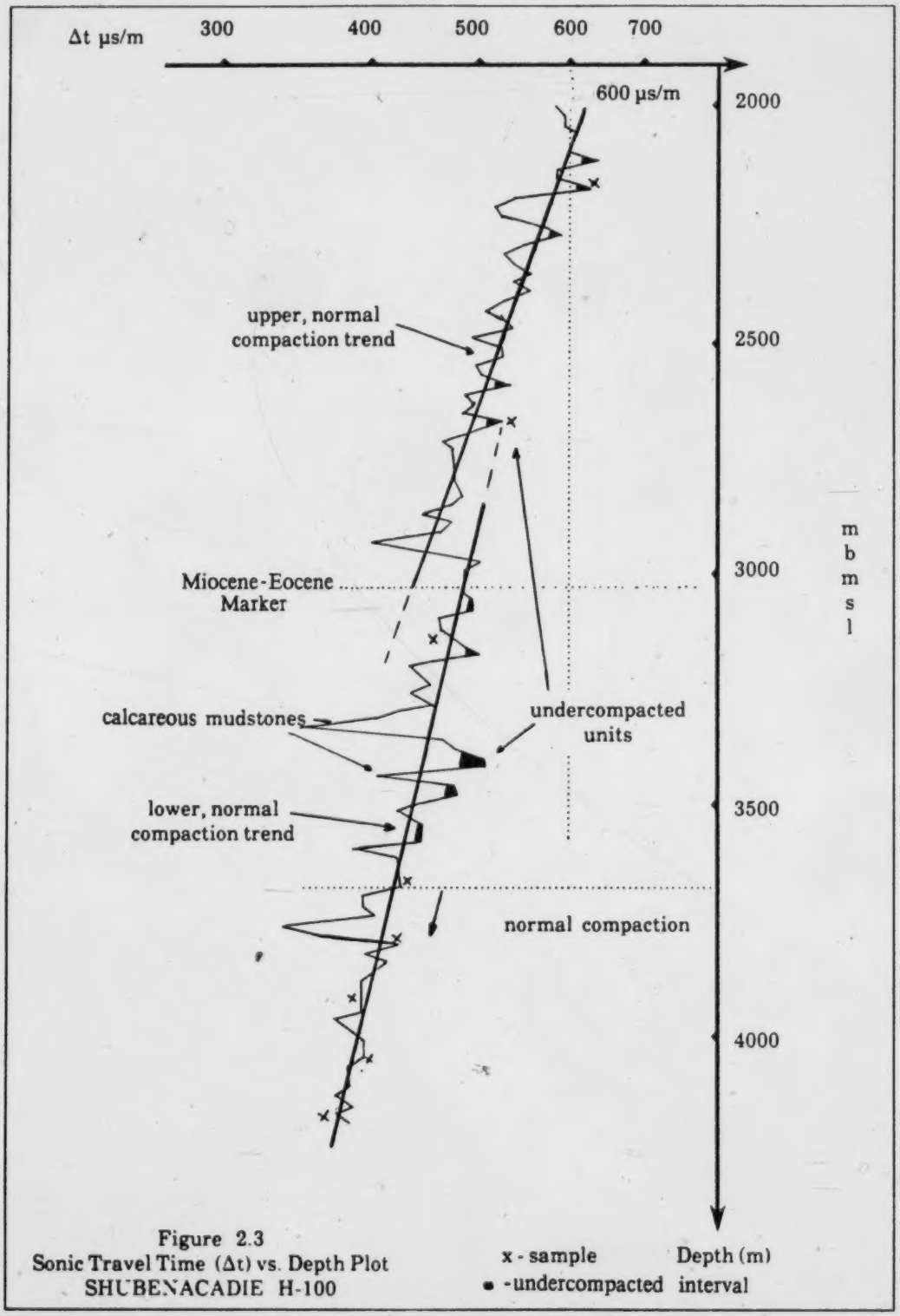

Figure 2.3
Sonic Travel Time (Δt) vs. Depth Plot
SHUBENACADIE H-100

seawater velocity variations with temperature and (iii) it permits characterization of uncompacted sediment by a velocity having a component of matrix.

Aside from measuring thicknesses of uncompacted sediment, two styles of undercompaction can be recognized. The lower compaction trend at Shubenacadie is characterized by marked deflections from the trend of normal compaction. Between 3050-3200 mbmsl and 3350-3600 mbmsl, several Δt deflections of up to 60 μs/m are observed; system noise may vary upto 10 μs/m. These deflections suggest that even in a normally compacting sequence of mudrocks, several intervals of high fluid content may be present. High velocity "kicks" corresponding to calcareous units are shown in Figure 2.3. These "kicks" were not included in linear regression determinations of the lower compaction trend because the petrophysical properties of carbonate matrix are not simlar to clay matrix.

Below 3600 mbmsl, undercompaction is not detected. Unlike shallower intervals, this segment exhibits a normal compaction sequence because it closely follows a "normal trend" (i.e., no compaction-related effects).

The upper compaction trend at Shubenacadie exhibits numerous low-velocity deflections of lesser intensity than the lower zone (i.e., 10-40 μs/m). This suggests that a milder degree of undercompaction is developed above the Miocene-Eocene marker. Numerous short Δt (i.e., high velocity) kicks correspond to certain silty mudstones and graywackes. However, Press (1966) suggests that no significant velocity difference exists between the matrix of graywackes and mudstones. Considering that continuous hole stability is apparent throughout the section, and that graywackes constitute certain low velocity intervals, weak undercompaction may exist in the upper section at Shubenacadie.

Synthetic seismographs also reveal the presence of undercompaction; raw wireline-velocity data define a synthetic, seismic impedence time-series. A seismic impedence, time-series accentuates intervals characterized by fluctuations in seismic velocity by defining spikes at lower boundaries of low velocity zones. In this way, a lithologically homogeneous sequence containing numerous low velocity, fluid-rich zones is characterized by the occurrence of significant seismic impedence. However evaluation of undercompaction by synthetic seismographs must be conducted with care; hole instability or high velocity carbonate stringers can create unrelated seismic events. For this study, lithology and hole conditions were considered to ensure that the seismic events which are attributed to undercompaction are not

influenced significantly by unrelated effects.

The synthetic seismograph for Shubenacadie verifies that below 3000 mbmsl, synthetic seismic events are common (Figure 2.4). In the absence of hole caving, these events may be attributed to the presence of high-velocity, calcareous lenses or low-velocity, undercompacted units. While several intense synthetic events correspond closely to calcareous mudstones, mild deflections in the synthetic wavelet occur throughout intervals of uniform lithology. These events may result from undercompacted lenses in the lower sequence.

The upper compaction trend exhibits a seismically noisy signal of lesser intensity than the lower sequence. As no high velocity matrix is detected in the upper sequence, seismicity is attributed to undercompaction.

Below approximately 3800 mbmsl, the sequence becomes more lithologically homogeneous and exhibits stable hole conditions. Over this interval, the synthetic wavelet becomes smoother indicating greater compaction at the base of the section.

PETROPHYSICAL CHARACTER - ACADIA

The upper slope section at Acadia is distinquished by three distinct compaction trends (Figure 2.5). The shallowest trend is characterized by long interval transit times of wide variability. From the top of the logged interval down to 1780 mbmsl, this zone exhibits essentially no indication of compaction with burial and frequently appears to be "washed-out" on the caliper log. It is suspected that this interval represents approximately 900 meters of uncompacted sediment with a high fluid content (i.e., long Δt). High velocity "kicks" may represent local zones of compaction or consolidated lithologies. The very fine and disaggregated nature of ditch cuttings from the upper section corroborates the friable, weakly compacted nature of this interval.

Below this low velocity zone, a trend of normal compaction is defined from 1780 - 2300 mbmsl. This compaction trend extrapolates to a Δt characteristic of uncompacted sediment at 1780 mbmsl (635 μs/m). The middle compaction trend contains numerous low-velocity deflections of up to 100 μs/m from the normal compaction trend, through an interval of stable hole conditions. While these undercompacted lenses are not as thick as those at Shubenacadie, they are numerous enough to suggest that this section is significantly undercompacted.

At Acadia, significant seismic impedence is defined throughout a lithologically homogeneous section (Figure 2.4). Synthetic seismographs from Acadia corroborate detection

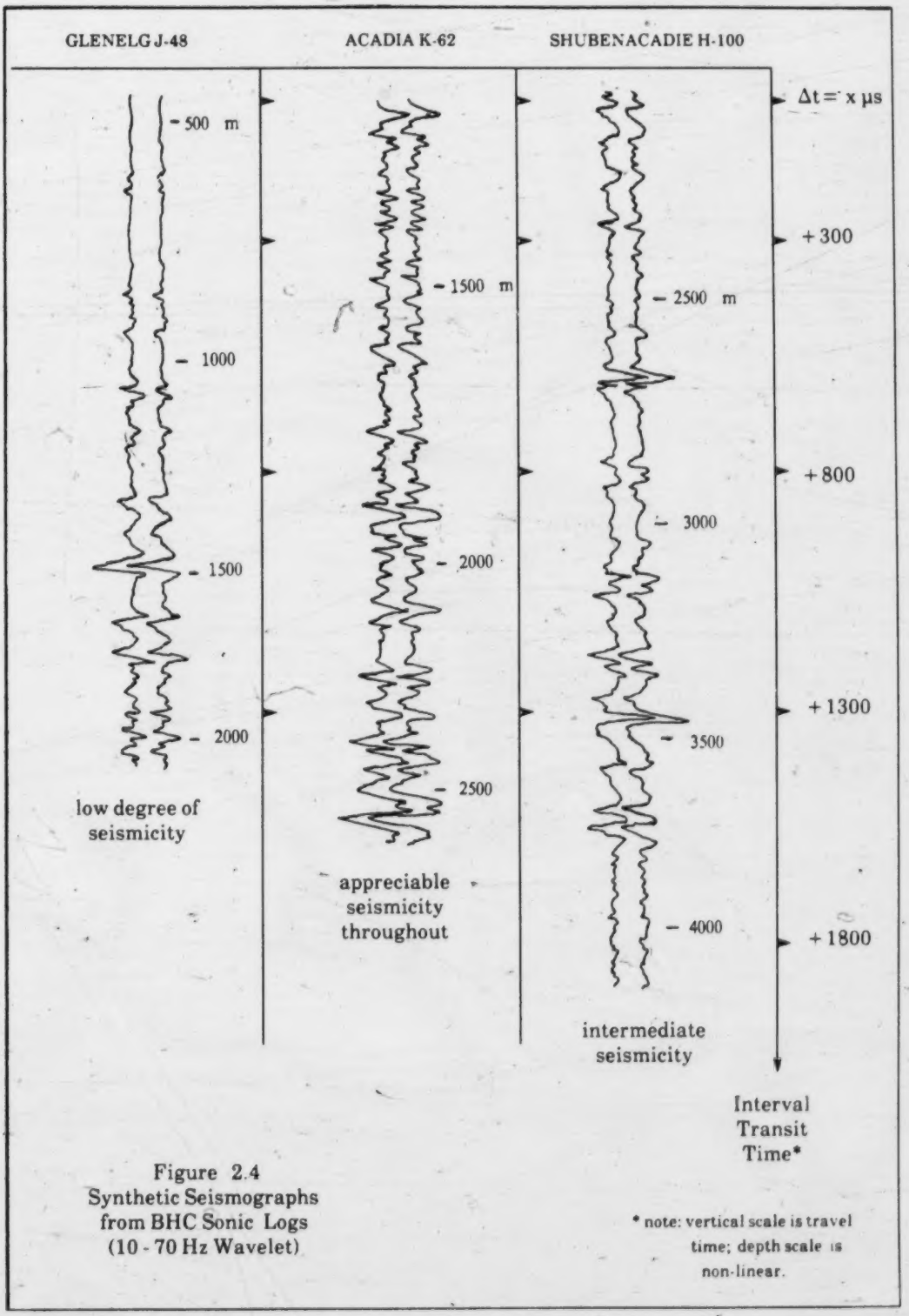

Figure 2.4
Synthetic Seismographs
from BHC Sonic Logs
(10 - 70 Hz Wavelet)

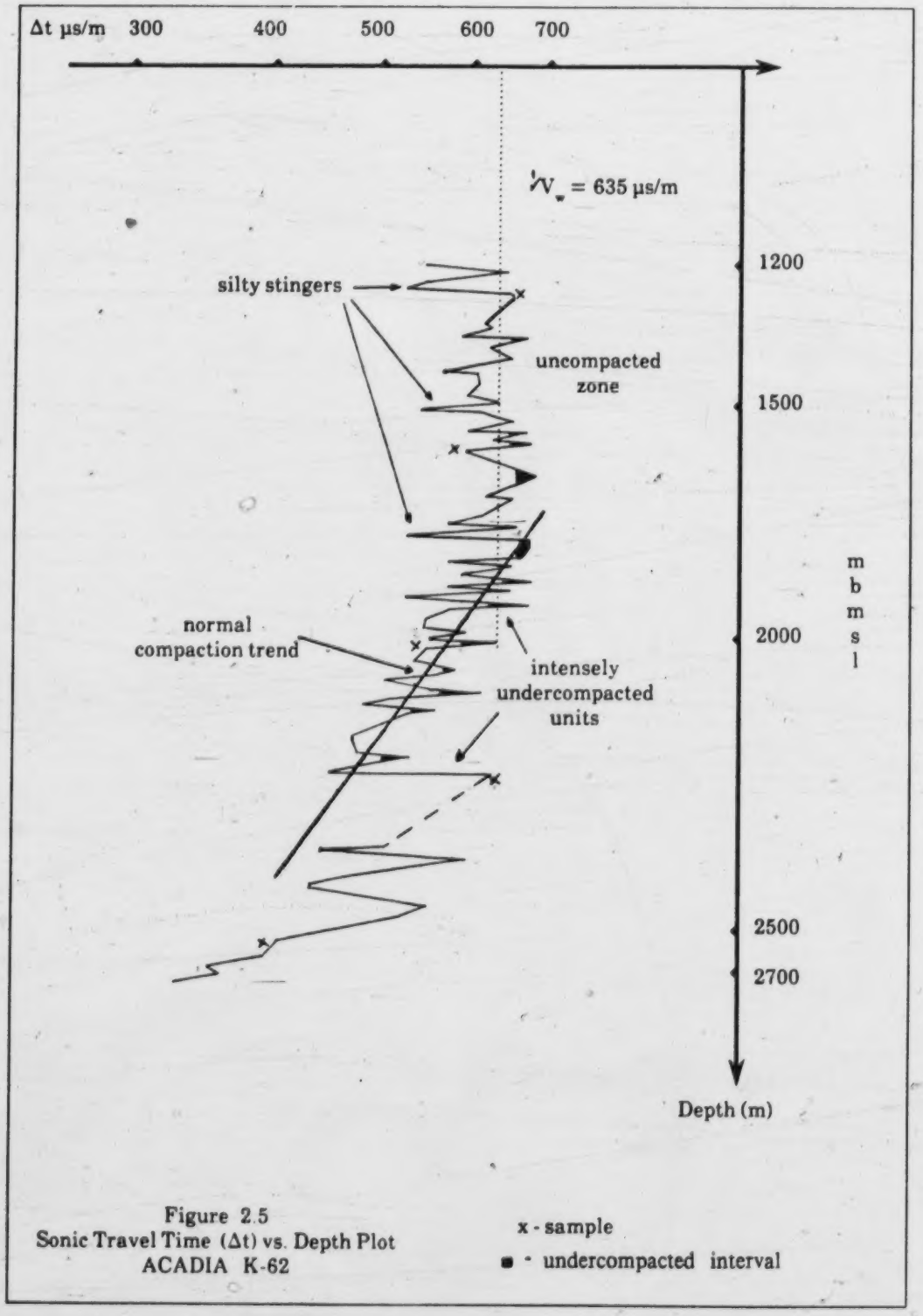

Figure 2.5
Sonic Travel Time (Δt) vs. Depth Plot
ACADIA K-62

of a shallow zone of uncompacted sediment and deeper undercompacted units, because the abundance of seismic impedence is likely a function of numerous undercompacted lenses and "wash-out" zones developed in soft mudrocks of high fluid content.

The lowest compaction trend at Acadia begins below 2300 mbmsl at the top of the Eocene section. This interval is characterized by a poorly developed compaction trend with several intense low-velocity deflections (i.e., 100's μs/m) where no hole caving is detected.

Mudstones in the lower section are more calcareous as confirmed by whole rock XRD. Although petrographic evaluation of this interval is not possible, non-calcareous mudstones in this region are likely thinner and have less vertical permeability due to frequent, calcareous mudstone interbeds. The lower trend extends downsection to roughly 2800 mbmsl where it contacts reef-related carbonates of the Jurassic Abenaki Formation (as indicated by a strong seismic event).

PETROPHYSICAL CHARACTER - GLENELG

The outer shelf section at Glenelg is characterized by two trends of compaction, in the Upper Cretaceous and Tertiary section (Figure 2.6). From 350 mbmsl down to 1650 mbmsl, a trend of normal compaction is defined. Moderately high velocity "kicks" are associated with siltstones, graywackes and silty mudstones which have similar gamma-log signatures. These high velocity "kicks" are included in the linear regression estimate of a normal compaction trend.

Moderate, low-velocity (i.e., long Δt) deflections occur from 1000-1100 mbmsl and below 1630 mbmsl. However, unlike Shubenacadie or Acadia, the deflections are of low intensity (i.e., 20-30 μs/m) suggesting only weak undercompaction.

In Figure 2.4, synthetic seismographs from Glenelg are quieter and reveal that this section has lower overall seismic impedence than the other wells. This observation agrees with predictions of minimal undercompaction at Glenelg. In the lower trend, appreciable impedence is associated with calcareous Wyandot mudstones.

When extrapolating Glenelg's trend of normal compaction to the interval transit time characteristic of uncompacted sediment at Shubenacadie and Acadia, an interesting observation is made. By this assumption, non-compaction is reached in excess of 200 meters *above* mean sea level (mamsl). Conversely, assuming uncompacted sediment is characterized by the Δt for 15°C seawater at 200 meters depth, estimates of non-compaction are reached even higher, in excess

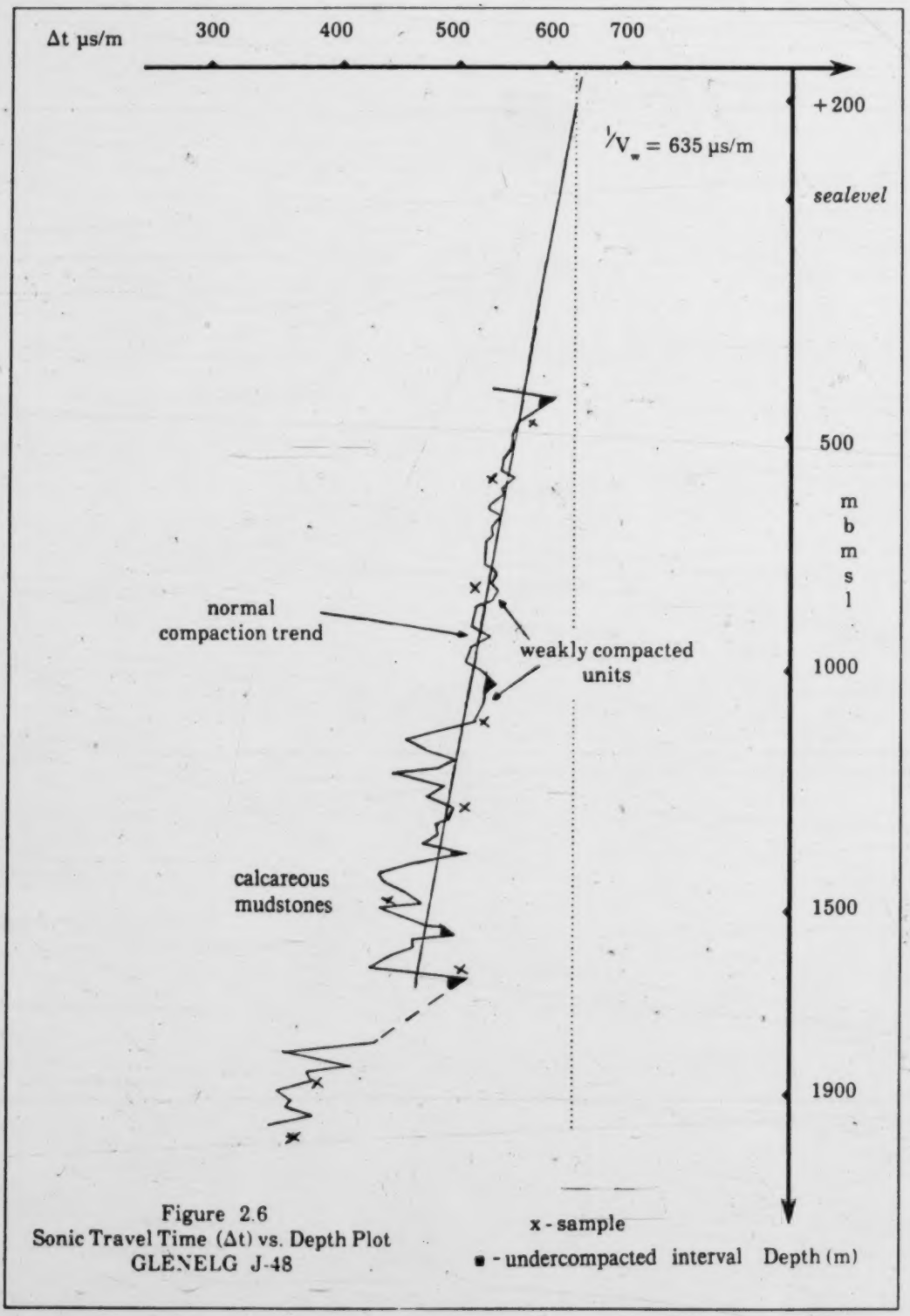

Figure 2.6
Sonic Travel Time (Δt) vs. Depth Plot
GLENELG J-48

of 700 mamsl.

Using these estimates of interval transit times characteristic of no compaction, between 300 and 800 meters of section apparently has been removed at this location on the outer shelf. Given that the sonic travel time of a hypothetical, uncompacted sediment is likely closest to the Δt of 15°C seawater, a realistic estimate of erosion at Glenelg may be closer to 600 meters. Possible mechanisms for erosion on the outer shelf include: (i) submarine debris flow off the shelf and/or (ii) subaerial erosion during a recent low stand in sealevel (McIver, 1972).

An important result of petrophysical analysis at Glenelg is that estimates of maximum burial for this section may be increased by roughly 600 meters beyond present burial. As well, Glenelg appears to be less highly undercompacted when compared to slope wells.

GEOTHERMAL GRADIENT OBSERVATIONS

Geothermal gradients have been calculated for each well using compensated, wireline-log, run-temperatures (Table 2.2). On the lower slope at Shubenacadie, a plot of temperature versus depth reveals two distinct geothermal trends with burial. The upper gradient is significantly cooler than the lower gradient and corresponds closely with the upper trend of porosity reduction recognised previously in the petrophysical analysis. Below the Miocene/Eocene marker, the geothermal gradient appears to increase significantly to a level in excess of other gradients recognised on the Nova Scotia shelf or slope; the result is a maximum temperature estimate of roughly 100°C at total depth (TD). The position of the hotter gradient corresponds closely with the lower interval of undercompaction. These observations suggest that the overlying, less compacted sediment has acted as a thermal insulator, serving to warm the lower section to a higher gradient. Given that the heat capacity of water exceeds that of rock material, significant thicknesses of weakly compacted mudstones and silty mudstones might inhibit heat flow through such a sequence.

Acadia's geothermal gradient consists of two distinct components which merge at roughly 2800 mbmsl, approximately the top of Jurassic Abenaki carbonates. The upper gradient, including most of the Upper Cretaceous and Tertiary sediments examined, is cool and of similar magnitude to the shallow gradient on the lower slope. The existence of such a cool gradient suggests fairly high, fluid-filled porosity in Upper Cretaceous and Tertiary mudrocks, an observation in agreement with petrophysical data.

TABLE 2.2. OFFSHORE-NOVA SCOTIA GEOTHERMAL GRADIENTS

WELL NAME	SETTING	GRADIENT ESTIMATE °C/km	MAXIMUM TEMPERATURE AT BASE
GLENELG J-48	OUTER SHELF	29.0	65°C
	86°C if buried 800 meters deeper		
TRIUMPH P-50	OUTER SHELF	28.9	
	below 2286 m	37.6	67°C
ACADIA K-62	UPPER SLOPE	22.8	
	below 2800 m	42.4	45°C
SHUBENACADIE H-100	LOWER SLOPE	22.5	
	below 3100 m	56.7	100°C

Compaction studies at Acadia suggest that significant erosion has not occurred within the Upper Cretaceous and Tertiary section. The present depth of these mudrocks probably represents a maximum since deposition. As the gradient over this interval is cool, the maximum burial temperature likely reached only about 43°C at 2640 mbmsl. From these data, the Upper Cretaceous and Tertiary section at Acadia is apparently very cool.

Two geothermal trends are also evident on the outer shelf at Triumph. The upper trend is warmer than shallow slope gradients and incorporates the Upper Cretaceous and Tertiary section examined. A geothermal gradient of 28.9°C/km (1.6°F/100 ft.) results in present-day burial temperatures of approximately 67°C at 2156 mbmsl (7080 ft.). As the lower section (pre-Upper Cretaceous strata) is characterized by a higher gradient of 37.6°C/km, (1.8°F/100 ft.), the upper section possibly provides an insulating influence similar to that described for slope wells.

In contrast to geothermal styles discussed previously, raw geothermal data from Glenelg suggest the existence of only one gradient of 29°C/km throughout the entire sequence measured. No indications of a cooler, shallow gradient or an underlying, hotter gradient have been observed.

At the geothermal gradient suggested, the present maximum temperature of this section is approximately 64°C at 2080 mbmsl. However, considering erosion estimates at Glenelg, maximum burial temperatures may be increased by between 9° and 23°C (likely 17°C). A resultant, maximum burial temperature of roughly 81°C can be estimated prior to erosion of the upper section at Glenelg.

PETROGRAPHIC INFORMATION

PETROGRAPHY - OUTER SHELF

Using various petrographic techniques, depositional and compactional fabrics and gross facies distributions were investigated. Considering information from Glenelg and Triumph, the outer shelf sections are characterized by the presence of four distinctive primary facies including: (i) a coarse lithoclastic facies, (ii) a graywacke facies, (iii) a silty mudstone facies and (iv) a calcareous mudstone facies.

The coarse lithoclastic facies consists of rocks containing diverse sedimentary rock fragments including silty and calcareous mudstone (Plate 2.1a). Average fragment dimensions

PLATE 2.1. THIN SECTION MICROGRAPHS

Plate 2.1a: Thin section micrograph of lithoclastic facies from outer shelf. Lithic fragments include mudstone and calcareous mudstone, containing cemented foram tests. Detrital quartz is also present in rock fragments. Triumph P-50, 1554 mbmsl (5100 ft.), 2.5X objective.

Plate 2.1b: Thin section micrograph of wacke containing glauconite and silt-size quartz in mud matrix. Triumph P-50, 1368 mbmsl (4490 ft.), 6.5X objective.

Plate 2.1c: Thin section micrograph of fossiliferous mudstone. Fossil tests and crosscutting fractures are filled with calcite. Triumph P-50, 1807 mbmsl (5930 ft.), 10X objective.

Plate 2.1d: Thin section micrograph of calcareous, fossiliferous mudstone. Numerous fossil tests are unaltered and partly filled with calcite. Glenelg J-48, 1510 mbmsl, 10X objective.

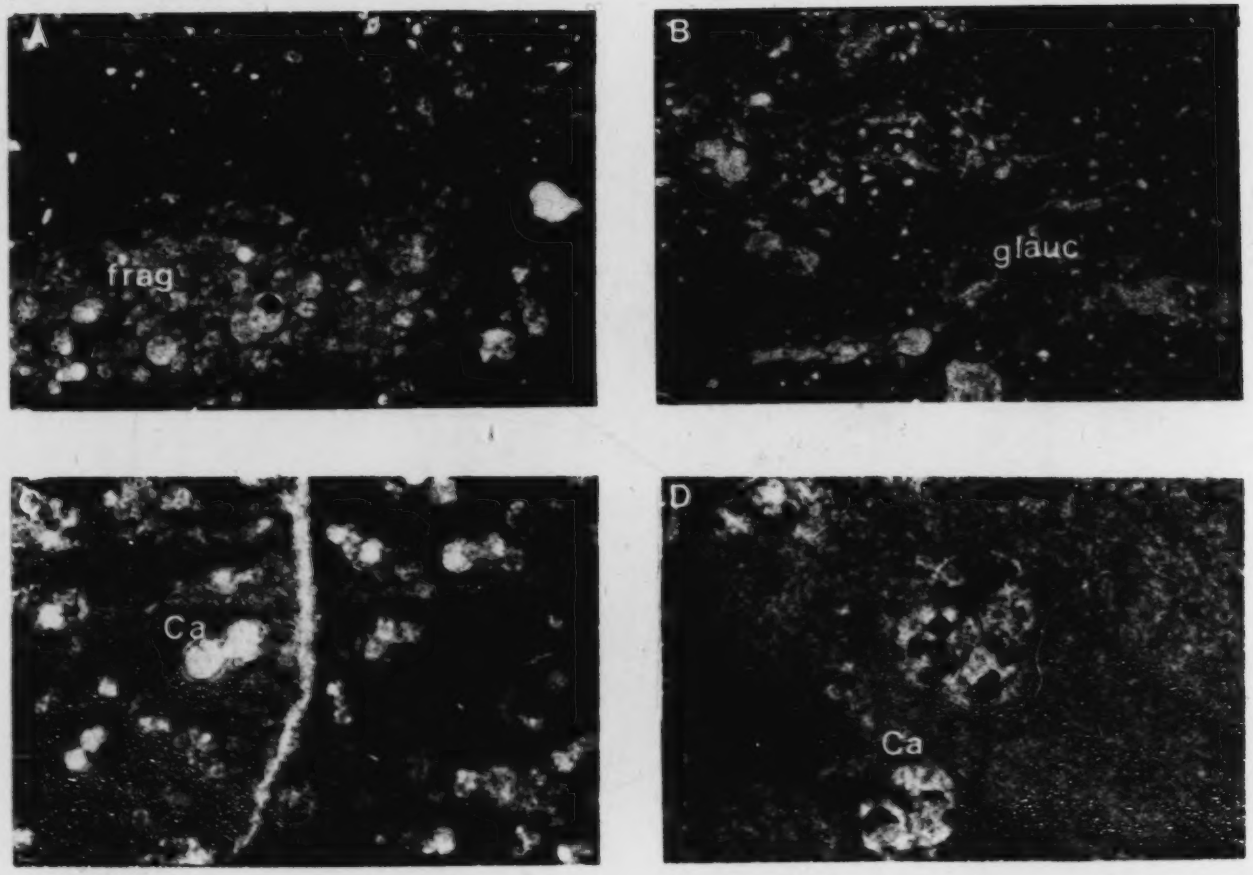
A
frag
B
glauc
C
Ca
D
Ca

are consistent at approximately 3mm long by 1.5 mm wide and indicate some degree of preferred orientation. Fine clay and silt occur adjacent to rock fragments and serve to consolidate the fragments.

The lithoclastic facies is distributed differently between outer shelf wells. At Triumph, closer to the upper slope, the lithoclastic facies occurs interbedded with silty units to a depth of approximately 1590.9 mbmsl (5220 ft.). Below 1590.9 mbmsl, this facies occurs infrequently. Farther shoreward at Glenelg, however, the lithoclastic facies is seldom observed and is not of major significance. This facies suggests higher energy conditions related to: (i) previous shedding of debris off the paleo-shelf during infilling of the outer shelf and/or (ii) erosion of the upper shelf during a recent, relative low stand in sealevel.

At Triumph, microfossils in lithoclasts of calcareous mudstone are filled with secondary calcite. It is uncertain whether secondary calcite present in these fossils represents a pre-erosional precipitate.

The graywacke facies consists of a coarse silty to very fine sandy rock-type with abundant matrix (Dott, 1964), occurring: (i) interbedded with mudstones, upsection at Glenelg and (ii) downsection from the lithoclastic facies at Triumph. At Glenelg, the graywacke facies becomes very sandy in isolated intervals. At Triumph, this facies is scarce and interbedded with the mudstone facies.

The graywacke facies contains primarily coarse silt to very fine sand-size quartz with lesser quantities of plagioclase, K-feldspar and microfossils in varying degrees of preservation, in a mud matrix. Coarse detritus does not exhibit grain corrosion, overgrowth or stress breakage. Exceptions occur in the lower section at Glenelg where minor etching and pitting of K-feldspar and plagioclase have occurred. In some samples, thin beds of glauconite occur containing concentric grains with a radiating internal structure (Plates 2.1b, 2.2a); the glauconite usually occurs only in isolated laminae.

Throughout Upper Cretaceous and Tertiary sections at Glenelg and Triumph, a silty mudstone facies occurs. It is most commonly interbedded with the graywackes facies in mid to lower portions of each section. Silt-size quartz and minor feldspar grains float in a matrix of detrital and authigenic clays. The pervasive occurrence of silty particles results in the absence of any extremely fine-grained lithologies such as claystones. A lack of diagenetic alteration including etching and pitting suggests that decreases in abundance of coarser constituents

PLATE 2.2. BACKSCATTERED ELECTRON SEM MICROGRAPHS

Plate 2.2a: Backscattered electron SEM micrograph of radiating glauconite grains in mudstone. Two levels of glauconite brightness suggest variation in the mean atomic number of each sample. Glenelg J-48, 1880 mbmsl, (see scale).

Plate 2.2b: Backscattered SEM micrograph of subparallel fabric in mudrock. Fossil fragments and platy illitic minerals are weakly oriented. A cluster of framboidal pyrite infills microporosity which has been deformed in response to compaction. Glenelg J-48, 1100 mbmsl, (see scale).

Plate 2.2c Backscattered electron SEM micrograph of calcareous mudstone. Very fine-grained, silt-size pieces of calcite and fossil debris comprise the matrix of calcareous mudstone (confirmed by EDA). Shubenacadie H-100, 3305 mbmsl, (see scale).

Plate 2.2d Backscattered electron SEM micrograph of microfossil tests partly filled with calcite (confirmed by EDA). Matrix contains a minor component of illite/smectite with kaolinite. Shubenacadie H-100, 3305 mbmsl, (see scale).

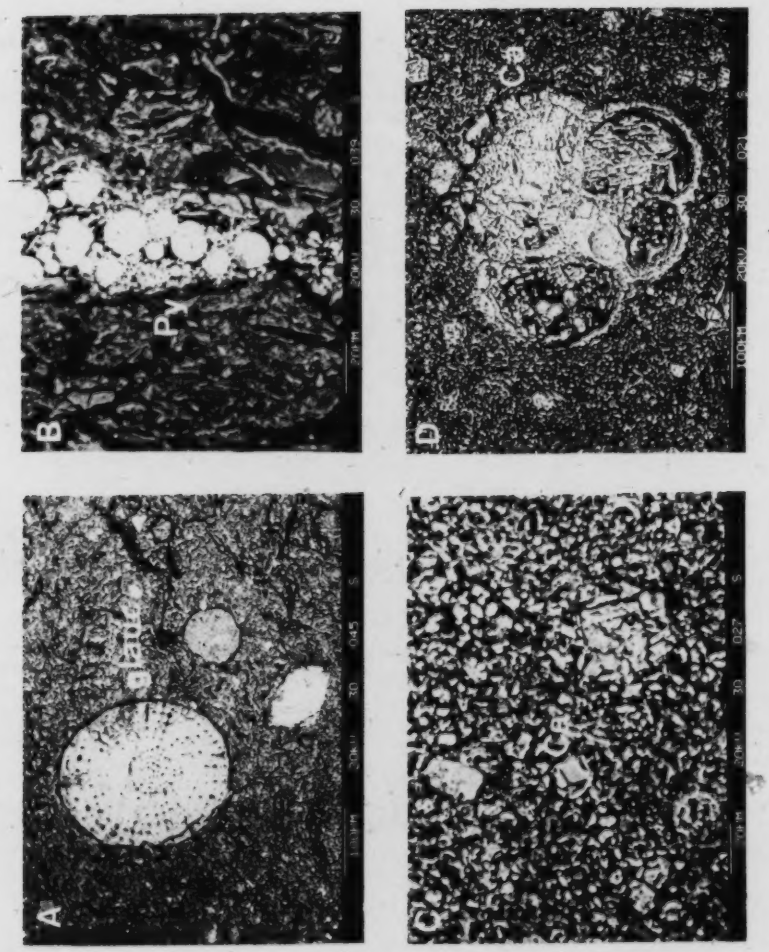
A
B
Pv
C
D

downsection is due to transition into deeper water facies containing less coarse detritus, rather than diagenetic dissolution or disaggregation. Microfauna tests are present in mudstones from each outer shelf sequence.

The calcareous mudstone facies occurs in the lower section of both shelf wells. At Triumph, its first occurrence is approximately 200 - 300 meters below its occurrence at Glenelg. This facies is characterized by abundant foram tests situated in a muddy, grey carbonate-rich matrix containing numerous small grains of calcite. The occurrence of calcareous mudstones and depletion of coarse silicate material suggest deposition in a deep water environment. Micropaleontological and palynological studies also indicate an open marine deposition for these mudstones (pers. comm., F. Brillo).

Fine clastic-rock fabrics from the Nova Scotia shelf were examined by a variety of petrographic techniques. Most samples from Glenelg and Triumph are considered to be soft as indicated by gouging during polishing of thin sections. As well, some samples are fractured by various processes. Subparallel fracture sets oriented perpendicular to the axis of the SWC are attributed to impact during acquisition by the sidewall coring gun. Polygonal fracture sets in thin section are associated with preparation techniques resulting from shrinkage of hydrated clays due to desiccation. However, minor fractures in the calcareous mudstones (i.e., brittle in handspecimen) are filled with secondary calcite (Plate 2.1c). As well, most samples do not exhibit well developed laminations and are not fissile.

As discussed earlier, some mudrocks throughout the sections from Glenelg and Triumph are silty. Preferred optical extinction of platy minerals suggests that certain intervals are characterized by grain alignment (Nuhfer et al., 1981). At Triumph, platy mineral alignment is not widely observed until a depth of roughly 1600 mbmsl (5250 ft.). Below this depth, most samples exhibit strong parallel alignment. However, at Glenelg, grain alignment is observed at a shallower depth of approximately 1100 mbmsl. Apparently some 500 meters of present burial separates levels at which platy mineral alignment is observed.

SEM images from Glenelg indicate that below 1100 mbmsl, a platy subparallel fabric has developed (Plate 2.2b, 2.3a), continuing downsection to TD. Secondary electron images from Glenelg also suggest burial deformation of fine micaceous clay (Plate 2.3b). At 1050 mbmsl and above, no alignment of detrital grains or platy minerals is observed, despite the absence of bioturbation.

PLATE 2.3. SECONDARY ELECTRON SEM MICROGRAPHS

Plate 2.3a: Secondary electron SEM micrograph of subparallel compaction fabric. Deformed clay is illitic in composition as determined by EDA and is wrapped around silt-size calcite particles. Glenelg J-48, 1865 mbmsl, (see scale).

Plate 2.3b: Secondary electron SEM micrograph close-up of compacted, highly illitic, mixed-layer clay (confirmed by EDA). Glenelg J-48, 1865 mbmsl, (see scale).

Plate 2.3c: Secondary electron SEM micrograph of coarse fossil debris little affected by compaction and breakage. Glenelg J-48, 469 mbmsl, (see scale).

Plate 2.3d Secondary electron SEM micrograph of fossil debris which has undergone mechanical degradation during burial. Glenelg J-48, 525 mbmsl, (see scale).

Plate 2.3e Secondary electron SEM micrograph of mudstone. Illitic clay flakes exhibit poorly oriented fabric despite present depth of burial. Unaltered K-feldspar is situated in matrix (confirmed by EDA). Shubenacadie H-100, 3410 mbmsl, (see scale)

Plate 2.3f Secondary electron SEM micrograph of mudstone. Unlike Plate 2.3e, illitic flakes exhibit subparallel microfabric and ductile wrapping around a coarser quartz grain. Shubenacadie H-100, 3900 mbmsl, (see scale).

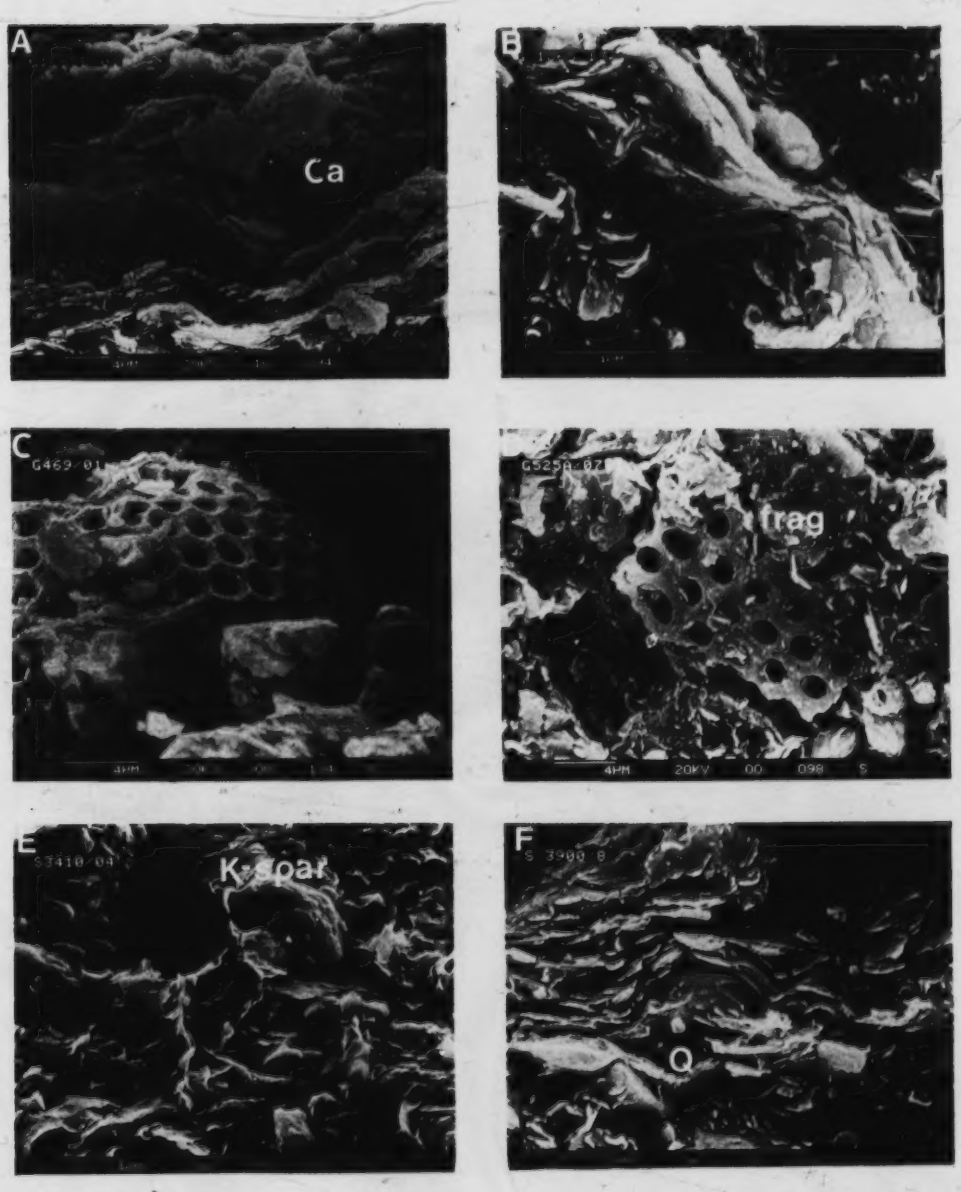
A
Ca
B
C
G469-01
G525B-07
frag
4MM 20KV 00 098 S
E
S3410-04
K-spar
F
S 3900 8
Q

The occurrence of zones of platy mineral alignment is partially independent of lithology. Graywackes occur both above and within regions of grain alignment, although graywackes are absent deeper in the section. In zones of platy mineral alignment, coarse grains in graywackes may also reflect some degree of preferred orientation. In contrast, Gibson (1966) found, through examination of more highly compacted sequences, that coarser grain sizes often inhibited development of preferred orientation in platy minerals.

The mechanical integrity of fossils provides additional insight into the compaction of these fine-grained clastic rocks. In many samples, coarse microfossils are broken and mechanically degraded at relatively shallow depths of burial (i.e., 400 - 600 mbmsl). At the top of the section at Glenelg, coarse fossil debris is observed which becomes progressively indurated downsection until the debris is absent in the lower section (Plates 2.3c, 2.3d). At Glenelg, large microfauna are sparse compared with Triumph, except in association with the calcareous Wyandot mudstone (Plate 2.1d). However very small microfauna are intact, with only minor secondary calcite infilling.

In contrast, coarse microfauna from Triumph are largely intact without evidence of corrosion or breakage. Intraskeletal porosity can be open or partly filled with secondary calcite. Relative to Glenelg, coarse and intact fossil material presently exists at significant burial depths. Triumph may represent a lesser degree of compaction relative to Glenelg.

PETROGRAPHY - LOWER SLOPE

Petrographic examination of the lower slope was conducted on sidewall core (SWC) and ditch cutting subsamples from Shubenacadie. A coarse-grained trend of interbedded graywackes and mudstones occurs in the upper section at Shubenacadie (2100 - 3050 mbmsl). Underlying the coarser trend, a finer-grained trend consisting of interbedded mudstones and calcareous mudstones is observed lying between 3050 mbmsl and TD. However, the lithoclastic facies has not been recognised throughout this slope sequence.

In the upper trend, graywackes contain fine sand-size grains of quartz, with lesser quantities of K-feldspar and plagioclase floating in a matrix of detrital and authigenic clay. Coarser grains were apparently not affected by corrosion or overgrowth. Downsection toward 2800 mbmsl, graywackes occur less frequently as mudstone predominates.

Occurring in both petrographic trends, a mudstone facies containing detrital and transformed clays comprises most of the lower slope section at Shubenacadie. Mudstones are

massively bedded and contain sparse silt-size quartz grains and intact microfossils. K-feldspar and plagioclase are only minor constituents of this facies. Infrequently, primary sedimentary laminations in mudstones are highlighted by lineations of fossil debris (Plate 2.4a). As on the shelf at Triumph, fossil tests in mudstones are frequently open or only partly filled with secondary calcite. As well, differential filling of fossils can be observed at Shubenacadie (Plates 2.4b, 2.4c).

In the lower trend, calcareous mudstones occur, interbedded with mudstones downsection below 3050 mbmsl (Miocene/Eocene marker). This trend is consistent with a transition into deeper water depositional conditions as has been determined for Shubenacadie using micropaleontology and palynology (pers. comm., F. Brillo). The calcareous mudstones are characterized by a massive matrix consisting of abundant silt-sized calcite fragments (Plate 2.2c). As well, calcareous mudstones from the lower slope contain numerous microfossils which are incompletely filled with secondary calcite, in contrast to calcareous mudstones from the outer shelf. Incomplete calcite infilling possibly is a response to inhibition of fluid flow throughout the sedimentary sequence in response to undercompaction and high fluid pressures.

When considering fine clastic-rock fabric on the lower slope, SWC subsamples from Shubenacadie were examined by light microscopy and combined backscattered/secondary electron SEM imagery. Considerable gouging and scratching suggest that samples from Shubenacadie are soft. Extreme sample softness correlates with undercompacted zones determined petrophysically.

In the upper trend, primary depositional laminations are highlighted by lenses of fossil debris. As well, the upper section is considerably coarser-grained compared to the lower trend. In contrast to the outer shelf, thin sections and backscattered electron images generally do not reveal strong preferred orientation of platy and coarse grains. However, as graywackes disappear toward the lower part of the upper petrographic trend, subparallel orientation (parallel extinction) of platy minerals occurs in some mudstones. A lack of preferred clay orientation upsection, in association with coarser-grained lithologies, agrees with Gibson (1966) and Nuhfer et al. (1981), who observed that platy minerals in the matrices of coarser lithologies are often poorly aligned.

Microfossils are mostly intact, being open or partly filled with secondary calcite. Unlike the outer shelf, intraskeletal porosity is infilled with secondary calcite to a much lesser degree.

PLATE 2.4. THIN SECTION MICROGRAPHS

Plate 2.4a: Thin section micrograph of fossiliferous mudstone. Laminations within mudstone are highlighted by scattered fossil debris. As well, intraskeletal porosity is open. Shubenacadie H-100, 3125 mbmsl, 2.5X objective.

Plate 2.4b: Thin section micrograph of intraskeletal porosity in mudstone. Fossils are intact and differentially filled . Secondary calcite completely fills several chambers. Shubenacadie H-100, 3650.3 mbmsl, 40X objective.

Plate 2.4c: Thin section micrograph of open intraskeletal porosity situated in deeply buried mudstone. This mudstone lies within an undercompacted unit. Shubenacadie H-100, 3650.3 mbmsl, 40X objective.

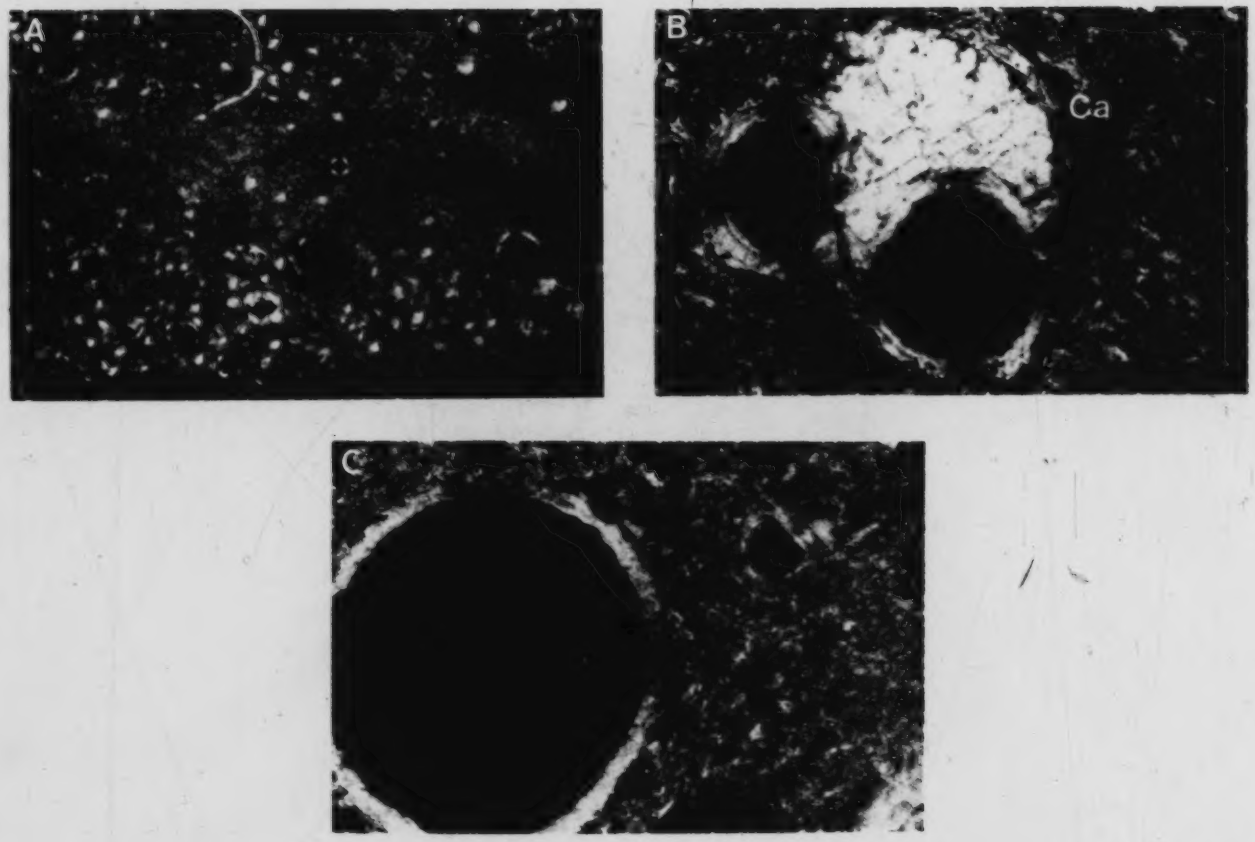
A
B
Ca
C

Below 3050 mbmsl in the lower petrographic trend, sample material appears to be very soft. Mudstones in the lower trend are massively bedded, with a disorganised microfabric (i.e., no preferred orientation/extinction). Microfossils situated in the lower petrographic trend generally are intact without suggestion of significant crushing or mechanical breakage. As well, they are generally empty or only partly filled with secondary calcite (Plate 2.2d).

Within the lower mudstone facies, grains of aggregated clay occur deeper in the section. These grain aggregates may represent flocculated clay. According to O'Brien (1970), the presence of flocculated clay may suggest an appreciable sediment supply and/or marine salinity at the time of original deposition.

Below 3600 mbmsl, thin section micrographs exhibit strong preferred orientation of platy minerals, as determined by parallel extinction under cross polarized light. Secondary electron images reveal platy grains to be poorly aligned at 3410 mbmsl in contrast to well aligned detrital flakes at 3900 mbmsl (Plate 2.3e, 2.3f). At 3900, platy grains exhibit compaction and deformation around detrital grains. Unlike shallower intervals, more deeply buried sections at Shubenacadie appear to be more highly compacted as suggested by increasing fabric orientation.

D. DISCUSSION OF COMPACTIONAL STYLE

The evolution of the Nova Scotia passive margin has been described using a classical rift/drift model of tensional tectonism, active from the Jurassic until present. Throughout this time, a compressive phase is not indicated.

Prior to deposition of the sections at Glenelg, Triumph, Acadia and Shubenacadie (Late Cretaceous and Tertiary time), Early Cretaceous tectonics were characterized by diminishing thermal subsidence in response to crustal cooling. By Late Cretaceous time, progressive sedimentation *dominated over* weakening thermal subsidence, resulting in steady infilling of the passive margin. This resulted in the deposition of regressive sequences on the outer shelf and slope. Petrographic and paleontologic/palynologic trends agree with progressive shallowing trends upsection at Glenelg and Shubenacadie.

During progressive sedimentation on the outer shelf and slope, fine-grained clastic sediments accumulated. The sections situated on the slope may have resulted partly from mass movement off the outer shelf (Stow, 1977). Observation of thinly laminated mudstones on the

lower slope, enhanced by fossil tests, also suggests down slope debris-movement.

In such a tectonic setting, progressive sedimentation during Late Cretaceous and Tertiary time resulted in fine-grained rock sequences of several thousand meters thickness on the outer shelf and slope. During early burial (tens' of meters), original fluid contents were likely between 60% - 80% of total sediment volume (Richards and Keller, 1962; Meade, 1966).

Depending on the rock type concerned, dewatering could have proceeded at different rates. For example, at shallow burial depths, slightly coarser mudrocks having a lower original fluid content and a coarser grain size, may have dewatered more completely compared to very porous, but poorly ordered mudstones (Meade, 1966). Similarly, Heling (1970) considered calcareous mudstones to compact more readily than non-calcareous mudstones. Although the permeabilites of fine-grained rocks were not tested, reduced porosity and increased compaction may have established weak seals associated with these units.

For mudstones which comprise the majority of each sequence examined, Meade (1966) described various parameters which can influence sediment compaction (i.e., grain size, salinity, deposition rates, clay composition). However sediments deposited under relatively uniform conditions (i.e., marine) generally undergo exponential porosity reduction with burial.

As sediment was compacted under increased burial load, imperfect dewatering could have resulted in localized lenses of fluid entrapment associated with the development of hydrodynamic seals. Such zones would be characterized by slightly higher porosities relative to adjacent, normally compacting sediments.

Considering concepts outlined above, an evaluation of the compaction of fine-grained rocks from offshore-Nova Scotia follows. From previous observations, fine-grained Upper Cretaceous and Tertiary clastic rocks generally were not highly compacted subsequent to deposition under marine conditions. These rocks generally exhibit an *immature style* of compaction and fabric development characterized by the existence of: (i) shallow, uncompacted mud sequences, (ii) significant zones of undercompaction, (iii) a lack of preferred, platy mineral orientation (except at depth) and (iv) a lack of extensive fracturing or detrital grain shearing.

Both slope sequences from offshore-Nova Scotia appear to have undergone only minor compaction. On the lower slope at Shubenacadie, some 2800 meters of fine-grained sediment has been deposited since Early Cretaceous time comprising two separate petrographic and

petrophysical trends. These fine-grained clastic sediments exhibit an immature style of compaction, despite present-day sediment thicknesses.

As previously mentioned, some 650 meters of unconsolidated mud lies below seafloor at Shubenacadie. Underlying this uncompacted sediment, progressive porosity-reduction is implied by a steady decrease in Δt. Petrophysical evaluation of porosity reduction with burial reveals that fine-grained clastic rocks from Shubenacadie contain numerous, sometimes extreme, units of undercompaction with respect to a normal, statistically-defined trend.

Upsection, petrophysical study implies that weak undercompaction exists relative to a normal compaction trend. Possibly, hydrodynamic seals are associated with slightly coarser clastic units (i.e., low permeability). However, the most intense undercompaction, relative to adjacent mudrocks, occurs in the lower compaction/petrographic trend. Undercompaction occurs here despite higher, overall compaction relative to the upper trend. Undercompaction is most extreme from 3300 to 3600 mbmsl in poorly oriented mudstones associated with calcareous mudstones. As calcareous mudstones may be expected to compact more quickly than normal mudstones (Heling, 1970), hydrodynamic seals may have formed inhibiting vertical migration of pore-fluid as predicted by Magara (1976a). However, the permeability of mudrocks is difficult to determine petrophysically (Schlumberger Log Interpretation Principles, 1970), and no permeability tests were conducted on samples taken.

Petrophysical estimates of weak compaction are corroborated by qualitative petrographic observations. In the lower section at Shubenacadie, platy and coarse minerals generally are not aligned through intervals that are relatively undercompacted (Gibson, 1966). However Heling (1970), O'Brien (1970) and Curtis et al. (1980) have considered alignment of platy minerals in muddy sediments to result from compaction strain during shallow burial (i.e., several hundred meters). A comparison of micrographs presented by O'Brien (1970) and Curtis et al. (1980) with samples from intervals of intense undercompaction at Shubenacadie indicates that a lack of preferred orientation in clay-rich mudrocks contrasts with *expectations after several thousand meters of burial*. Further, the presence of numerous unbroken fossil tests, throughout the top of the lower trend at Shubenacadie, implies that sediment load *upon individual grains* was not sufficient to cause breakage. As well, fossil tests generally were not filled with secondary calcite, suggesting that widespread circulation of fluids has not affected these mudrocks. Inhibition of fluid circulation may be associated with high fluid pressures due

to sediment undercompaction.

Upsection, petrophysical detection of weak undercompaction is also corroborated petrographically. Unlike the lower section, the graywacke/mudstone trend exhibits varying degrees of preferred orientation associated with coarse and platy grains suggesting some degree of compaction (Meade, 1966). Further, certain elongated detrital micas suggest early deformation upon burial. However, the degree of compaction is still weak as revealed by: (i) fossil tests containing very little secondary calcite and (ii) a higher overall porosity suggested by a slower interval velocity (Δt).

Although no petrographic evaluation of Acadia was performed, petrophysical evidence indicates that undercompaction at Acadia is more extreme than at Shubenacadie. Much of the upper section from seafloor to approximately 1780 mbmsl is essentially uncompacted as indicated by: (i) extreme sample softness and friability, (ii) considerable borehole instability associated with a lack of consolidation and (iii) very slow Δt at shallow depths where the borehole was stable. Below the interval of hole caving, a normal compaction trend is recognised. The presence of numerous undercompacted lenses suggests a lack of compaction despite considerable burial thicknesses. Further, interbedded mudstones and calcareous mudstones downsection may have established a similar zone of low permeability as at Shubenacadie.

Examination of geothermal gradients from each slope sequence provides additional substantiation of compaction trends. Both Acadia and Shubenacadie are characterized by two-component geothermal gradients. The upper, less consolidated material is associated with a low geothermal gradient of 23°C/km for both Acadia and Shubenacadie. Suppression of geothermal gradients may be a function of greater heat capacity in response to higher, fluid-filled porosity (Zierfuss, 1969).

However hotter gradients of 42° and 57°C/km are measured downsection at Acadia and Shubenacadie, respectively. While these gradients appear to be abnormally warm, higher gradients may be due to: (i) greater compaction (i.e., less fluid-filled porosity), (ii) the insulation effect of an overlying blanket of fluid-saturated sediment, (iii) a higher carbonate content associated with calcareous mudstones and (iv) higher regional heat flow along this part of the margin (Reiter and Jessop, 1985). According to Zierfuss (1969), limestones have a fairly high heat conductivity allowing for shallower geothermal gradients.

The entire section at Acadia lies within the cooler gradient, resulting in a maximum burial temperature of approximately 43°C at 2640 mbmsl. At Shubenacadie, the upper petrographic and petrophysical trend, above 3050 mbmsl, lies within the cooler gradient and is characterized by cooler temperatures reaching 37°C. However the lower section is characterized by: (i) greater net compaction and (ii) carbonate stringers (high heat conductivity). The resulting gradient gives a maximum burial temperature of approximately 100°C at TD.

On the outer shelf, two different styles of compaction are recognised at Glenelg and Triumph. Although petrophysical compaction could not be evaluated at Triumph, petrography reveals that Triumph has not been subjected to extreme compaction. Unbroken fossil tests, partly filled with secondary calcite, and a lack of platy mineral alignment until roughly 1600 mbmsl burial (5220 ft) suggests that minimal sediment compaction has occurred. However a lack of petrophysical evidence does not permit estimation of whether any section was removed by erosion or whether extensive undercompaction exists.

The petrographic style at Triumph is similar to the upper section at Shubenacadie and the shallowest section at Glenelg. However Glenelg differs in its style of compaction. Examination of petrophysical compaction at Glenelg reveals a somewhat "normal" compaction trend containing few undercompacted zones, each of low intensity, from a normal compaction trend. Glenelg exhibits a greater degree of compaction as suggested by: (i) alignment of platy minerals at shallower depths, (ii) occurrence of abundant, broken fossil debris and (iii) a significantly lower, overall at than equivalent depths on the slope (Nafe and Drake, 1957). As mentioned previously, orientation of platy minerals occurs 400 - 500 meters above the level of similar orientation at Triumph. As well, the level of first major calcareous mudstone occurrence is roughly 200 - 250 meters above the same event at Triumph. These data suggest that Glenelg may have experienced between 250 to 800 meters of erosion (i.e., approximately 600 m) in agreement with petrophysical data.

The occurrence of erosion may be due to Glenelg's position relative to potential growth faults or to a recent low stand in sea level. As Triumph is located farther oceanward, that section may be downdropped relative to Glenelg and subsequently filled by sediment.

Geothermal gradients determined by compensated, log-run temperatures for Glenelg and Triumph are in agreement with petrophysical and petrographic observations from the outer shelf. Table 2.2 indicates that the geothermal style at Triumph is similar to styles determined

for both slope sections. The upper part of Triumph's gradient at 29°C/km is cool, relative to the lower component. However the upper gradient is hotter than those determined for shallow sections at Shubenacadie and Acadia. As at Acadia, the entire sequence examined at Triumph lies within the upper gradient resulting in a maximum, present burial temperature of approximately 67°C.

In contrast, Glenelg's geothermal gradient of 29°C/km is consistent throughout showing no indication of multiple components. This gradient also suggests a similar degree of compaction (i.e., similar fluid-filled porosity) with Triumph (Zierfuss, 1969). Using the above gradient, maximum present burial temperatures for Glenelg may reach 65°C. However, by including 300 - 800 meters of additional sediment possibly eroded from the top of the section, estimates of maximum burial temperature can be elevated from 65°C to between 74° and 87°C (i.e., 81°C estimating 600 m erosion). In this way, a greater degree of compaction may result in higher estimates of geothermal gradient and lower estimates of undercompaction (i.e., overpressure).

E. SUMMARY OF COMPACTION AND FABRIC STUDY

1. Fine-grained, Upper Cretaceous and Tertiary rocks from offshore-Nova Scotia exhibit an immature style of compaction. Such behavior is suggested by:
   a. The existence of significant thicknesses of uncompacted sediment at Acadia and Shubenacadie;
   b. The occurrence of weakly compacted sediment and zones of undercompaction at Triumph, Acadia and Shubenacadie (i.e., above 3600 mbmsl);
   c. The measurement of very low geothermal gradients in association with shallow petrophysical and/or petrographic trends at Acadia and Shubenacadie (i.e., above 3600 mbmsl);
   d. The observation of intact microfossils and coarse detrital grains;
   e. The existence of random grain orientation in shallow sections at Glenelg, Triumph and Shubenacadie.
2. Undercompaction and weak overpressure may have developed in certain shallowly buried mudstone sequences where hydrodynamic barriers formed in response to preferred

compaction of slightly coarser clastic units (i.e., silty mudrocks) or calcareous mudstones. As a result, these sequences were probably not open to extensive fluid movement. Pore-fluids likely contain a large constituent of original marine waters.

3. Geothermal gradients developed on offshore-Nova Scotia are strongly influenced by the degree of compaction in a sequence:
   a. Acadia exhibits a cool, estimated maximum burial temperature (43°C) at depth in agreement with a lower degree of compaction and a shallow maximum burial depth (i.e., 2000 m);
   b. Triumph exhibits a warm gradient as at Glenelg, but may not have experienced higher temperatures if erosion has not not affected this section to the same extent as at Glenelg;
   c. Glenelg and Shubenacadie (below 3600 mbmsl) exhibit warm estimated maximum burial temperatures (80° - 100°C) associated with: (i) a greater degree of compaction, (ii) greater estimated maximum burial depth (2500 - 2700 m) and (iii) higher heat flow throughout this region.
4. Petrophysical determination of: (i) relative trends in porosity reduction with burial and (ii) geothermal gradients, provide regionally useful information for assessing compaction histories. Petrographic examinations of fine-grained rock fabric can be used to substantiate petrophysical trends.

F. BIBLIOGRAPHY

Athy, L.F., 1930, Density, porosity, and compaction of sediments: Am. Assoc. Petroleum Geologists Bull., v. 14, p. 1-35.

Curtis, C.D., Lipshie, S.R., Oertel, G. and Pearson, M.J., 1980, Clay orientation in some Upper Carboniferous mudrocks, its relationship to quartz content and some inferences about fissility, porosity and compactional history: Sedimentology, v. 27, p. 333-339.

Dott, R.H., 1964, Wacke, graywacke and matrix - what approach to immature sandstone classification: Jour. Sedimentary Petrology, v. 34, p. 625-632.

Gibson, M., Jr., 1966, A study of the relations of depth, porosity and clay mineral orientation in Pennsylvanian shales: Jour. Sedimentary Petrology, v. 36, p. 888-903.

Gillott, J.E., 1969, Study of the fabric of fine-grained sediments with the scanning electron microscope: Jour. Sedimentary Petrology, v. 39, p. 90-105.

Hackbarth, D.A., 1978, Application of the drill-stem test to hydrogeology: Groundwater, v. 16, p. 5-11.

Hall, M.G. and Lloyd, G.E., 1981, The SEM examination of geological samples with a semiconductor back-scattered electron detector: Am. Mineralogist, v. 66, p. 362-368.

Hedberg, H.D., 1936, Gravitational compaction of clays and shales: Am. Jour. Science, v. 31, p. 241-287.

Heinrich, K.F.J., 1981, Electron Beam X-ray Microanalysis: Van Nostrand Reinhold Company, New York, N.Y., 578 pp.

Heling, D., 1970, Micro-fabrics of shales and their rearrangment by compaction: Sedimentology, v. 15, p. 247-260.

Kaarsberg, E.A., 1959, Introductory studies of natural and artificial argillaceous aggregates by sound and x-ray diffraction methods: Jour. Geology, v. 67, p. 447-472.

Krinsley, D.H., Pye, K. and Kearsley, A.T., 1983, Application of backscattered electron microscopy in shale petrology: Geol. Magazine, v. 120, p. 109-114.

McIver, N.L., 1972, Cenozoic and Mesozoic stratigraphy of the Nova Scotian shelf: Can. Jour. Earth Sciences, v. 9, p. 54-70.

Magara, K., 1976a, Water expulsion from clastic sediments during compaction - directions and volumes: Am. Assoc. Petroleum Geologists Bull., v. 60, p. 543-553.

Magara, K., 1976b, Thickness of removed sedimentary rocks, geopore pressure, and paleotemperature, southwestern part of Western Canada basin: Am. Assoc. Petroleum Geologists Bull., v. 60, p. 544-565.

Meade, R.H., 1966, Factors influencing the early stages of the compaction of clays and sands - review: Jour. Sedimentary Petrology, v. 36, p. 1085-1101.

Nafe, J.E. and Drake, C.L., 1957, Variation with depth in shallow and deep water marine sediments of porosity, density and the velocities of compressional and shear waves: Geophysics, v. 22, p. 523-552.

Nuhfer, E.B., Vinopal, R.J., Hohn, M.E. and Klanderman, D.S., 1981, Applications of SEM in petrology of mudrocks (results of studies of Devonian mudrocks from West Virginia and Virginia): Scanning Electron Microscopy, 1981/I, p. 625-632.

O'Brien, N.R., 1970, The fabric of shale - an electron microscope study: Sedimentology, v. 15, p. 229-246.

Press, F., 1966, Seismic velocities: *in* S.P. Clark, Jr., ed., Handbook of Physical Constants - Revised Edition, chapter 9, Geol. Soc. America Memoir 97, p. 195-218.

Pye, K. and Krinsley, D.H., 1984, Petrographic examination of sedimentary rocks in the SEM using backscattered electron detectors: Jour. Sedimentary Petrology, v. 54, p. 877-888.

Reiter, M. and Jessop, A.M., 1985, Estimates of terrestrial heat flow in offshore eastern Canada: Can. Jour. Earth Sciences, v. 22, p. 1503-1517.

Richards, A.F. and Keller, G.H., 1962, Water content variability in silty clay core from off Nova Scotia: Limnology and Oceanography, v. 7, p. 426-427.

Schlumberger Log Interpretation, Volume 1 - Principles, 1972, Schlumberger Limited, New York, N.Y., 113 pp.

Stow, D.A.V., 1976, Deep water sands and silts on the Nova Scotian continental margin: Maritime Sediments, v. 12, p. 81-90.

White, S.H., Shaw, H.F. and Huggett, J.M., 1984, The use of back-scattered electron imaging for the petrographic study of sandstones and shales: Jour. Sedimentary Petrology, v. 54, p. 487-494.

Wyllie, M.R.J., Gregory, A.R. and Gardner, I.W., 1956, Elastic wave velocities in heterogeneous and porous media: Geophysics, v. 21, p. 41-70.

Zierfuss, H., 1969, Heat conductivity of some carbonate rocks and clayey sandstones: Am. Assoc. Petroleum Geologists Bull., v. 53, p. 251-260.

III. MINERALOGY AND GEOCHEMISTRY

A. INTRODUCTION

Trends in mineralogy and geochemistry of certain detrital, transformed and authigenic phases provide information concerning the nature of chemical diagenesis during burial of fine-grained clastic rocks from the Nova Scotia shelf and slope. Such information includes: (i) the chemical composition of fluids involved in diagenesis, (ii) the evolution of pore-fluids with burial and (iii) the manner in which particular stratigraphic sections have been affected by organic and inorganic diagenetic reactions.

To evaluate changes in mineralogy and geochemistry with burial, samples were selected from Glenelg, Triumph, Acadia and Shubenacadie (Table 3.1). Samples were examined by: (i) thin section and scanning electron microscopy (SEM), (ii) x-ray diffraction (XRD), (iii) inductively coupled, plasma emission spectrography (ICP), (iv) x-ray microanalysis (EDA) and (v) light stable isotope analysis.

B. METHODOLOGY

PETROGRAPHIC EXAMINATION

Techniques of petrography were discussed in Chapter 2. Petrographic samples used for fabric analyses were examined during the present investigation to evaluate: (i) alteration of detrital constituents (i.e., corrosion, formation of overgrowths) and (ii) the character of authigenic minerals.

XRD ANALYSIS

Samples from each sequence were initially prepared for whole rock XRD analysis to evaluate trends in mineralogy. Sample material consisted of ditch cuttings which were prewashed and wet sieved to remove excess drilling fluid by Shell Canada Resources. All cuttings were then examined under a binocular microscope to evaluate residual drilling fluid contamination. While most samples were found to be relatively clean, any remaining drilling fluid contaminant was removed manually.

TABLE 3.1. SAMPLES INVESTIGATED

SAMPLE NUMBER	ROCK TYPE	DEPTH mbmsl	THIN SECTION	SIZE-FRACTION FOR XRD				ELEMENTAL ANALYSIS	ISOTOPE ANALYSIS	SEM
				finest fraction	<0.2 μm	0.2 - 2.0 μm	Whole Rock			
GLENELG J-48										
G460	Qw	460.0	X	<0.2	X	X	X			
G580	Qw	580.0	X				X			X
G820	Md	820.0	X	<0.2	X	X	X		X	
G1100	Md	1100.0	X	<0.2	X	X	X		X	X
G1290	Qw	1290.0	X	<0.05	X	X	X		X	
G1480	clc Md	1480.0	X	<0.05	X	X	X	carb	X	X
G1630	clc Md	1630.0	X	<0.05	X	X	X	carb	X	
G1865	Md	1865.0	X	<0.05	X	X	X		X	X
G2080	clc Md	2080.0		<0.05			X		X	
TRIUMPH P-50										
T1590	Lithic	484.6		<0.1			X			
T2845	Lithic	867.1	X	<0.1			X		X	
T4220	Lithic	1286.2	X	<0.1			X		X	
T5160	Md	1572.7	X	<0.1			X		X	
T5670	clc Md	1728.1	X	<0.1			X		X	
T5930	clc Md	1807.4	X	<0.1			X		X	
T7080	Md	2157.9		<0.1			X		X	

TABLE 3.1. CONTINUED

SAMPLE NUMBER	ROCK TYPE	DEPTH mbmsl	THIN SECTION	SIZE-FRACTION FOR XRD				ELEMENTAL ANALYSIS	ISOTOPE ANALYSIS	SEM
				finest fraction	<0.2 μm	0.2 - 2.0 μm	Whole Rock			
ACADIA K-62										
A1270	Qw	1270.0		<0.2	X	X	X			
A1600	Md	1600.0		<0.2	X	X	X			
A2010	Md	2010.0		<0.2	X	X	X			
A2304	Md	2304.0		<0.2	X	X	X		X	
A2640	clc Md	2640.0		<0.2	X	X	X		X	
SHUBENACADIE H-100										
S2165	Qw	2165.0		<0.1	X	X	X	clay		
S2675	Qw	2675.0	X	<0.1	X	X	X	clay		X
S3140	Md	3140.0	X	<0.1	X	X	X	clay	X	X
S3660	clc Md	3660.0	X	<0.1	X	X	X	clay,carb	X	X
S3785	clc Md	3785.0	X	<0.1				clay, carb	X	
S3910	Md	3910.0	X	<0.1	X	X	X	clay, carb	X	X
S4040	Md	4040.0	X	<0.1				clay	X	
S4165	Md	4165.0	X	<0.1	X	X	X	clay	X	X

Samples were lightly crushed using a mortar and pestal to reduce fine-grained rock to its original disaggregated grain size. A portion of whole rock sample was taken for XRD examination in random orientation. Samples generaily were scanned over at least 2 - 60 ° 2θ (CoKα radiation).

After whole rock XRD study, clean cuttings were selected for examination of the clay size-fraction. Cuttings were immersed in a 4% Na hexa-metaphosphate solution to disaggregate fine-grained clastic rocks *without grinding*. The resulting mixture was sonified, using a high frequency probe to assist disaggregation. The clay suspension was then poured into settling columns to perform gravitational extraction of the <2.0 μm size-fraction.

After isolating the majority of <2.0 μm clay, this material was treated with bleach in a hot bath for 2 days to: (i) destroy organic matter and (ii) to assist flocculation of clay from suspension. Clean clay-size material was then resuspended for extraction of very fine size-fractions.

During investigation, fine size-fractions were extracted to isolate mixed-layer phases, which might have experienced diagenetic modifications (i.e., illite/smectite). Size-fractions ranging from <0.2 to <0.05 μm were separated by low speed centrifuge using settling times accounting for: (i) angular centrifuge velocity (rpm), (ii) settling distance within test tubes, (iii) ambient temperature and (iv) grain size desired (Jackson, 1961).

A homogeneous slurry from the finest size-fractions was divided into two portions for saturation with K^+ and Ca^{2+}. Samples were repeatedly immersed in saline solutions to obtain effective saturation of interlayer sites with the appropriate cation. As well, coarser size-fractions from Glenelg, Acadia and Shubenacadie were saturated with Ca^{2+}, K^+ and Na^+ (i.e., bleach). Following saturation, samples were washed with distilled water until clean of excess solute.

After freeze-drying, 10 to 20 milligrams of each saturated clay was resuspended in methanol and oriented onto a glass slide. Orientation was required to enhance basal reflections and suppress non-integral reflections permitting easier XRD analysis.

All K^+ saturated clays were scanned from 2 - 22° 2θ under diagnostic conditions. K^+ slides were first heated to 107°C for 24 hours in order to expel interlayer water and collapse swelling clays to their minimum d-spacing. After heating, slides were taken quickly from oven to XRD and scanned at 0% relative humidity (RH) to avoid expansion by atmospheric

moisture. This test is necessary to determine: (i) whether swelling clays are present and (ii) if interlayer sites are propped open by inorganic hydroxy-compounds (x-ray amorphous) as revealed by a low-angle *hump or shoulder* on a 10 Å peak.

After heat treatment, K^+ slides were exposed to 54% RH for at least 48 hours. Slides were scanned at 54% RH to prevent changing interlayer thickness due to non-standard ambient RH. Atmospheric equilibration with a supersaturated solution of $MgNO_3$ maintained 54% RH in the x-ray chamber.

By examining charts of K^+ saturated clay at 54% RH, a qualitative evaluation of the charge density on 2:1 layer silicates can be obtained. The extent to which a shoulder or secondary peak develops on the low-angle side of the 10 Å peak indicates whether layer charge is sufficient to hold the smectite structure closed. If layer-charge density is sufficiently high, K^+ will be held in interlayer sites preventing extensive rehydration under the conditions prescribed above.

After humidity treatments, K^+ slides were heated to 300° and 550°C for 3 and 2 hours respectively. These heat treatments permit reliable identification of: (i) chlorite, (ii) chloritic properties associated with 2:1 layer silicates and (iii) kaolinite.

Ca^{2+} slides were first scanned at 54% RH to expand swelling clays to a standard thickness having two molecular layers of water in interlayer sites. Ca^{2+} saturated clays were then solvated with ethylene glycol and glycerin by exposure to hot vapours as described by Jackson (1961). The 54% RH, ethylene glycol and glycerin treatments permitted detailed identification of swelling clay types (i.e., montmorillonite versus beidellite).

Randomly oriented clay mounts were examined to determine whether 2:1 layer silicates observed are primarily dioctahedral or trioctahedral (Reynolds, 1980). These samples were scanned from 68 - 76° 2θ at a rate of 1/4° 2θ/minute. A lower scan rate was selected to boost signal from a potential, high-angle 2:1 layer peak (060). Samples containing minimal kaolinite were examined to avoid interference from overlapping peaks. However, in samples containing some kaolinite, broadening of a dioctahedral (060) peak toward larger d-spacings was observed.

TECHNIQUES FOR XRD DATA EVALUATION

The relative abundance of various clay phases was *estimated* using peak heights. As most illite appears to be detrital, 10 Å clay is likely of uniform crystallinity.

Form factors used to weight calculations accounting for variations in crystallinity between clay types were obtained from Scafe (pers. comm.) and are indicated as follows:

1. Illite (10 Å) = 1.0
2. Kaolinite (7 Å) = 7 Å peak height/(2.5 x 10 Å peak height)
3. Smectite (17 Å) = 17 Å peak height/(4 x 10 Å peak height)
4. Chlorite (14 Å) = 14 Å peak height/(3 x 10 Å peak height)

Chlorite occurrence inhibits accurate determination of kaolinite using the 7 Å peak. The presence of kaolinite was confirmed by a peak doublet defining the kaolinite (002) and chlorite (004) peaks. To determine the semi-quantitative abundance of kaolinite, the percentage of chlorite was subtracted from the estimated percentage of kaolinite (7 Å) to account for contribution of the chlorite (002) peak to the combined 7 Å peak. All estimates were then normalized to 100 percent.

Coarser clay size-fractions frequently contain significant levels of impurity including quartz and calcite. The abundance of these phases with respect to clay minerals was estimated using calibration diffractograms for oriented <2.0 μm kaolinite and quartz.

Estimates of the degree of smectite/illite interstratification associated with the 10 and 17 Å clay phases have been determined following standard tables of Hower (1981). All determinations were verified using techniques described by Środoń (1980, 1981 and 1984). However, no attempt was made to account for variations in expandability resulting from differential expansion between montmorillonite and beidellite.

CHEMICAL INVESTIGATION

Elemental analyses were performed on certain very fine-grained clay and secondary calcite samples. Analyses determined: (i) the relative abundance of major elements in certain phases and (ii) their changes through the burial sequence. Two independent techniques were used to estimate elemental compositions: (i) inductively coupled, plasma emission spectrography (ICP) and (ii) energy dispersive x-ray microanalysis (EDA) from an SEM.

To perform x-ray microanalysis on clays, NH_4^+ saturated samples were suspended in distilled water and oriented onto glass microprobe slides to a thickness of 30-40 μm. After preparation, the slides were heated to 107°C for 24 hours and stored in a dessicator to minimize interparticulate- and interlayer-water content.

Prior to mounting in the SEM, samples were coated with a thin veneer of carbon to provide suitable conductivity during exposure to the electron beam. After carbon coating, samples remained in a 5 x 10^{-6} torr vacuum overnight to draw out remaining water.

An exitation potential of 20 KeV generated characteristic x-ray energies from the sample. Spectra were collected for 100 seconds at several locations across most samples. A standard, cobalt spectrum was collected after every third unknown spectrum to calibrate beam drift. Data were processed using the Link Systems® ZAF-FLS (fitted least squares) deconvolution program. The results from all spectra for each sample were averaged and standard deviations for each element determined.

As each clay sample was an aggregate of several clay types, accurate determination of formulae for each mineral phase from "% Oxides" was not possible. The final presentation consists of a statistically averaged "Weight % Element" for each element with respect to all elements analysed.

ICP analysis was conducted independently on identical sample material. A minimum mass of 50 mg was consumed during analysis. Samples were dissolved and diluted to obtain the appropriate volume for analysis and corrections made for dilution. The resulting analyses are expressed in parts per million (ppm). Data for each element were converted to "Weight % Element" of elements analysed to facilitate comparison with SEM and U.S.G.S standard data.

Pore-filling, secondary carbonates were examined using polished thin sections. Although shaly samples were difficult to polish because of their softness, uncovered thin sections were prepared for EDA analysis. Using backscattered electron imagery, secondary calcite infillings from Glenelg and Shubenacadie were located. Spectra were collected and processed to determine the relative proportion of major cations in each carbonate cement as described above. Corrections (ZAF) permitted accurate estimation of the apparent concentration of each major cation.

Whole rock samples from each interval at Shubenacadie were examined by ICP analysis. Elemental analyses are required to determine trends in the whole rock distribution of major elements including Si, Al, K, Ca and Fe. Results of whole rock elemental analyses were compared with petrography and bulk XRD.

STABLE ISOTOPE ANALYSIS

Whole rock samples from throughout Glenelg, Triumph, Acadia and Shubenacadie were selected for isotope analysis of carbonate minerals ($\delta^{13}C$; $\delta^{18}O$). Cuttings were examined first to remove contamination from drilling fluids and then lightly crushed in a mortar and pestal. To avoid isotopic contamination from organic materials, cuttings were bleached as described earlier and washed thoroughly.

Samples were examined by XRD prior to and after bleaching to evaluate which carbonate minerals were present and in what proportions. CO_2 was extracted from bleached calcite by reaction with 100% phosphoric acid for 1 hour at 25°C following the method of McCrea (1950).

Once extracted, the isotopic character of evolved CO_2 gasses was compared with CO_2 derived from a standard calcite using a mass spectrometer. Isotopic ratios relative to standard calcite were adjusted to give permill deviations from international standards (i.e., PDB for carbon, Craig, 1957; SMOW for oxygen, Craig, 1961).

C. OBSERVATIONS

WHOLE ROCK XRD DATA

Results of whole rock XRD indicate that fine-grained clastic rocks from the Nova Scotia shelf and slope are quartz-rich. Plagioclase and K-feldspar are present in appreciable quantities in the upper parts of each shelf and slope section (Table 3.2). However, both feldspar types diminish to trace levels in lower parts of most sections. Most feldspar and quartz are detrital and without significant alteration suggesting that depletion in these grains downsection represents transition into deeper depositional environments, rather than mineral dissolution.

Shelf sections generally contain much less clay material than the slope. Shelf clays consist mainly of kaolinite and 10 Å phases. In contrast, the slope contains varying amounts of kaolinite and 10 Å clay, as well as a phase indicated by a very diffuse peak on the low-angle side of 10 Å. Low-angle phases are probably smectitic.

Carbonates also occur in various parts of each section. XRD suggests that calcite abundance varies considerably. Calcite-rich intervals generally correspond with: (i) abundant

TABLE 3.2. WHOLE ROCK XRD SUMMARY

SAMPLE NUMBER	ROCK TYPE	Quartz	Plagioclase	K-spar	Calcite	Siderite	Dolomite	Pyrite	Halite	7 Å clay	10 Å clay
GLENELG J-48											
G460	Qw	M	mM	m	m	mt	mt	t	nd	mt	mt
G580	Qw	M	m	mM	mt	nd	nd	m	mt	m	m
G820	Md	M	mt	m	m	nd	nd	mt	m	m	m
G1100	Md	M	nd	nd	mM	nd	nd	mM	m	m	m
G1290	Qw	M	mM	m	mM	nd	nd	mt	mt	m	mM
G1480	clc Md	mM	m	nd	M	nd	nd	mt	m	mt	mM
G1630	clc Md	M	nd	nd	M	nd	nd	mt	m	nd	m
G1865	Md	M	m	mt	m	nd	nd	mt	mt	mM	m
G2080	clc Md	M	mt	nd	M	nd	t	t	mt	mt	mt
TRIUMPH P-50											
T1590	Lithic	M	mM	nd	mt	mM	nd	mt	nd	m	m
T2845	Lithic	M	mt	nd	mM	nd	nd	m	nd	m	m
T4220	Lithic	M	mt	mt	mM	nd	nd	m	nd	m	m
T5160	Md	mM	nd	nd	M	mt	nd	m	m	nd	mt
T5670	clc Md	mM	nd	mt	M	mt	nd	mt	mt	mt	mt
T5930	clc Md	t	nd	nd	M	nd	nd	nd	nd	nd	nd
T7080	Md	M	mt	mM	m	mt	nd	t	mt	mM	m

TABLE 3.2. CONTINUED

SAMPLE NUMBER	ROCK TYPE	Quartz	Plagioclase	K-spar	Calcite	Siderite	Dolomite	Pyrite	Halite	7 Å clay	10 Å clay
ACADIA K-62											
A1270	Qw	M	mM	mM	m	m	mt	mt	nd	mt	m
A1600	Md	mM	m	m	mM	m	nd	mt	m	mt	m
A2010	Md	M	mM	mM	m	mM	nd	m	nd	m	mM
A2304	Md	mM	m	m	M	m	nd	m	nd	mt	m
A2640	clc Md	mM	mt	nd	M	mt	nd	mt	nd	mt	mt
SHUBENACADIE H-100											
S2165	Qw	M	mM	nd	m	m	m	mt	m	m	mM
S2675	Qw	mM	mM	mM	m	m	nd	mt	nd	mt	m
S3140	Md	M	mM	nd	mM	m	nd	m	nd	m	mM
S3660	clc Md	mM	nd	nd	M	mt	nd	nd	nd	t	mt
S3910	Md	mM	nd	nd	M	nd	nd	mt	m	m	m
S4165	Md	M	nd	nd	mM	nd	nd	mt	m	mM	m

skeletal debris, (ii) secondary pore-fillings and (iii) minor calcite fracture-fillings. Calcite occurs in greatest abundance associated with calcareous mudstones downsection (see Chapter 2, calcareous Wyandot mudstones).

Dolomite and siderite are present in upper portions of shelf and slope sections. Only siderite has been recognised in SEM and EDA. Dolomite is not observed downsection and is present only in the uppermost interval of each well. Siderite is more pervasive and is present at low abundance throughout the sequences from Acadia and Triumph.

Acadia varies slightly from other wells by having a higher feldspar content which persists throughout the section. Although petrographic examination of feldspar at Acadia was not possible, the feldspar trend from XRD is similar to shallow sections at other wells.

Halite is present in whole rock samples; it may represent minor drilling fluid contamination.

PETROGRAPHY

Petrographic investigation has revealed the nature of the alteration of detrital grains and the occurrence of authigenic minerals. Thin sections, backscattered and secondary electron SEM imaging were used to evaluate diagenetic petrography.

Detrital phases comprising shaly sections from the shelf and slope consist primarily of quartz, plagioclase, K-feldspar, calcareous and siliceous fossil tests and clays. Quartz usually occurs as round to subangular grains of high sphericity. However no evidence of quartz overgrowth or corrosion was observed. Similarly no geochemical alteration of siliceous fossil material could be recognised. However, as discussed in Chapter 2, physical degradation of fossil tests is recognised at certain intervals (e.g., Glenelg).

Coarse feldspar grains also appear to be mechanically intact. However, unlike quartz, petrographic evidence suggests that detrital plagioclase and K-feldspar grains have experienced some dissolution (Plate 3.1a, 3.1b). However, the lack of severe pitting and the occurrence of pitting only deep in the sequence, suggests that feldspar dissolution is at an immature state.

Detrital carbonate fossils are generally intact, despite minor mechanical breakage at some locations. Although recrystallization of aragonite to calcite may have occurred during early burial (XRD), calcite dissolution has not been observed. Calcite, comprising fossil fragments, is coarse compared to recent samples, suggesting recrystallization. As well, fossil

PLATE 3.1. SECONDARY ELECTRON SEM MICROGRAPHS

Plate 3.1a: Secondary electron SEM micrograph of minor corrosion on detrital K-feldspar grain (confirmed by EDA). Fine clays situated inside cavity are probably kaolinite. Grain is situated in a matrix of illite/smectite and kaolinite. Glenelg J-48, 1420 mbmsl, (see scale).

Plate 3.1b: Secondary electron SEM micrograph of detrital plagioclase (confirmed by EDA) in a matrix of illite/smectite and kaolinite. Solution cavity along plagioclase grain edge is not filled with authigenic clay. Glenelg J-48, 1865 mbmsl, (see scale).

Plate 3.1c: Secondary electron SEM micrograph of euhedral pyrite grain situated adjacent to secondary calcite. Material resting on pyrite is unidentified. Shubenacadie H-100, 3900 mbmsl, (see scale).

Plate 3.1d Secondary electron SEM micrograph of euhedral pyrite grain from Plate 3.1c. Pyrite was precipitated in a cavity rimmed by secondary, low-iron calcite. Shubenacadie H-100, 3900 mbmsl, (see scale).

Plate 3.1e Secondary electron SEM micrograph of secondary calcite infilling early microporosity. Calcite grains exhibit classical rhombic habit without dissolution. Shubenacadie H-100, 3900 mbmsl, (see scale).

A
K-spar

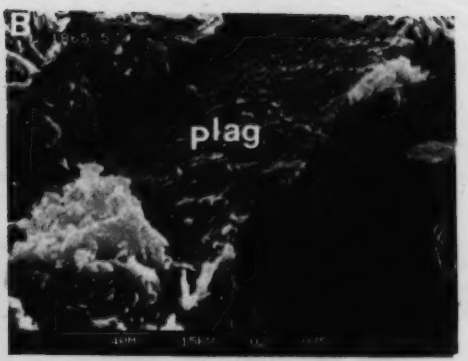
B
plag

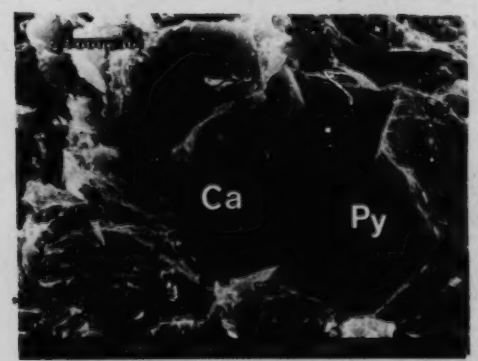
Ca
Py

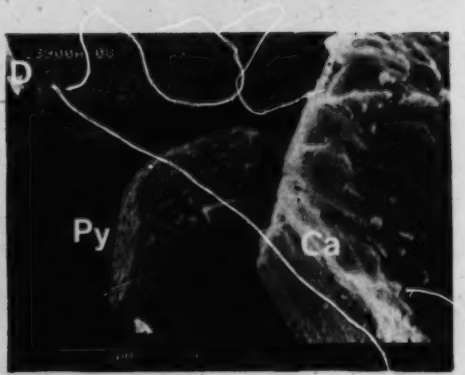
D
Py
Ca

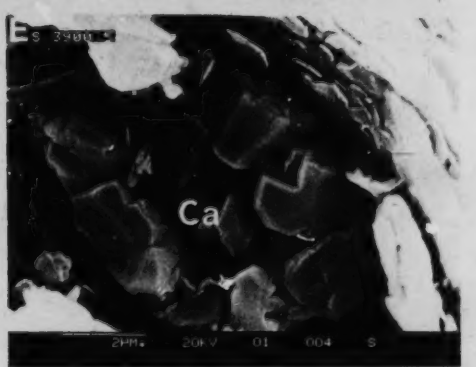
E
Ca

tests are partly infilled with secondary calcite.

Some authigenic clays are associated with small cavities developed during early feldspar dissolution. However dissolution cavities are very small and resulting clays are very fine-grained and scarce. As a result, their nature was difficult to determine by energy dispersive, elemental analysis under an SEM.

Pyrite occurs pervasively throughout all sequences examined. Most commonly it exists as framboidal aggregates of small, bipyramidal grains. Undeformed framboidal aggregates generally occupy large, void spaces suggesting precipitation during an early stage of compaction. However some framboidal pyrite infills compaction-related voids (Plate 2.2b). Certain samples contain euhedral pyrite which postdates secondary calcite precipitation (Plates 3.1c, 3.1d). Variations in pyrite morphology indicate that multiple generations of pyrite occur in these sequences (Coleman and Raiswell, 1981).

Secondary calcite is also a common constituent of the shale rocks examined (i.e., except Glenelg). Typically it occurs: (i) infilling intraskeletal porosity or fractures and (ii) as small aggregates of rhombs infilling early porosity (Plates 3.2a, 3.1e). In all cases, secondary calcite does not indicate subsequent corrosion during burial. The occurrence of secondary calcite: (i) infilling large void spaces during burial and (ii) intimately associated with early pyrite (Plate 3.1e) suggests that calcite precipitation occurred early in diagenesis.

0.2 - 2.0 μm XRD DATA

Upon completion of whole rock XRD, <2.0 μm material was extracted from whole rock sample. Clay-size material was subsequently separated into <0.2 μm and 0.2 - 2.0 μm size-fractions. As the coarser fraction constitutes the majority of clay-size material by mass, 0.2 - 2.0 μm material will be considered when discussing trends in clay-mineral distribution. Table 3.3 lists estimates of mineral abundance and expandable clay data from each well examined.

Examination of this size-fraction offers insight into the: (i) mineralogic character of detrital clays from the shelf and slope and (ii) the distribution of these clays through the burial sequence. Each sample contains significantly more kaolinite, chlorite and 10 Å clay than finer fractions from the same interval. Most phases are well crystallized and are not interstratified.

PLATE 3.2. THIN SECTION MICROGRAPH

Plate 3.2a: Thin section micrograph of mudstone. Fossil tests are intact and in early stages of secondary calciite infilling. Triumph P-50, 1515 mbmsl (4970 ft.), 10X. objective.

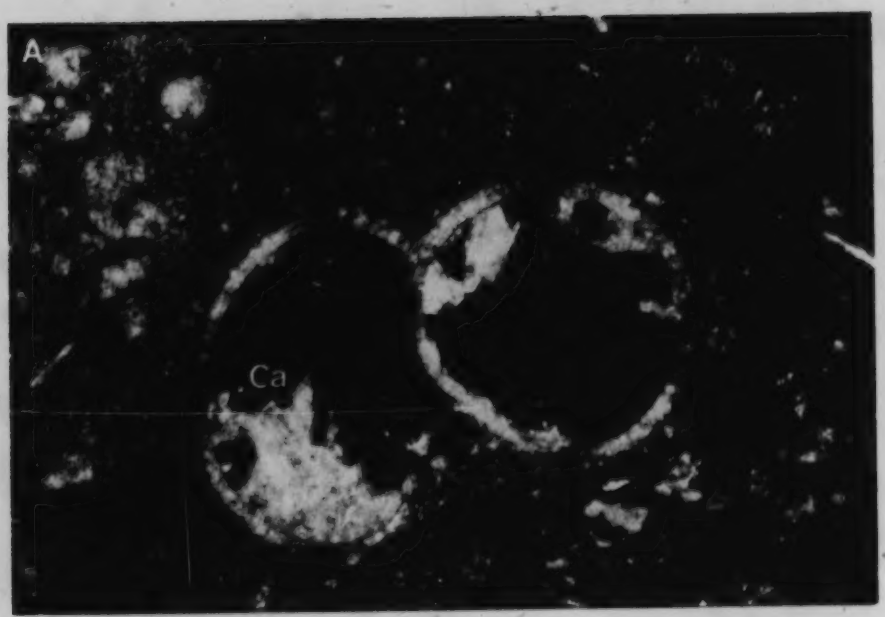
A
Ca

TABLE 3.3. 0.2 - 2.0 μm XRD DATA

SAMPLE	SETTING	MINERAL ABUNDANCES Sm	I	K	Cl	Q	Ca	S:I	%Sm¹ in 10 Å clay	%Sm¹ in 17 Å clay
GLENELG J-48										
G460	OUTER	mt	M	t	mM	mM	nd	0.11	<10	nd
G820	SHELF	m	mM	mM	mt	mM	nd	0.26	<10	nd
G1100	"	m	mM	mM	t	mM	nd	0.27	<10	nd
G1290	"	m	mM	mM	t	mM	m	0.33	<10	nd
G1480	"	mM	mM	mt	mt	mM	m	0.77	10	77
G1630	"	t	m	t	nd	M	mM	0.23	<10	nd
G1865	"	t	mM	M	m	mM	nd	0.06	<10	nd
ACADIA K-62										
A1270	UPPER	mt	mM	m	m	M	t	0.08	<10	nd
A1600	SLOPE	mt	m	t	mt	mM	M	0.59	<10	nd
A2010	"	m	mM	mM	m	M	t	0.28	<10	nd
A2304	"	mM	mM	m	mt	M	mM	0.53	<10	nd
A2640	"	mt	m	mt	nd	mM	M	0.56	<10	nd
SHUBENACADIE H-100										
S2165	LOWER	mM	mM	mM	m	mM	nd	0.49	5	nd
S2675	SLOPE	M	M	m	mM	nd	nd	0.78	5	nd
S3140	"	mM	mM	mM	mt	mM	nd	1.02	<10	79
S3660	"	mM	mM	mt	t	mM	M	1.22	<10	76
S3910	"	t	m	m	t	M	mM	0.19	<10	nd
S4165	"	mt	mM	mM	m	mM	mt	0.15	10	nd

%Sm¹: Apparent %Smectite from 10 and 17Å Phases Following Hower (1981)

At Glenelg, kaolinite and 10 Å clay are the dominant clay types except for a smectitic lense from roughly 1290 to 1480 mbmsl (Table 3.3). The ratio of smectite:illite abundance (S:I) in this size-fraction increases downsection toward 1480 mbmsl, compatible with $<0.2\ \mu m$ trends (Figure 3.1). Variations in smectite:illite abundance toward 1480 mbmsl result from transition into deeper water facies. Relative to 10 Å clay, kaolinite abundance is widely variable downsection and reaches relatively high levels at 1100 and 1865 mbmsl.

Estimation of smectitic interstratification associated with 17 Å clay is difficult for this size range. Measurements in Table 3.3, from certain 10 and 17 Å phases, indicate that these phases are highly illitic and smectitic respectively. Mixed-layer clays containing subequal amounts of interstratified illite and smectite layers were not recognised in this size-fraction.

Examination of the low-angle region of 10 Å peaks at 0% RH (K^+ saturation) reveals that little shouldering is developed down to 1480 mbmsl. Below this level to TD, slight broadening at the base of 10 Å peaks suggests minor occurrences of degraded illite (i.e., depotassified mica). However examination of a full suite of K^+ saturated, 0% RH x-ray charts (i.e., 107°, 300° and 550°C) indicates no extensive shouldering on the 10 Å peak.

Samples from Acadia contain less illite and discrete kaolinite than the outer shelf. Table 3.3 suggests that smectite becomes enriched relative to illite at shallow levels and then remains fairly constant in abundance with burial.

At Acadia, the percentage of smectite interstratification associated with 17 Å clay cannot be measured. However, 10 Å clay is highly illitic, having <10% expandable layers throughout the section. Examination of a full suite of 0% RH charts reveals that 10 Å clays from Acadia are highly crystalline and do not exhibit pronounced shouldering on their low-angle side. However, 10 Å peaks broaden and exhibit low-angle shoulders below 2304 mbmsl.

The lower slope section at Shubenacadie contains significant amounts of smectite, 10 Å clay and kaolinite. As mentioned previously, kaolinite, 10 Å clay and chlorite are considered to be detrital, with no indications of transformation. Kaolinite increases in abundance with depth relative to other phases. However no indication of kaolinite interstratification is detected in this study, although kaolinite reaches maximum abundance at 4165 mbmsl.

With burial, S:I increases downsection to a maximum between 3140 and 3660 mbmsl. However, below this level, smectite diminishes relative to other phases. Variations in detrital

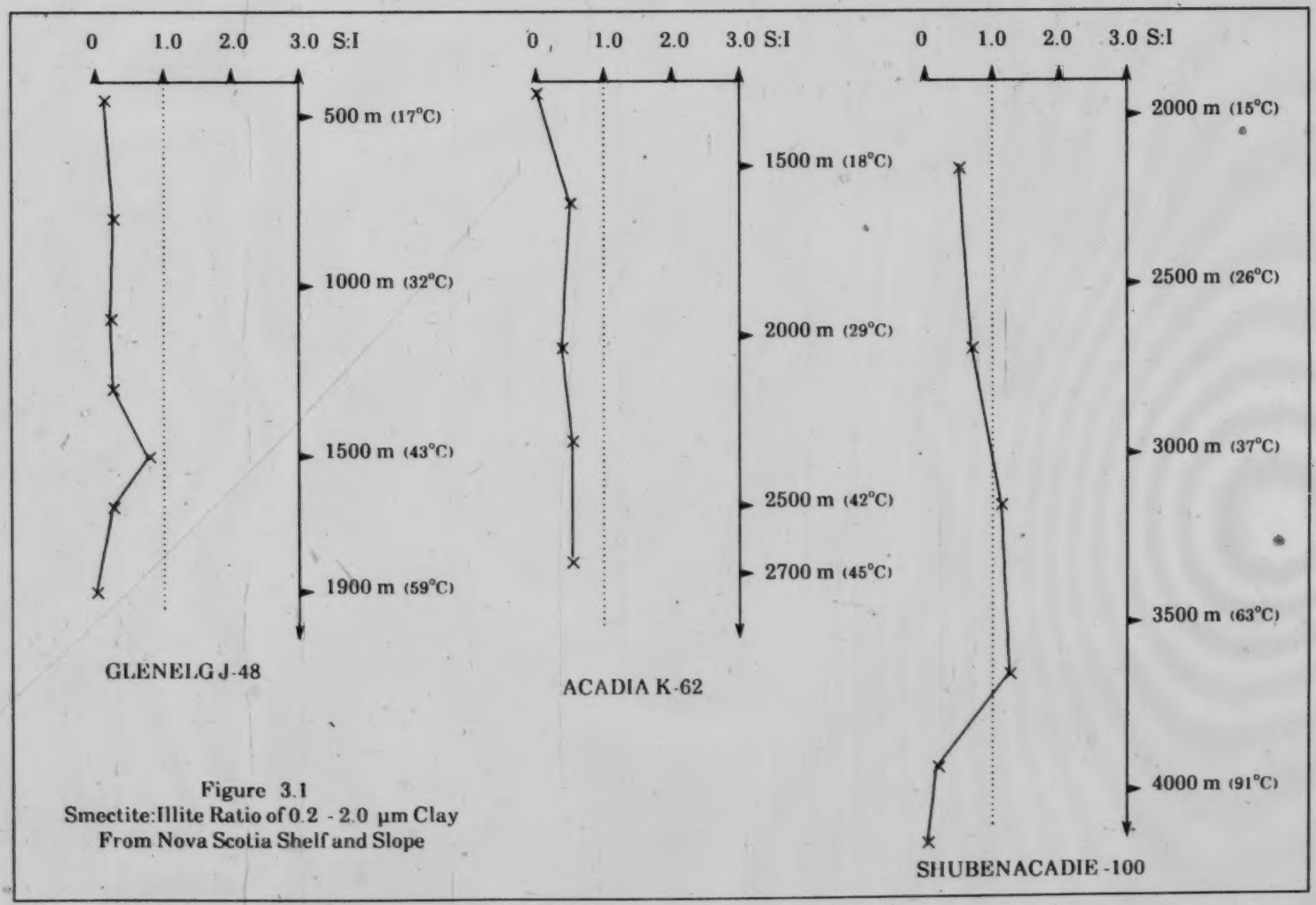

Figure 3.1
Smectite:Illite Ratio of 0.2 - 2.0 μm Clay
From Nova Scotia Shelf and Slope

S:I ratio downsection may result from transition into deeper water facies (Gibbs, 1970).

Where measurement is possible, 17 Å clay contains in excess of 75% interstratified smectite. With burial at Shubenacadie, 17 Å clay in this size range persists and does not become more illitic. As well, the low-angle side of the 10 Å peak exhibits only very minor shouldering down to 2675 mbmsl. Below this depth, shouldering increases slightly toward 4165 mbmsl. However no significant shouldering is detected on any 0% RH heat-treatments, suggesting a lack of degraded illite.

<0.2 μm XRD DATA

Results from XRD investigations of very fine size-fractions from Glenelg, Triumph, Acadia and Shubenacadie are listed in Table 3.4. The mean diameter of the finest size-fraction examined from each sequence varies because finer separations were performed in certain cases to isolate as pure a sample of mixed-layer illite/smectite as possible.

When evaluating the character of very fine size-fractions, which should have been most sensitive to diagenesis, <0.2 μm material from Glenelg was considered initially. The degree of smectite interstratification in 10 and 17 Å phases was determined using techniques of Hower (1981) and Środoń (1980, 1981, 1984). Both methods yielded fairly consistent results.

Kaolinite appears to be discrete because (001) and (002) peaks are invariant and do not exhibit shouldering. Chlorite is detected in low abundance at the top and bottom of the section. However, the chlorite exhibits no indication of interstratification, as determined by XRD.

In the <0.2 μm fraction, 17 Å clay is not abundant. Large amounts of kaolinite and 10 Å clay obscure evaluation of the degree of interstratification in expandable, 2:1 layer phases. To more reliably determine the nature of mixed-layer phases, below 1290 mbmsl a finer size-fraction (<0.05 μm) was used to concentrate illite/smectite (Table 3.4). This fraction was analyzed using standard Ca^{2+} treatments.

In the <0.05 μm fraction, smectitic and illitic phases were recognised throughout the sequence associated with the 17 and 10 Å peaks respectively. In general, 10 Å clay contains a low proportion of expandable layers (<25%) (Figure 3.2). In comparison with 0.2 - 2.0 μm clays, the 10 Å clays in the <0.05 μm fraction apparently contain *more expandable layers* with depth, except at 2080 mbmsl (Tables 3.3, 3.4). However, variations in 10 Å clay expandability may not be caused by fundamental changes in the crystal structure and elemental composition

TABLE 3.4. FINE SIZE-FRACTION XRD DATA

SAMPLE NUMBER	SIZE FRACTION (μm)	MINERAL ABUNDANCES Sm	I	K	Cl	SMECTITE POLYTYPE	%Sm[1] in 10 Å CLAY	%Sm[1] in 17 Å CLAY	%Sm[2] in 17 Å CLAY	TYPE OF 17 Å CLAY INTERSTRATIFICATION[3]
GLENELG J-48										
G460	<0.2	mM	M	nd	mM	nd	5	nd	nd	nd
G820	<0.2	mM	mM	M	nd	nd	10	nd	nd	nd
G1100	<0.2	mM	mM	mM	nd	nd	10	76	nd	nd
G1290	<0.05	M	mM	m	nd	Mnt	15	69	68	RANDOM
G1480	<0.05	M	mM	nd	nd	Mnt	nd	75	63	RANDOM
G1630	<0.05	M	M	nd	nd	Mnt	22	60	67	RANDOM
G1865	<0.05	M	mM	m	nd	Mnt	23	68	69	RANDOM
G2080	<0.05	M	mM	mM	nd	Mnt	12	58	57	RANDOM
TRIUMPH P-50										
T1590	<0.1	mM	M	mM	nd	Mnt/Bd	9	42	51	RANDOM
T2845	<0.1	M	mM	mM	nd	Mnt	10	61	65	RANDOM
T4420	<0.1	M	mM	mM	nd	Mnt	16	56	56	RANDOM
T5160	<0.1	M	mM	mt	nd	Mnt	20	59	60	RANDOM
T5670	<0.1	M	mM	mt	nd	Mnt	10	68	72	RANDOM
T7080	<0.1	mM	M	M	nd	Bd/Mnt	9	nd	nd	nd

TABLE 3.4. CONTINUED

SAMPLE NUMBER	SIZE FRACTION (μm)	MINERAL ABUNDANCES Sm	I	K	Cl	SMECTITE POLYTYPE	%Sm¹ in 10 Å CLAY	%Sm¹ in 17 Å CLAY	%Sm² in 17 Å CLAY	TYPE OF 17 Å CLAY INTERSTRATIFICATION³
ACADIA K-62										
A1270	<0.2	mM	M	t	mM	nd	12	nd	nd	nd
A1600	<0.2	mM	M	mM	nd	nd	9	100	72	RANDOM
A2010	<0.2	M	mM	mM	nd	nd	10	78	77	RANDOM
A2304	<0.2	M	mM	mM	nd	nd	10	80	76	RANDOM
A2640	<0.2	Mt	mM	m	t	nd	10	83	87	RANDOM
SHUBENACADIE II-100										
S2165	<0.1	M	mM	mM	nd	Mnt	15	65	73	RANDOM
S2675	<0.1	M	mM	m	nd	Mnt	12	73	71	RANDOM
S3140	<0.1	M	mM	m	nd	Mnt	11	78	74	RANDOM
S3660	<0.1	M	mM	mt	nd	Mnt/Bd	13	65	65	RANDOM
S3785	<0.1	M	M	m	nd	Mnt/Bd	15	57	63	RANDOM
S3910	<0.1	mM	mM	M	nd	Mnt/Bd	14	58	64	RANDOM
S4040	<0.1	M	M	mM	nd	Mnt/Bd	18	50	59	RANDOM
S4165	<0.1	mM	M	M	nd	Mnt:Bd	12	nd	nd	nd

%Sm¹: Apparent %Smectite from 10 and 17 Å Phases Determined Following Hower (1981)
%Sm²: Apparent %Smectite Determined Following Sfodoń (1981,1984)
INTERLAYERING³: Type of Interstratification Determined Following Sfodoń (1981,1984)

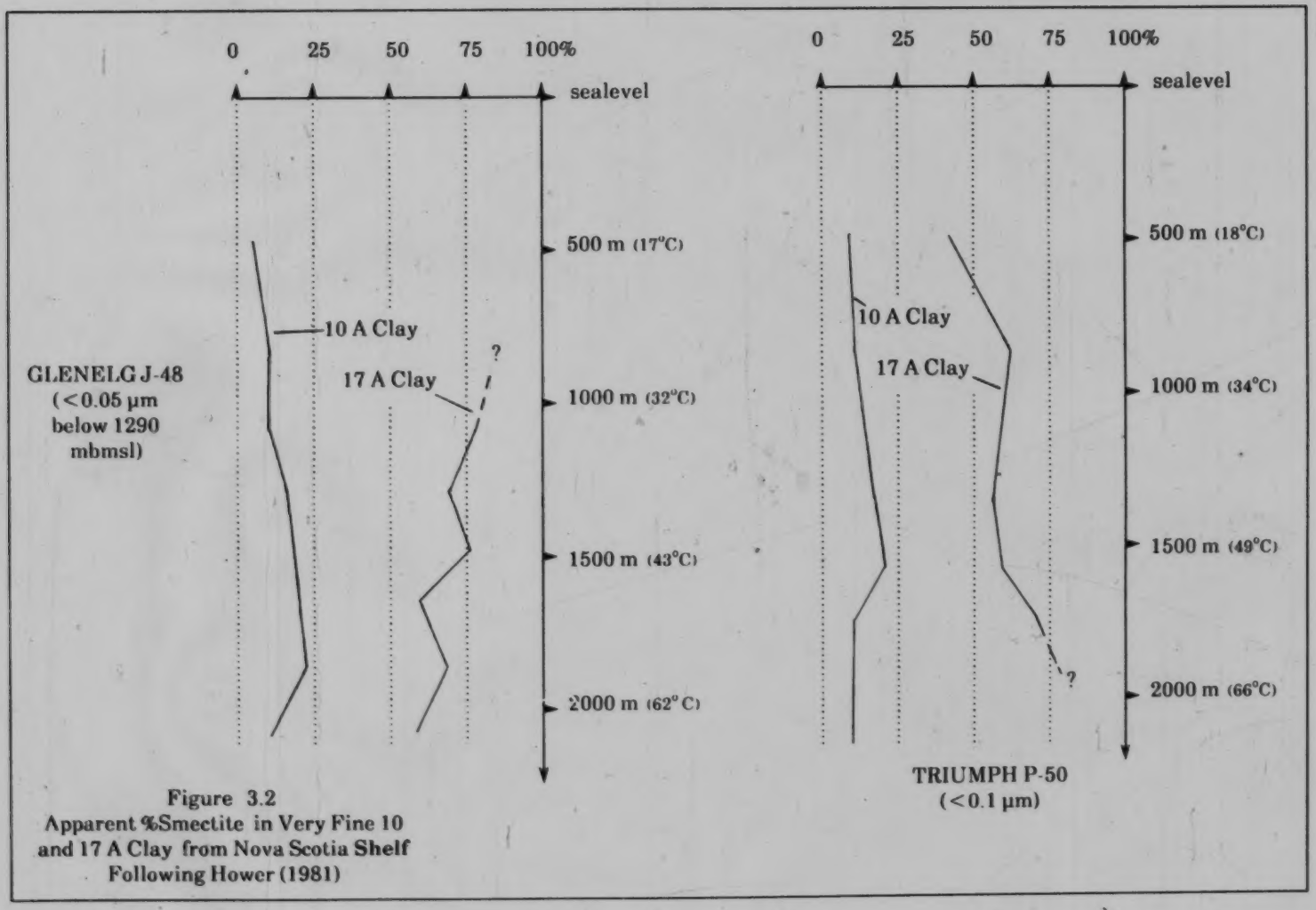

Figure 3.2
Apparent %Smectite in Very Fine 10 and 17 A Clay from Nova Scotia Shelf Following Hower (1981)

of 2:1 silicate layers. Rather, changing expandability may be due only to leaching of K^+ from the edges of mica.

The smectitic phase remains randomly interstratified throughout the section, with a moderate decrease in smectite interstratification from 75% to 57% downsection. Decline in 17 Å clay expandability appears to begin at temperatures as cool as 32°C. However, although smectite interstratification decreases moderately with burial, no beidellitic phases are observed, as would have been indicated by lower expandability in response to Ca^{2+}-glycerin solvation (Spiers et al., 1984). Smectite mineralogy is composed primarily of montmorillonite at Glenelg.

To augment information concerning the mineralogical character of fine, outer shelf clays, <0.1 μm size material was extracted from Triumph. Results from Ca^{2+} and K^+ treatments are listed in Table 3.4. At Triumph, fine clays consist primarily of smectitic and illitic phases with only minor kaolinite. As at Glenelg, very fine-grained kaolinite is discrete.

Throughout Triumph, 17 Å phases contain a large proportion of smectitic material which is randomly interstratified. In contrast to Glenelg, 17 Å clay becomes *more smectitic* with burial, from <50% smectite interstratification uphole to 70% downsection. While beidellite occurs at 2158 mbmsl (7080 ft.), montmorillonite is the dominant smectite polytype throughout the section. Despite the high degree of smectite interstratification, K^+-saturated 17 Å clay does not rehydrate markedly upon equilibration with 54% RH in any sample. Interlayer-charge density may be sufficiently high to prevent rehydration.

Heat treatments of K^+ saturated clay do not reveal chlorite or chloritic phases. However minor low-angle shouldering, suggestive of degraded illite, is recognised at 2158 mbmsl (7080 ft.) in Cenomanian age rock. The 10 Å clay reveals a weaker trend toward increasing expandability (i.e., depotassification) toward 1572 mbmsl (5160 ft.) compared to Glenelg.

On the upper slope at Acadia, <0.2 μm size material was examined after Na^+ saturation. As on the shelf, smectitic and illitic clays and kaolinite constitute this size-fraction. Similar to Triumph, the degree of smectite interstratification in 17 Å clay increases with depth. However, smectite interstratification is higher, ranging from >72% upsection to 84% at 2640 mbmsl. The high degree of randomness associated with smectite interstratification despite burial suggests that significant alteration of 17 Å clay has not occurred.

As at Glenelg and Acadia, <0.2 μm size material was examined initially at Shubenacadie. Although 17 Å clay is more abundant in this fraction than at Glenelg, a finer

fraction (<0.1 μm) was examined to: (i) minimize contamination from detrital kaolinite and 10 Å clay and (ii) to improve determination of smectite/illite interstratification.

A low intensity peak lying between 1.49 - 1.50 Å indicates that 2:1 layer silicates are primarily dioctahedral (i.e., aluminous). Following techniques of Hower (1981) and Sfodoń (1981), the degree of smectitic interstratification associated with 17 Å clay was found to increase slightly downsection toward 3140 mbmsl (Figure 3.3). Below 3140 mbmsl, smectite interstratification diminishes from 78% to 50% over 1000 meters of burial, beginning at approximately 40°C. However 17 Å clay remains *randomly interstratified* throughout the entire burial sequence. Unfortunately, while 17 Å clay is recognised at 4165 mbmsl, the degree of smectite interstratification is difficult to determine because $(002)_{17}$ and $(003)_{17}$ peaks are of low intensity.

Ca^{2+}-glycerin treatments indicate that smectite polytype varies with burial, unlike other sequences (Table 3.4). Upsection, smectite is composed primarily of montmorillonite down to 3140 mbmsl. However, with burial mixtures of montmorillonite and beidellite are recognised by high-angle shoulders on 17 Å peaks. At 4165 mbmsl, glycerin treatment indicates two peaks in the range of 14 to 18 Å. This indicates that the 17 Å glycol peak actually contains both montmorillonitic and beidellitic phases.

The 10 Å clay has a low degree of smectite interstratification (i.e., expandability) with burial. However the degree of expandability associated with 10 Å clay is slightly greater than in coarser fractions from Shubenacadie. Consistent with other wells, 10 Å material is probably detrital.

OBSERVATIONS FROM ELEMENTAL ANALYSIS

CLAY ELEMENTAL DATA

Elemental analyses of <0.1 μm clay samples from Shubenacadie were conducted because this sequence was suspected of exhibiting the greatest degree of diagenetic alteration. Table 3.5 indicates that ICP analysis is more accurate than x-ray microanalysis from SEM for accurately reproducing U.S.G.S. wet chemical analyses for clay standards. Although x-ray data generally follows similar trends to ICP data and are independent verification of ICP trends, only ICP results will be used for numerical determination of elemental trends. All raw data was recalculated to *weight % of each element* relative to elements analysed. Normalized <0.1 μm

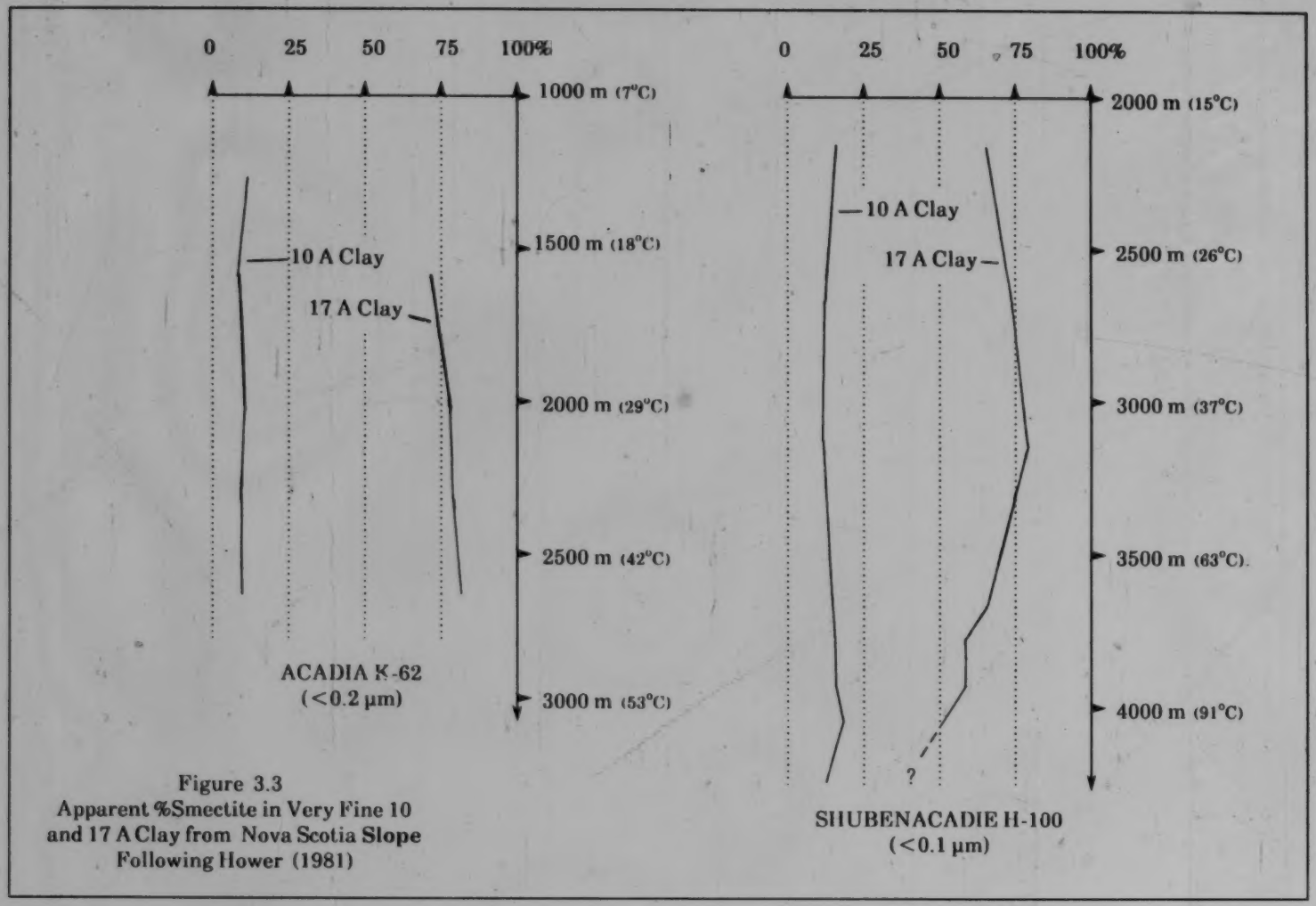

Figure 3.3
Apparent %Smectite in Very Fine 10 and 17 A Clay from Nova Scotia Slope Following Hower (1981)

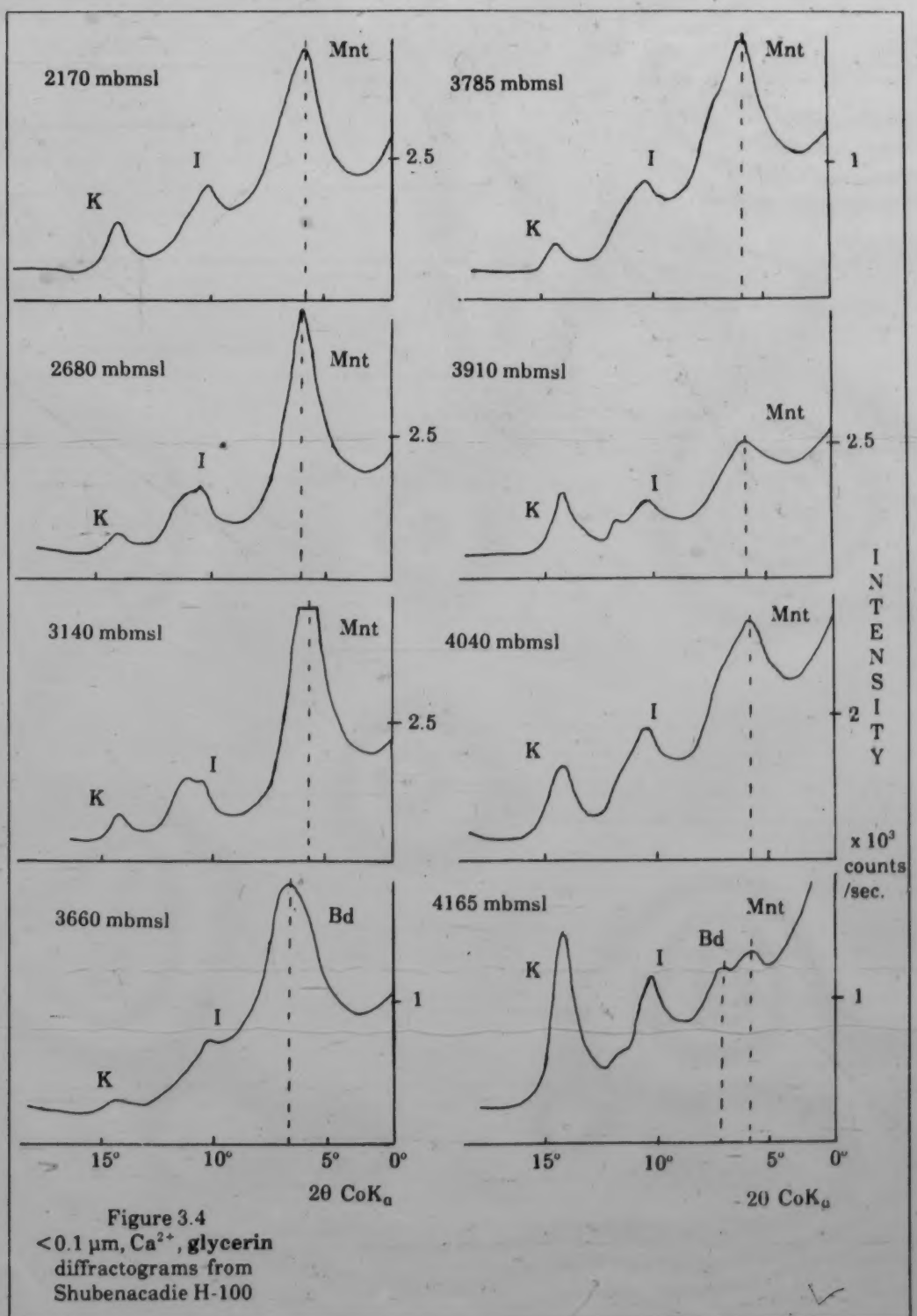

Figure 3.4
<0.1 μm, Ca^{2+}, glycerin diffractograms from Shubenacadie H-100

TABLE 3.5. ELEMENTAL ANALYSES OF STANDARDS

Analyses Expressed as "%Element of Total Elements Analysed"

Element	U.S.G.S. Standard	ICP	X-ray Analysis
K-Ga1, Georgia Kaolinite			
Na	0.02	0.09	na
Mg	0.04	0.04	na
Al	49.17	46.85	47.01
Si	48.36	50.35	50.80
S	nd	0.04	na
K	0.10	0.09	na
Ca	nd	0.01	na
Ti	1.95	2.17	1.82
Fe	0.36	0.36	0.38
Syn-1, Synthetic Mica-Montmorillonite			
Na	0.44	0.62	1.36
Mg	0.02	0.24	0.96
Al	46.18	44.29	41.38
Si	53.05	54.29	50.76
S	0.23	0.29	5.37
K	0.02	0.06	0.02
Ca	nd	0.06	na
Ti	0.03	0.02	0.07
Fe	0.03	0.14	0.08
SWy-1, Wyoming Montmorillonite			
Na	2.42	2.54	2.22
Mg	3.91	3.41	3.34
Al	22.07	20.80	18.49
Si	62.40	63.50	52.09
S	0.11	0.18	9.71
K	0.93	1.10	0.20
Ca	2.55	2.60	8.11
Ti	0.12	0.14	0.44
Fe	5.50	5.68	5.42

data are presented in Table 3.6.

From 2160 mbmsl, the Al/Si ratios decrease steadily from 0.41 to a value of 0.33 at 3140 mbmsl (i.e., Miocene-Eocene marker) (Figure 3.5). This trend agrees with <0.1 μm XRD data confirming a relative increase in smectite:illite (S:I) toward 3140 mbmsl; the Al/Si ratio of Wyoming montmorillonite is 0.35 and OECD standard illite is 0.45. Below 3140 mbmsl, Al/Si ratios increase irregularly downsection toward the first significant occurrence of kaolinite at 3910 mbmsl. Relative Al/Si highs correspond with zones of kaolinite or beidellite enrichment indicated by XRD; Al/Si ratios suggest mixing of a montmorillonitic phase and kaolinite (Al/Si of Georgia kaolinite = 1.01). However, in zones of abundant kaolinite, Al/Si ratios in the 2:1 layer phases are difficult to assess.

A distinct trend of K/(Si/Al) ratios occurs with depth (Figure 3.5). K^+ becomes depleted relative to Si/Al down to 3140 mbmsl in agreement with: (i) increases in smectite:illite ratios and (ii) abundant smectite interstratification in 17 Å clay as determined by XRD. However, below 3140 mbmsl, K^+ content increases as Si/Al ratios decrease. Increases correspond with progressive reduction in: (i) smectite:illite abundance ratios and (ii) the percentage of expandables as determined by XRD. An exception to this trend occurs at 4040 mbmsl where K^+ is slightly depleted and Si/Al is enriched relative to adjacent samples. As well, the high smectite:illite ratio and high percentage of smectite interstratification in illite/smectite is anomalous compared to samples from adjacent intervals.

Evaluation of total alkali and alkali-earth cations analysed, "Total Cations", reveals a trend similar to K/(Si/Al) ratios with burial, except at 3785 and 4040 mbmsl. At 3785 mbmsl, a minor calcite constituent observed on XRD elevates "Total Cations" by a marked increase in Ca^{2+}. By ignoring Ca^{2+}, this sample lies more along a trend of increasing "Total Cation" content with decreasing Si/Al ratio. From elemental analysis, alkali and alkali-earth cations (especially K^+) are more abundant in fine clays of the lower section. As kaolinite is present downsection, K^+-enrichment in the clay mixture can result from the occurrence of 17 Å clay of higher ordering and/or highly illitic, 10 Å clay.

The <0.1 μm clays derived from calcareous mudstones are generally depleted in Ca^{2+}. Free Ca^{2+} in solution has not been incorporated into these clays. However an exception occurs at 4040 mbmsl where K^+ is relatively depleted yet total cation content is fairly high. Table 3.6 indicates that Ca^{2+} content in this fraction may compensate for a lack of K^+. Possibly

TABLE 3.6. NORMALIZED <0.1 μm ELEMENTAL ANALYSES: SHUBENACADIE

Analyses Expressed as %Element of Total Elements Analysed

SAMPLE	Na	Mg	Al	Si	S	K	Ca	Ti	Fe
S2165									
ICP	0.20	3.73	23.29	56.71	0.05	4.48	0.34	0.35	10.85
x-ray				not analysed					
S2675									
ICP	0.28	3.82	21.75	58.92	0.10	3.36	0.45	0.62	10.70
x-ray	nd	2.82	20.15	62.28	0.43	4.73	0.17	0.52	8.93
S3140									
ICP	0.14	3.61	20.28	62.30	0.05	3.18	0.14	0.51	9.80
x-ray	nd	2.83	19.73	64.01	0.24	4.20	0.13	0.29	2.47
S3665									
ICP	0.24	3.44	25.05	56.38	0.06	3.79	0.12	0.55	10.35
x-ray				not analysed					
S3785									
ICP	0.20	3.61	23.16	56.27	0.12	4.75	1.13	0.34	10.42
x-ray				not analysed					
S3910									
ICP	0.26	2.85	27.37	53.28	0.04	4.82	0.21	0.31	10.8
x-ray	nd	2.29	23.741	57.99	0.38	4.91	0.04	0.29	10.36
S4040									
ICP	0.21	2.95	26.50	54.92	0.05	4.74	0.39	0.31	9.92
x-ray				not analysed					
S4160									
ICP	0.28	2.48	30.07	48.65	0.04	4.75	0.16	0.30	13.27
x-ray	nd	2.08	26.39	53.00	0.35	4.82	0.09	0.30	12.98

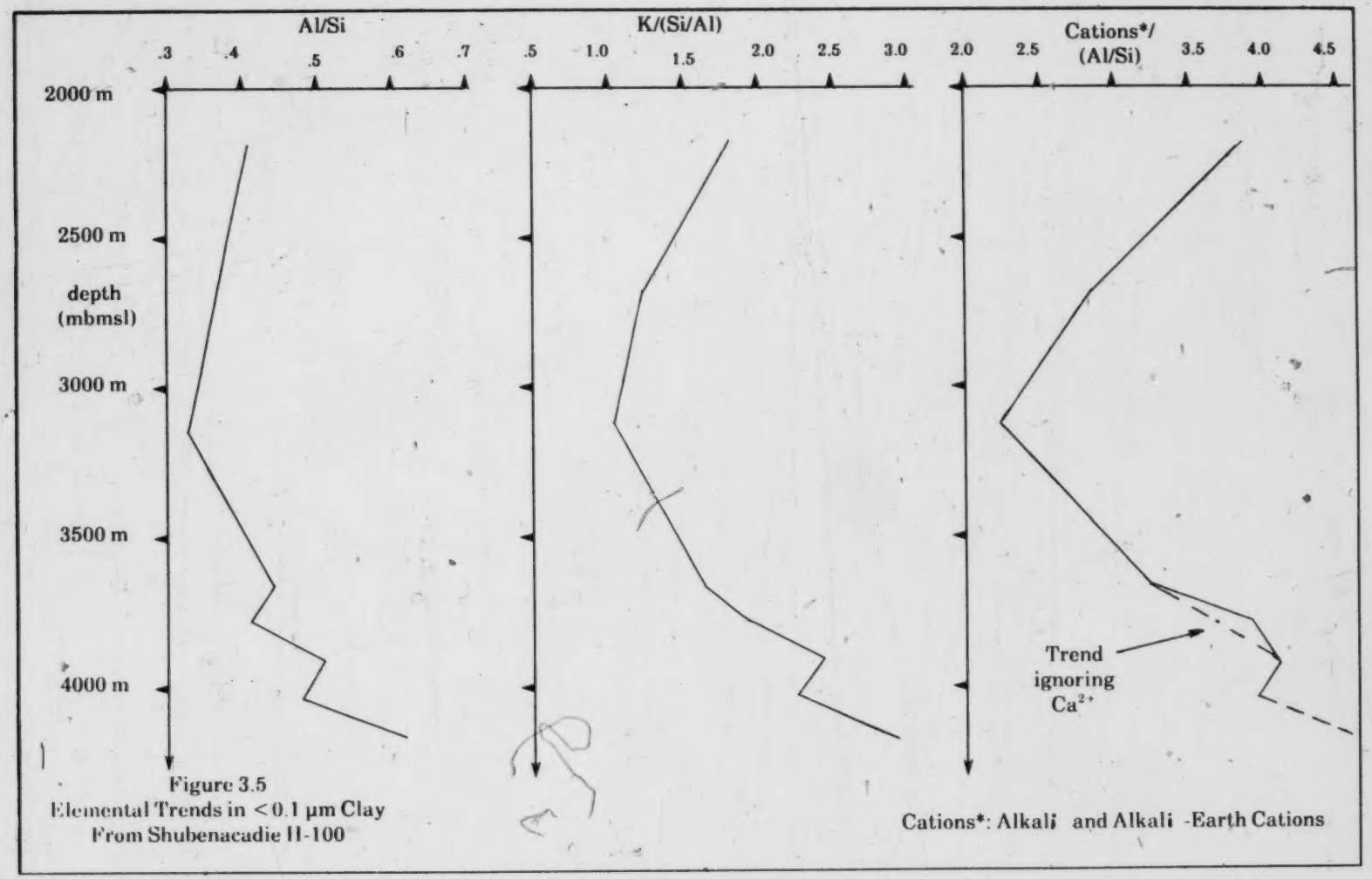

Figure 3.5
Elemental Trends in < 0.1 μm Clay
From Shubenacadie H-100

pore-fluids were depleted sufficiently in K^+ so that Ca^{2+} was fixed into interlayer sites despite the higher hydration energy of Ca^{2+} (Eberl, 1978).

Variations in the Mg^{2+} content of <0.1 μm clay compared to Al^{3+} are shown in Figure 3.6. In the low kaolinite zone upsection, Mg/Al increases with depth although 2:1 layer phases are primarily dioctahedral. Despite kaolinite occurrence downsection, Mg^{2+} becomes somewhat depleted relative to Al^{3+} suggesting that 2:1 layer phases are still dioctahedral with burial.

With depth, iron remains somewhat constant in this size range. Relative to Si/Al trends, there is no marked change in iron until an increase at 4165 mbmsl. In this case, iron enrichment may correspond to minor low-angle shouldering on the 10 Å peak (550°C) corresponding to the development of Fe-bearing, amorphous interlayer material (Figure 3.6).

WHOLE ROCK ELEMENTAL DATA

Whole rock elemental analyses indicate that significant Ca^{2+} occurs between 3660 and 4040 mbmsl (Table 3.7). Ca^{2+} enrichment corresponds with calcareous mudstones observed in whole rock XRD, in thin sections and on compaction curves/synthetic seismographs. By ignoring the bulk of Ca^{2+} in calcareous samples, trends of other major elements can be examined with depth.

Unadjusted for high Ca^{2+}, K^+ appears to remain fairly constant with depth. However, the highest levels of K^+ occur in sediment associated with calcareous mudstones, as observed when Ca^{2+} is ignored. Consideration of whole rock XRD and petrography suggests that K^+ resides increasingly in 10 Å clay with depth rather than feldspar.

Downsection, whole rock Al/Si ratios remain fairly constant until 3660 mbmsl, at which point the Al/Si ratios increase. Relative increases in Al/Si are in agreement with quartz/feldspar depletion and kaolinite enrichment with depth as determined by petrography and XRD.

CARBONATE ELEMENTAL DATA

To constrain the chemical composition of authigenic, pore-filling calcites, samples were chosen from the lower portions of two wells recognised as being most diagenetically active (Glenelg and Shubenacadie). Polished thin sections were prepared, permitting x-ray elemental analysis of secondary calcite.

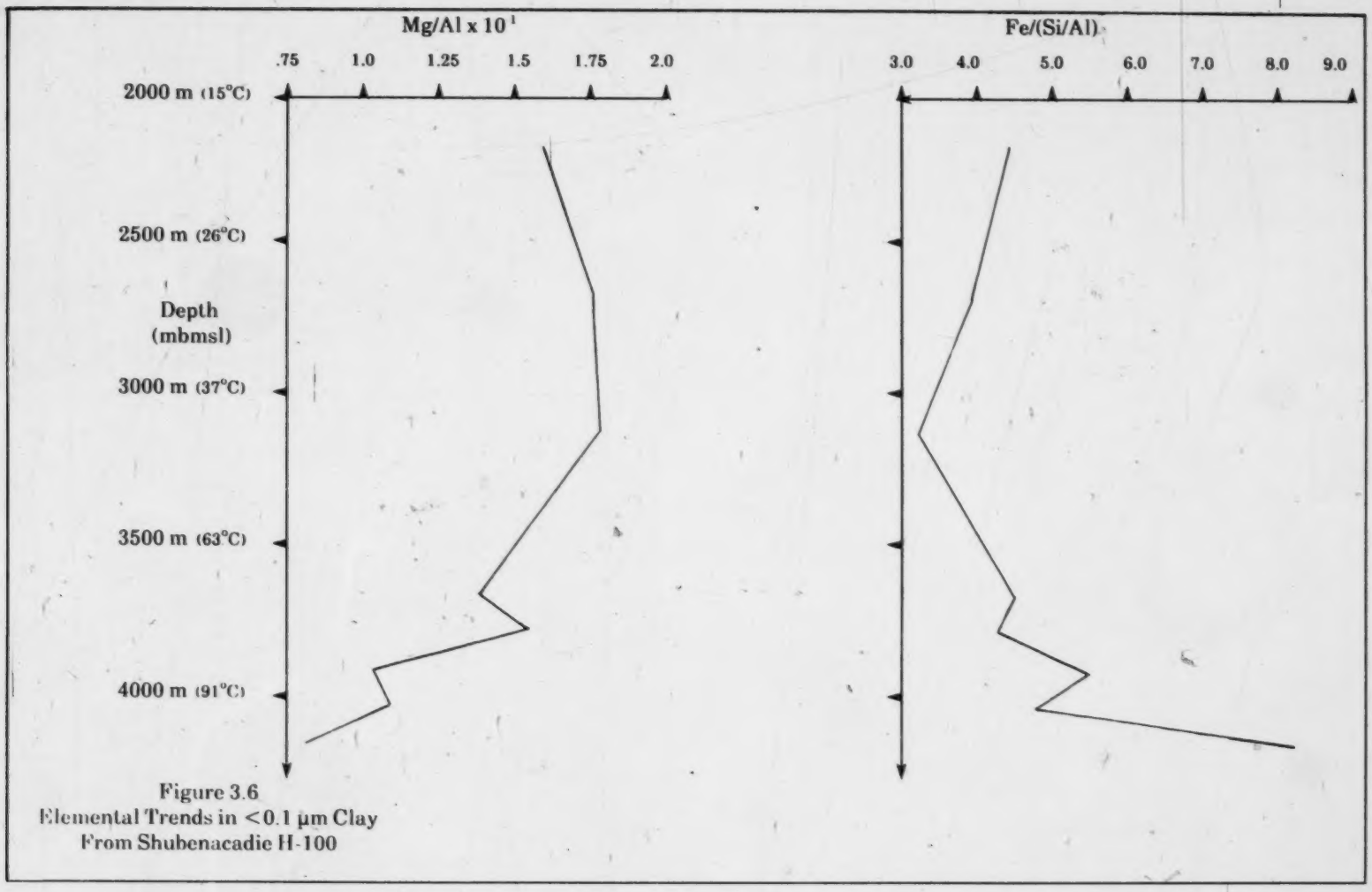

Figure 3.6
Elemental Trends in <0.1 µm Clay
From Shubenacadie H-100

TABLE 3.7. NORMALIZED WHOLE ROCK ELEMENTAL ANALYSES: SHUBENACADIE

Analyses Expressed as %Elements of Total Elements Analysed

SAMPLE	Na	Mg	Al	Si	S	K	Ca	Ti	Fe
S2165 ICP	1.66	3.08	17.16	59.01	0.53	4.00	2.05	0.91	11.58
S2675 ICP	1.99	2.62	15.52	60.29	0.87	3.68	4.43	0.85	9.75
S3140 ICP	1.31	2.54	16.20	63.33	0.58	3.17	2.70	0.87	9.29
S3665 ICP	0.51	1.80	10.68	47.03	0.70	3.66	27.04	0.64	7.95
S3785 ICP	0.43	1.49	10.51	41.33	0.09	4.23	36.31	0.59	5.02
S3910 ICP	0.46	1.51	14.55	50.08	1.03	3.50	16.47	0.91	11.50
S4040 ICP	0.62	1.67	15.11	49.30	0.26	4.88	20.81	0.83	6.51
S4160 ICP	0.61	1.63	19.05	56.23	0.63	3.24	7.34	1.17	10.10

In each case, Figure 3.7 indicates that secondary carbonate pore-fillings contain in excess of 96% Ca^{2+} in cationic sites. Only minor Mg^{2+} and Fe^{2+} components are present. These data agree with whole rock XRD which indicates d-spacings characteristic of high purity calcite.

STABLE ISOTOPE DATA FOR CARBONATE MINERALS

Carbon- and oxygen-isotope ratios were analyzed from samples containing mixtures of primary and secondary calcite (Table 3.8). $\delta^{13}C$ values range between -1.8 to +1.5‰ (PDB), with the exception of one sample with $\delta^{13}C$ = -8.6‰ at Glenelg (820 mbmsl). At least three carbon reservoirs can contribute to measured $\delta^{13}C$ ratios: (i) primary fossil-derived carbon ($\delta^{13}C$ = 0‰), (ii) carbon produced by oxidation of organic material ($\delta^{13}C$ = -25‰) and (iii) carbon produced by fermentation of organic material ($\delta^{13}C$ = +16‰) (Irwin, 1980). The carbon-isotope ratios obtained for these samples (except $\delta^{13}C$ = -8.6‰) suggest that the calcite mixtures contain carbon primarily derived from a marine reservoir (Hudson and Friedman, 1976; Irwin, 1980). Petrographic recognition of abundant skeletal debris throughout each section is in agreement with carbon-isotope information.

Although the $\delta^{13}C$ values of many samples are dominated by primary marine carbon (Keith and Weber, 1964), some values are *either* slightly enriched or depleted in ^{13}C. Slightly lower or higher values suggest a very minor contribution of carbon derived from bacterial reactions such as the oxidation and/or fermentation of organic matter (Rosenfeld and Silverman, 1959; Irwin, 1980).

Although primary fossil-derived calcite dominates the carbon-isotope signature of secondary calcite, limits on the $\delta^{13}C$ of secondary calcite can be estimated assuming that secondary calcite comprises only 10 to 30% of any mixture. If the $\delta^{13}C$ of primary calcite is approximately 0‰ (Keith and Weber, 1964), the maximum $\delta^{13}C$ of calcite, containing a component of isotopically heavy carbon from organic fermentation, reaches +4.8‰. Conversely, the minimum $\delta^{13}C$ of calcite, containing isotopically light carbon from organic oxidation, reaches -5.9‰. However, given the potential variability of $\delta^{13}C$ in detrital carbonates (Gross, 1964), only very limited organic reactions may have occurred in these sequences despite significant burial depths.

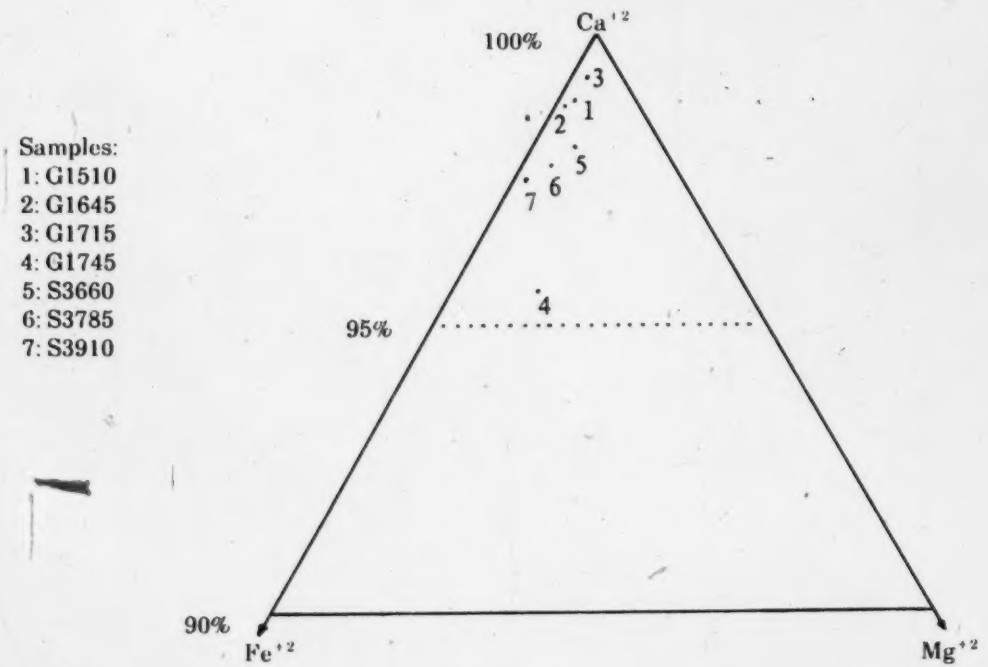

Figure 3.7
Major Cation Distributions in Secondary Carbonates from Glenelg J-48 and Shubenacadie H-100

TABLE 3.8. STABLE ISOTOPE DATA FOR CARBONATE MINERALS

SAMPLE	$\delta^{13}C$‰ (PDB)	$\delta^{18}O$‰ (SMOW)	$\delta^{18}O$‰ (PDB)	BURIAL TEMPERATURE (°C)	ESTIMATED TEMPERATURE (°C) ($\delta^{18}O$ fluid = 0‰)	ESTIMATED TEMPERATURE (°C) ($\delta^{18}O$ fluid = -3‰)
GLENELG J-48						
G820	-8.6	24.4	-6.2	25	46	30
G1100	-0.7	30.7	-0.1	37	15	3
G1290	-1.5	30.5	-0.3	41	15	3
G1480	-0.1	28.5	-2.3	47	25	11
G1630	0.0	28.3	-2.5	51	26	12
G1865	0.1	27.2	-3.6	57	31	17
G2070	0.7	24.1	-6.6	64	48	32
TRIUMPH P-50						
T2845	-1.6	31.0	0.2	29	13	2
T4220	-1.0	31.3	0.4	37	12	1
T5160	0.7	28.6	-2.2	51	24	11
T5670	0.3	26.9	-3.8	56	32	18
T5930	1.2	25.9	-4.8	57	38	23
T7080	0.4	26.8	-3.9	68	33	19

TABLE 3.8. CONTINUED

SAMPLE	$\delta^{13}C$ ‰ (PDB)	$\delta^{18}O$ ‰ (SMOW)	$\delta^{18}O$ ‰ (PDB)	BURIAL TEMPERATURE (°C)	ESTIMATED TEMPERATURE (°C) ($\delta^{18}O$ fluid = 0‰)	ESTIMATED TEMPERATURE (°C) ($\delta^{18}O$ fluid = -3‰)
ACADIA K-62						
A2304	0.3	29.1	-1.7	37	22	9
A2640	1.3	27.9	-2.9	45	28	14
SHUBENACADIE H-100						
S3140	-0.1	30.3	-0.6	44	17	4
S3665	1.4	27.7	-3.0	72	28	15
S3785	1.4	28.0	-2.8	79	27	14
S3910	-1.8	26.9	-3.9	86	33	18
S4040	1.0	27.4	-3.4	94	30	16
S4165	-1.0	26.1	-4.7	101	37	22

Ratios of oxygen-isotopes (versus SMOW) from mixtures containing greater than 70% detrital calcite, are plotted against present sample depth (Figure 3.8). These ratios ($\delta^{18}O$ = +32 to +24‰) indicate that calcite mixtures generally become depleted in ^{18}O with burial. Glenelg and Triumph follow burial trends which are similar below 1000 meters. The only two samples analyzed from Acadia plot at slightly higher $\delta^{18}O$ values at equivalent burial depths. In contrast, $\delta^{18}O$ values at Shubenacadie are enriched by over 2.5‰ compared to other wells at similar burial depths.

As samples contain primarily detrital calcite, consideration is given to its oxygen-isotope properties. Prior to any isotopic reequilibration, most marine fossils are in equilibrium with seawater at low temperatures (e.g., 5°C) (Keith and Weber, 1964; Anderson and Arthur, 1983). At high temperatures (i.e., >190°C), Clayton (1959) determined that calcite reequilibrates completely with ambient pore-fluids. However solid-state, isotopic reequilibration becomes less efficient at lower temperatures (i.e., <100°C) (Hudson and Friedman, 1976; Millikan et al., 1981).

Although mixtures containing abundant detrital calcite are not expected to exhibit extensive reequilibration over the temperature ranges examined, some reequilibration *must have occurred* to produce observed ^{18}O-depletion. Hudson and Friedman (1976) and Anderson and Arthur (1983) considered that ^{18}O-depletion is due to equilibration at: (i) higher temperatures and/or (ii) from isotopically light pore-fluids. Estimates of equilibration temperatures for calcite mixtures can be obtained using measured $\delta^{18}O$ values and estimates of $\delta^{18}O$ for pore-fluids, in the equation for the fractionation of calcite and H_2O proposed by Friedman and O'Neil (1977):

$$1000\ln\alpha = 2.78\times10^{6}(T^{-2}) - 2.89.$$

When evaluating the implications of ^{18}O-depletion with burial, a first approximation involves partial reequilibration of calcite in the presence of pore-fluids which have not undergone post-depositional ^{18}O-enrichment or depletion (i.e., remaining near 0‰). This is a reasonable assumption because extensive ^{18}O-depletion of pore-fluids in fine-grained sediments, by infiltration of meteroic waters through submarine aquifers originating on land, is not anticipated. These sections generally have remained in a marine setting along a passively subsiding margin. As well, compaction and geochemical (i.e., XRD, petrography) information suggest that pore-fluids have not circulated widely and have not evolved significantly from a

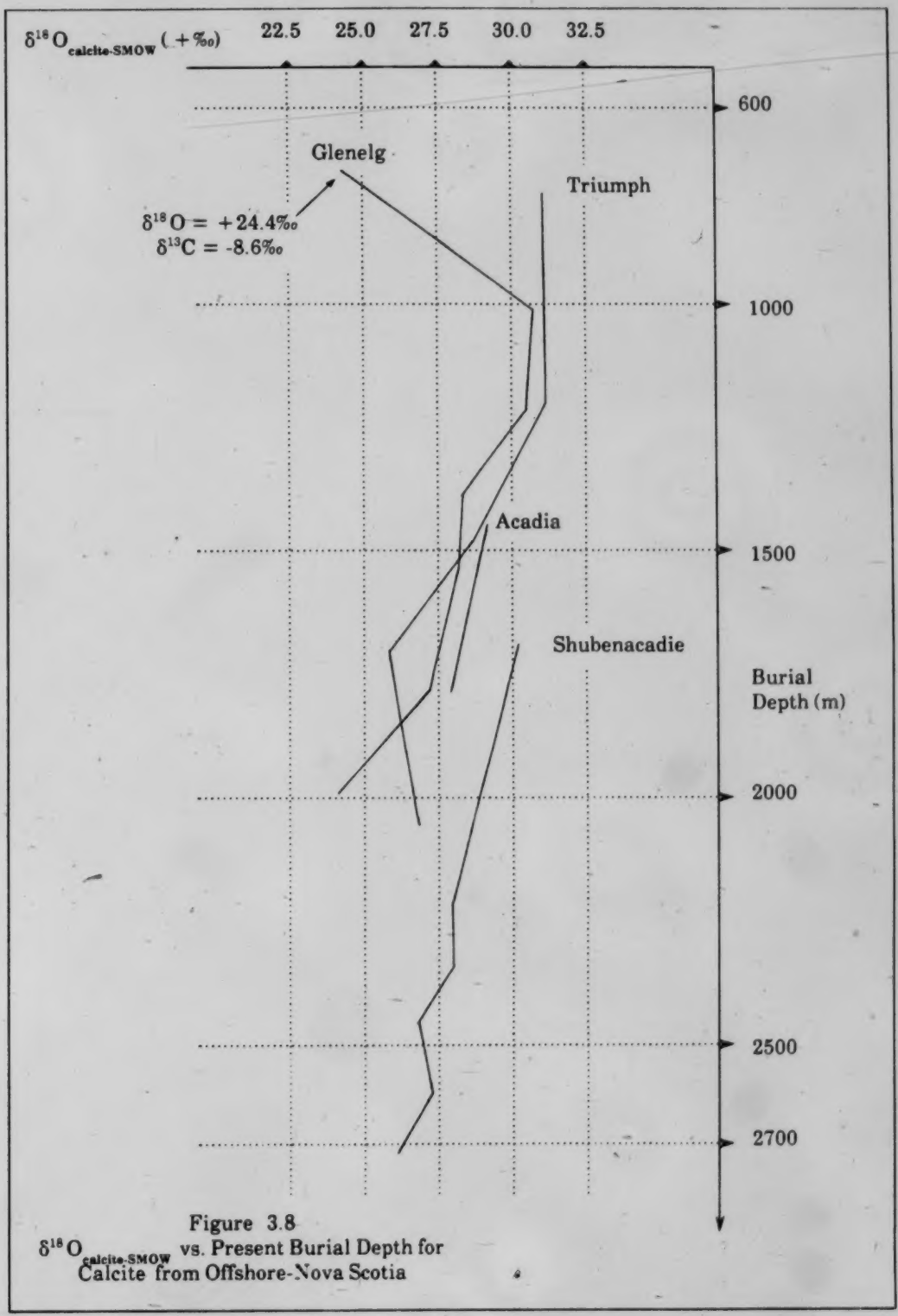

Figure 3.8
$\delta^{18}O_{calcite\text{-}SMOW}$ vs. Present Burial Depth for Calcite from Offshore-Nova Scotia

marine composition.

Assuming that the $\delta^{18}O$ of pore-fluids have remained near $0‰$, isotopic temperatures can be calculated that increase with depth, but remain lower than burial temperatures estimated by petrophysical methods (Table 3.8).

Minor ^{18}O-depletion of pore-fluids in fine-grained sediments, in response to early chemical reactions, has been reported during shallow burial to several hundred meters (Irwin, 1977). Assuming ^{18}O-depletion of pore-fluid by $3‰$, isotopic temperatures are now *very much lower* than petrophysical estimates of present burial temperatures (Table 3.8). Such low isotopic temperatures suggest a low degree of reequilibration of detrital calcite in agreement with Hudson and Friedman (1976) and Millikan et al. (1981).

The previous two cases suggest that if minimal reequilibration has occurred in these sequences, minor ^{18}O-depletion of pore-fluids is possible. Although ^{18}O-depletion is expected for shallowly buried pore-fluids, this constrasts with pore-fluids which have become ^{18}O-enriched in response to the transformation of smectite to illite during deep burial (Suchecki and Land, 1983). However, ^{18}O-depletion in pore-fluids may not be as great at Shubenacadie where calcite mixtures are more deeply buried and are slightly enriched in ^{18}O compared to other wells. Shubenacadie also exhibits a greater degree of illitization than other wells.

In summary, ^{18}O-depletion in detrital calcite with burial is likely due to partial isotopic reequilibration. $\delta^{18}O$ values suggest that pore-fluids may have become slightly depleted in ^{18}O by upto $3‰$.

At Glenelg (820 mbmsl), an isotopically light $\delta^{18}O$ value of $+24.4‰$ was measured, corresponding to the anomalous $\delta^{13}C$ value of $-8.6‰$ cited above. Considering that this sample is shallowly buried at present, these low isotopic ratios suggest that this calcite has equilibrated with pore-fluids containing a significant component of meteoric water.

D. DISCUSSION OF CHEMICAL DIAGENESIS

Fine-grained clastic rocks from the shelf and slope are composed primarily of detrital or transitional phases, without abundant authigenic constituents. Secondary and altered minerals indicate that Upper Cretaceous and Tertiary rocks from offshore Nova Scotia are *diagenetically immature*. In this discussion, a geochemical model is proposed to explain the diagenetic observations from these deeply buried, fine-grained rocks.

Understanding the nature of pore-fluid chemistry is important because it can significantly affect subsequent diagenetic processes (Hurst and Irwin, 1982). As most of these fine-grained rocks were deposited in marine environments, early pore-fluids were dominated by seawater. Throughout their burial history, pore-fluids probably have evolved only slightly from a marine precursor characterized by high, total dissolved solids and pH; the *maximum* ^{18}O-depletion is roughly -3‰. An exception may have occurred at the shallowest depths of Glenelg where meteoric influences are suggested by ^{18}O- and ^{13}C-depletion, possibly resulting from sub-aerial erosion.

During the earliest stages of burial, pyrite and calcite precipitated as secondary phases. Pyrite occurs both in framboidal and euhedral forms, suggesting that geochemical conditions varied during burial. Coleman and Raiswell (1981) attributed variations in pyrite habit to the early diagenetic transition from: (i) open marine-sulphate replenishment to (ii) a closed sulphate reservoir during sulphate reduction, occurring after only several meters of burial. This mechanism suggests that secondary pyrite is formed very early (i.e., neoformed). Early pyrite formation is corroborated texturally; the framboids precipitated in large micropores prior to extensive compaction.

In association with early pyrite, secondary calcite precipitated as an early phase: (i) rimming micropore walls and (ii) infilling micropores as interlocking rhombs. From textural relations, euhedral pyrite and secondary calcite appear to have formed contemporaneously during early burial. Calcite could have precipitated in response to: (i) increased pH through sulphate reduction and (ii) diminished calcite solubility as fluid temperatures increased with burial. $\delta^{13}C$ data support this interpretation; the $\delta^{13}C$ values are typical of carbonate derived from a marine reservoir with only a minor, organically-derived component. Stable isotope results do not suggest the occurrence of secondary carbonate minerals derived from higher temperature, organic reactions such as described by Irwin et al. (1977).

A possible mechanism for secondary calcite formation, modified from Irwin (1980), is:

$$CH_2O + 2SO_4^{-} + FeOOH + 14H^{+} + 11e^{-} \rightarrow FeS_2 + HCO_3^{-} + 8H_2O \quad (1).$$

Although mechanism (1) is active only in the presence of *free sulphate ions*, during its operation alkalinity is increased. By this mechanism, sulphate and amorphous iron compounds are reduced through bacterial oxidation of organic matter, producing HCO_3^{-1}, Fe^{2+} and HS^{-}. Pyrite precipitates in response to very low solubility over most pH ranges (pers. comm., A.

Crowe). During pyrite formation, calcite which precipitates is characterized by low iron contents because pyrite formation buffers available Fe^{2+} activity to very low levels. As well, bicarbonate ions, released into solution to form secondary calcite, have a slightly depleted ^{13}C signature. Secondary calcite also can incorporate ^{13}C-enriched carbonate being produced by early fermentation reactions (Rosenfeld and Silverman, 1959).

Mechanism (1) suggests that the formation of early pyrite and calcite is mutually dependent upon the Eh-pH conditions established by sulphate and amorphous iron reduction. Once free sulphate is consumed in a closed system, further oxidation or fermentation of organic material (CH_2O) produces CO_2 which dissolves into the pore-fluids of fine-grained rocks, changing their $\delta^{13}C$ values accordingly. Although Fe^{2+} may be available to crystallize in Fe-calcite because HS^- is buffered to low activities, increased CO_2 in solution stops carbonate precipitation, and possibly begins consuming *existing* carbonate to buffer the decline in pH according to the following mechanism:

$$CaCO_3 + CO_2 + H_2O \rightarrow Ca^{2+} + 2HCO_3 \text{ (Stumm and Morgan, 1981) (2).}$$

Mechanism (2) implies that: (i) pore-fluids become weakly acidic in response to organic reactions, (ii) calcite dissolution is directly proportional to pore-fluid flux, (iii) secondary Fe-carbonate is not precipitated during early organic activity and (iv) existing secondary calcite is likely an artifact of earlier neoformation during shallow sulphate reduction. In this way, existing detrital and neoformed calcite can be corroded during subsequent organic reactions, possibly accounting for a lack of secondary calcite throughout much of the section at Glenelg. The $\delta^{13}C$ value of residual calcite likely remains unchanged as observed.

The diagenesis of shelf and slope sections can be interpreted beyond early burial. The shelf section at Glenelg exhibits post-depositional alteration of detrital feldspars at present temperatures as low as 40°C. As well, <0.05 μm, 10 Å clay exhibits a trend toward increasing expandability with burial (depotassification of mica) not observed in coarser 10 Å clays or fine clays from other wells. Complementing these observations, neoformed calcite is uncommon at Glenelg.

Acidity is a likely cause of mineral dissolution because high, total dissolved solid concentrations, typical of marine-derived pore-fluids, preclude solubility disequilibria as a dominant influence on mineral dissolution (Hurst and Irwin, 1982). Fluid acidity could have been generated by solution of CO_2, produced by organic reactions, into pore-fluids during

deeper burial. Possibly, pore-fluid acidity was more effective at Glenelg because of greater pore-fluid mobility than elsewhere on the outer shelf or slope.

The incipient dissolution of deeply buried, detrital feldspar observed only at Glenelg can be described by an incongruent reaction mechanism cited by Hurst and Irwin (1982):

$$2KAlSi_3O_8 + 2H^+ + H_2O \rightarrow Al_2Si_2O_5(OH)_4 + 4SiO_2 + 2K^+ \quad (3).$$

This mechanism suggests that feldspar is dissolved in the presence of weakly acidic pore-fluids, producing kaolinite (aluminum conservation) and evolving silica and K^+. However Surdam et al. (1984) suggested that aluminosilicate dissolution by carbonic acid is not viable because Al^{3+} can be transported; unrealistically high pore-fluid fluxes would be required to compensate for low Al^{3+} solubility in the presence of this acid. They suggested that aliphatic acids, which form in response to kerogen maturation, are responsible for feldspar dissolution by increasing Al^{3+} solubility in response to complexation with oxalate anions ($C_2O_4^{2-}$).

At Glenelg, dissolution cavities in feldspar do not contain abundant authigenic kaolinite. This suggests that Al^{3+} *was transported* by complexing agents away from sites of pitting in contrast to reaction (3). *Possibly*, kerogen maturation and associated organic acid production were initiated in mudrocks at Glenelg at temperatures as low as 40°C (53°C if buried more deeply). However, although early oxalate production from kerogen oxidation *may have occurred* at cool burial temperatures, pitting could have been inhibited by reaction of oxalate anions with calcite to produce Ca-oxalate salt. Preferential consumption of calcite (Glenelg) by oxalate anions would have reduced Al^{3+} mobility.

In contrast to Glenelg, Triumph and Shubenacadie are characterized by: (i) intact secondary calcite having a marine $\delta^{13}C$ signature, (ii) unaltered feldspar and (iii) 10 Å clay of low expandability. Preservation of these phases suggests that pore-fluids were not highly corrosive. However, even if limited organic reactions were occurring, pore-fluid mobility was probably diminished, inhibiting flushing of constituent grains by weakly acidic fluids.

The nature of expandable clay alteration also can characterize the style of diagenesis in these fine-grained rocks. Shubenacadie is discussed first because this section exhibits the greatest degree of clay alteration. Results from <0.1 μm XRD data suggest that below 3140 mbmsl, 17 Å clay has undergone *limited transformation* to a more highly ordered, mixed-layer structure (i.e., illitization). Despite the presence of detrital illite and kaolinite, XRD results suggest that randomly ordered, smectite interstratification in 17 Å clay has decreased from

>75% at 3140 mbmsl to <55% at 4040 mbmsl. As well, the 17 Å clay polytype has changed with burial from essentially pure montmorillonite upsection to a mixture with some beidellite downhole. From this evidence, illitization appears to be at *a preliminary stage* on the lower slope.

The illitization reaction may be ongoing to some degree via layer by layer transformation of smectite to illite. Part of the process may require that montmorillonitite transform to an intermediate, smectitic mixture containing a beidellitic component by the following mechanism:

$$Si_8(Al,Mg)_4(OH)_4O_{20}\ (\text{Montmorillonite}) + xAl^{3+} \rightarrow$$
$$(Si,Al)_8(Al,Mg)_4(OH)_4O_{20}\ (\text{Beidellitic Smectite}) + xSi^{4+}\ (4).$$

This mechanism requires that layer-charge density increase via isomorphous substitution in the tetrahedral layer with depth. However appreciable cation fixation (e.g., K^+) *is not* anticipated. In contrast to Boles and Franks (1979), an illitization mechanism involving mobile Al^{3+} is preferred because: (i) Al^{3+} can apparently be complexed and (ii) illitization by tetrahedral substitution may be easier at lower temperatures.

Elemental data confirm that below 3140 mbmsl, certain cations are held within interlayer sites in <0.1 μm clay (i.e., specifically K^+). Even in regions of high kaolinite content below 3140 mbmsl, increases in Al/Si ratios with burial indicate that progressive illitization has occurred. Yet throughout Shubenacadie, K/(Si/Al) and Al/Si ratios are most similar to smectitic phases having a low degree of isomorphous substitution. This was determined by comparison of elemental data from Shubenacadie with standard montmorillonites and micas. Presuming that partial illitization has occurred at Shubenacadie, collapse of interlayer sites may have resulted in only minor expulsion of Ca^{2+}, Fe^{2+} and other cations into the pore-fluids of fine-grained clastic rocks (Boles and Franks, 1979).

Oxygen-isotope data from calcite at Shubenacadie indicate that over the temperature range examined, calcite samples are slightly enriched in ^{18}O compared to other wells. As partial isotopic reequilbration is likely, ^{18}O-enrichment suggests that pore-fluids at Shubenacadie were not as depleted as elsewhere, perhaps because of fluids derived from partial illitization (Suchecki and Land, 1983).

Examination of the slightly coarser, <0.2 μm fraction confirms that diagenetic clay alteration is most common only in a small portion of any slope sample. In this size range, 17 Å

clay generally contains a higher proportion of smectite interstratification, with less illitization than in the <0.1 μm material. This observation implies that <0.2 μm clay has remained comparatively inert.

From Glenelg, <0.05 μm size clay exhibits a weaker degree of illitization than on the lower slope. This is anticipated as maximum burial temperatures of Upper Cretaceous and Tertiary sequences are cooler than at Shubenacadie, even when adjusted for possible erosion.

In contrast, smectite interstratification in <0.2 μm, 17 Å clay increases with depth at Acadia. Highly smectitic 17 Å clay is observed throughout the entire size-fraction in all samples. In brief, <0.2 μm clay from Acadia appears to be diagenetically inert relative to similar size-fractions from the lower slope or outer shelf. Correspondingly, although Acadia is situated physiographically between Glenelg and Shubenacadie, below roughly 2304 mbmsl present burial depth, Acadia contains 17 Å clay which is *more randomly interstratified* than similar age clays from the previous two wells. This trend is corroborated by examination of <0.1 μm clay data from Triumph. A lack of illitization in the latter sections suggests diagenetic inmaturity relative to Glenelg or Shubenacadie (i.e., lower burial temperatures, less compaction).

When examining illitization trends across the outer shelf and slope, consideration must be given to the source of K^+ and Al^{3+} required for this transformation. Coarser size-fractions from Glenelg, Acadia and Shubenacadie contain highly illitic, 10 Å clay. However, with the exception of <0.05 μm 10 Å clay from Glenelg, only minimal depotassification was observed in the lower parts of Glenelg and Shubenacadie. Recognition of unaltered 10 Å clay suggests that mica alteration has not contributed significant K^+ to pore-fluids from the Nova Scotia shelf or slope. As well, these sections are feldspar-poor. Petrographic work indicates that K-feldspar is unaltered and shows only minor evidence of dissolution at Glenelg. As a result, K-feldspar also *is not* likely a major source of K^+ and Al^{3+} within this stratigraphic sequence.

If limited illitization is occurring, K^+ and Al^{3+} required for transformation may be transported from more deeply buried units. At Glenelg, this is possible because this section is thought to have undergone a greater degree of compaction. As well, Glenelg is underlain by coarser clastic units which may have undergone sufficient feldspar dissolution to provide cations required for illitization.

Cation transport from depth likely is less important at Shubenacadie where permeabilities are thought to be lower. Probably, fluid movement has been inhibited through such a thick sequence of weakly overpressured, fine-grained rocks. Throughout the burial sequence, this is suggested by intact microfossils which are either open or partly filled with secondary calcite. In specific instances, differential filling of microporosity occurs within a few meters of burial. As well, Shubenacadie is not thought to be underlain by appreciable sediment which is K-feldspar rich.

Diagenesis of the clay fraction may be summarized by noting that ***only the finest expandable constituents are diagenetically active***. Although smectitic phases contained within the original detrital input were mixed with significant amounts of illite and kaolinite, sufficient 17 Å clay is thought to have existed, to be available for illitization under suitable conditions. Inhibition of illitization may be a response to: (i) low burial temperatures, (ii) poor sources for *in-situ* K^+ and (iii) low pore-fluid fluxes.

Illitization has progressed further on the lower slope than on the outer shelf; maximum burial temperatures are higher on the lower slope. However examination of temperatures measured at various stages of illitization between each well do not reveal strong temperature dependence. Diagenesis in these rocks appears to be most *significantly influenced* by pore-fluid interactions controlled by undercompaction and associated high fluid pressures.

Illitization reactions may expel cations and silica into the pore-fluids of fine-grained rocks. However, extensive expulsion is not likely to have occurred even in the most diagenetically active sections (Glenelg and Shubenacadie) because this process is at an early stage.

The only indication of late stage exposure and non-burial related influences occurs in the shallowest section at Glenelg. $\delta^{18}O$ and $\delta^{13}C$ values for calcite suggest isotopic exchange with isotopically light pore-fluids, containing some organically-derived carbon. The possibility of meteoric influence agrees with the suggestion in Chapter 2 of erosion in the upper section at Glenelg.

E. SUMMARY OF MINERALOGICAL AND GEOCHEMICAL STUDY

1. Secondary pyrite and calcite were precipitated during very shallow burial. A possible reaction mechanism is the reduction of sulphate and amorphous iron through bacterial oxidation of organic material. During such an event:
   a. Pore-fluids are characterized by low Eh and high pH (alkalinity);
   b. Upon consumption of SO_4^{2-}, pore-fluid chemistry becomes mildly acidic as dissolved CO_2 is generated by organic reactions. Subsequent ^{13}C-enrichment or depletion is not recorded in secondary carbonate cements because pore-fluid chemistry was not conducive to carbonate precipitation.
2. Corrosion of detrital aluminosilicates is recognised only at Glenelg:
   a. Although pore-fluids likely became acidic during shallow burial, extensive feldspar dissolution did not occur until the onset of kerogen maturation;
   b. Alteration of detrital feldspars without precipitation of abundant kaolinite indicates that complexing agents removed small amounts of Al^{3+} in solution. Fluid flux may have been sufficient in this sequence to flush away Al^{3+} complexes.
3. After some 1000 meters burial, partial illitization reactions are observed at Glenelg and Shubenacadie, but not at Triumph and Acadia. At Glenelg and Shubenacadie, incomplete illitization resulted in persistance of 17 Å clay toward the bottom of each sequence:
   a. At Shubenacadie, smectite is less randomly ordered with depth reaching approximately 50% smectite downsection. As well, montmorillonite is associated with beidellite below 3140 mbmsl. In agreement, elemental data indicate increases in Al/Si and K/(Si/Al) ratios with burial. $\delta^{18}O$ data suggest that pore-fluids are less depleted in ^{18}O than other wells, commensurate with partial illitization;
   b. At Glenelg, partial illitization is recognised in <0.05 μm clay. However the transformation has: (i) not proceeded as far as at Shubenacadie and (ii) is not recognised as strongly in coarser fractions.
4. The diagenesis of fine-grained rocks on the Nova Scotia shelf and slope is immature:
   a. Detrital constituents do not exhibit extensive depotassification. Probably, abundant K^+ was not derived from within these sections;
   b. Isotopic analyses of carbonates suggests that pore-fluids were of seawater composition

in $\delta^{18}O$ ($0/_{00}$), or have undergone minor ^{18}O-depletion. Significant evolution from an initial marine precursor has not occurred;

c. Inhibition of mineral alteration during intermediate burial suggests that: (i) pore-fluids were not rich enough in required cations (i.e., K^+ and Al^{3+}), and (ii) ambient conditions (i.e., pH, temperature) were not favorable for mineral transformation.

5. Temperature may not be a major control on illitization of deeply buried shaly sequences. Pore-fluid mobility may have strongly influenced authigenic mineral precipitation, detrital grain corrosion and clay transformation.

6. Recognition of isotopically light $\delta^{18}O$ and $\delta^{13}C$ values for calcite at the top of Glenelg provide supporting evidence for late stage erosion of this sequence.

F. BIBLIOGRAPHY

Anderson, T.F. and Arthur, M.A., 1983, Stables isotopes of oxygen and carbon and their application to sedimentological and paleoenvironmental problems: *in* Stable Isotopes in Sedimentary Geology, Soc. of Economic Paleontologists and Mineralogists Short Course Notes No. 10, Dallas, TX., p. 1-1 - 1-149.

Boles, J.F. and Franks, S.G., 1979, Clay diagenesis in Wilcox Sandstones of southwest Texas: implications of smectite diagenesis on sandstone cementation: Jour. Sedimentary Petrology, v. 49, p. 55-70

Clayton, R.N., 1959, Oxygen isotope fractionation in the system calcium carbonate-water: Jour. Chemical Physics, v. 30, p. 1246-1250.

Coleman, M.L. and Raiswell, R., 1981, Carbon, oxygen and sulphur isotope variations in concretions from the Upper Lias of N.E. England: Geochimica et Cosmochimica Acta, v. 45, p. 329-340.

Craig, H., 1957, Isotopic standards for carbon and oxygen and correction factors for mass spectrometer analysis of carbon dioxide: Geochimica et Cosmochimica Acta, v. 12, p. 133-149.

Craig, H., 1961, Standards for reporting concentrations of deuterium and oxygen-18 in natural waters: Science, v. 133, p. 1833-1834.

Eberl, D., 1978, The reaction of montmorillonite to mixed-layer clay: the effect of interlayer alkalai and alkalai earth cations: Geochimica et Cosmochimica Acta, v. 42, p. 1-7.

Friedman, I. and O'Neil, J.R., 1977, Compilation of stable isotope fractionation factors of geochemical interest: *in* M. Fleischer, ed., Data of Geochemistry, U.S. Geological Survey Professional Paper, 440-KK, 6th ed.

Gibbs, R.J., 1977, Clay mineral segragation in the marine environment: Jour. Sedimentary Petrography, v. 47, p. 237-243.

Gross, M.G.; 1964, Variations in the O^{18}/O^{16} and C^{13}/C^{12} ratios of diagenetically altered limestones in the Bermuda Islands: Jour. Geology, v. 72, p. 170-194.

Hower, J., 1981, X-ray diffraction identification of mixed-layer clay minerals: *in* F.J. Longstaffe, ed., Clays and the Resource Geologist, Mineralogical Assoc. Canada Short Course Notes, Calgary, AB. p. 39-59.

Hudson, J.D. and Friedman, I., 1976, Carbon and oxygen isotopes in concretions: relationship to pore-water changes during diagenesis: *in* J. Cadek and T. Paces, eds., Proceedings of the International Symposium on Water-Rock Interaction, Czechoslovakia, 1974, Prague Geological Survey, p. 331-339.

Hurst, A. and Irwin, H., 1982, Geological modelling of clay diagenesis in sandstones: Clay Minerals, v. 17, p. 5-22.

Irwin, H., 1980, Early diagenetic carbonate precipitation and pore fluid migration in the Kimmeridge Clay of Dorset, England: Sedimentology, v. 27, p. 577-591.

Irwin, H, Curtis, C. and Coleman, M., 1977, Isotopic evidence for the source of diagenetic carbonates formed during burial of organic-rich sediments: Nature, v. 269, p. 209-213.

Jackson, M.L., 1961, Soil Chemical Analysis - Advanced Course, 2nd Ed.: published by author, Madison, WI., 895 pp.

Keith, M.L. and Weber, J.N., 1964, Carbon and oxygen isotope composition of selected limestones and fossils: Geochimica et Cosmochimica Acta, v. 28, p. 1787-1816.

McCrea, J.M., 1950, On the isotopic chemistry of carbonates and a paleotemperature scale: Jour. Chemical Physics, v. 18, p. 849-857.

Millikan, K.L., Land, L.S. and Loucks, R.G., 1981, History of burial diagenesis determined from isotopic geochemistry, Frio Formation, Brazoria County, Texas: Am. Assoc. Petroleum Geologists Bulletin, v. 65, p. 1397-1413.

Reynolds, R.C., 1980, Interstratified clay minerals: *in* G.W. Brindley and G. Brown, eds., Crystal Structures of Clay Minerals and Their X-ray Identification, Mineralogical Soc. Monograph No. 5, p. 249-303.

Rosenfeld, W.D. and Silverman, S.R., 1959, Carbon isotope fractionation in bacterial production of methane: Science, v. 130, p. 1658-1659.

Spiers, G.A., Pawluk, S. and Dudas, M.J., 1984, Authigenic mineral formation by solodization: Can. Jour. Soil Science, v. 64, p. 515-532.

Sfodoń, J., 1980, Precise identification of illite/smectite interstratification by X-ray powder diffraction: Clays and Clay Minerals, v. 28, p. 401-411.

Sfodoń, J., 1981, X-ray identification of randomly interstratified illite-smectite in mixtures with discrete illite: Clay Minerals, v. 16, p. 297-304.

Sfodoń, J., 1984, X-ray powder diffraction identification of illitic minerals: Clays and Clay Minerals, v. 32, p. 337-349.

Suchecki, R. K. and Land, L.S., 1983, Isotope geochemistry of burial-metamorphosed volcanogenic sediments, Great Valley sequence, northern California: Geochimica et Cosmochimica Acta, v. 47, p. 1487-1499.

Surdam, R.C., Boese, S.W. and Crossey, L.J., 1984, The chemistry of secondary porosity: *in* D.A. McDonald and R.C. Surdam, eds., Clastic Diagenesis, Am. Assoc. Petroleum Geologists Memoir 37, p. 127-149.

Stumm, W. and Morgan, J.J., 1981, Aquatic Chemistry - An Introduction Emphasizing Chemical Equilibria in Natural Waters: John Wiley and Sons, New York, N.Y., 780 pp.

IV. GENERAL DISCUSSION AND CONCLUSIONS

A. INTRODUCTION

Considering information and concepts presented in previous chapters, a diagenetic model is proposed for fine-grained Upper Cretaceous and Tertiary sequences from offshore-Nova Scotia. This model then can be compared to models of the diagenesis of fine-grained rocks developed from other passive margins. Such a comparison can reveal whether similarities exist between the style of diagenesis from the Nova Scotia shelf and slope, and styles from other settings. As well, a critical appraisal of the Nova Scotia model may provide new insights into physical and chemical processes active during burial diagenesis of shaly sediments in such a geologic setting.

B. MODEL OF THE DIAGENESIS OF FINE-GRAINED CLASTIC ROCKS IN OFFSHORE-NOVA SCOTIA

Tectonic information presented in Chapter 1 established a framework for studying the diagenesis of fine-grained clastic rocks from offshore-Nova Scotia. In this framework, continuous deep-marine deposition of very fine-grained sediments resulted in high initial porosities containing pore-fluids of marine character. The thickest sequences of fine-grained Upper Cretaceous and Tertiary rocks were deposited along the outer shelf and slope. For this reason, investigation of burial diagenesis in fine-grained rocks is best suited to sequences examined in this study.

Throughout this region, subsidence has diminished since the Early Cretaceous. As a result, geothermal gradients are presently low and stable so that current burial conditions reflect maximum temperatures experienced throughout the history of these rocks. In general, uplift and exposure are not suggested from offshore-Nova Scotia sequences. Only at the shallowest depths of the most landward well (Glenelg) are exposure and meteoric influence indicated.

As uplift generally has not affected these sequences, local tectonic history has resulted in the strong influence of early compaction. Tectonically controlled deposition of fine-grained sediment, in a marine setting, has resulted in sections that are poorly compacted despite burial.

On the Nova Scotia slope, appreciable undercompaction occurs in sections that are overlain by hundreds' of meters of *unconsolidated material*. The presence of abnormally high porosities despite burial suggests that slightly higher fluid pressures occur in certain intervals. As a result, these fine-grained rocks are: (i) somewhat closed to upward fluid circulation and are (ii) not suitably compacted despite present burial conditions. Compaction characteristics of these sequences are immature compared to sections having less porosity variability. Weak compaction in these deeply buried slope sequences may inhibit pore-fluid flux from outside the system and suppress geothermal gradients resulting in cool temperatures at maximum burial.

Exceptions to this trend are observed at Glenelg and the lower part of Shubenacadie. These sections exhibit a more mature style of compaction resulting in: (i) higher maximum burial temperatures, (ii) increased fluid flux in response to compaction and dewatering and (iii) a greater potential for fluid circulation because hydrodynamic barriers related to undercompaction are diminished.

Chemical alteration of fine-grained clastic rocks from the Nova Scotia shelf and slope was strongly influenced by compaction. Chemical diagenesis is immature because: (i) detrital phases dominate whole rock mineralogy and (ii) early diagenetic phases persist to great depths in certain sequences (i.e., Shubenacadie).

Mineral phases resulting from early diagenesis suggest a strong marine influence, indicative of precipitation in sediments that were neither deeply buried nor significantly uplifted (Coleman and Raiswell, 1981). During the *earliest stages* of diagenesis, necessary ingredients for the formation of secondary minerals were derived from ambient pore-fluids of low mobility. No deeply derived fluid flux was required to supply Fe^{2+}, Ca^{2+}, HS^- and HCO_3^- for the formation of neoformed pyrite and calcite.

An exception to the trend of early phase preservation occurs at Glenelg. Aside from calcareous mudstone units, secondary calcite is uncommon. As well, preliminary feldspar dissolution is recognised. Sources of required acidity include: (i) CO_2 produced by oxidation and/or fermentation of organic material and (ii) production of aliphatic acids by kerogen maturation or oxidation. Early calcite remnants suggest that the ambient pH of pore-fluid was in a moderate to high range designated as the optimum range for aliphatic acid production. Possibly, acid production was not far advanced.

Immaturity of chemical diagenesis is suggested further by clay mineralogy. In these sequences, most clay minerals are either detrital or have undergone limited mineralogic transformation. For example, although montmorillonite is the dominant smectite polytype throughout most of these sections, some degree of smectite transformation to a more illitic, mixed-layer clay is recognised.

As discussed in Chapter 3, illitization of 17 Å clay has not been extensive. This transformation is most readily observed in very fine size-fractions from Glenelg and the deeper section at Shubenacadie. The proportion of interstratified smectite diminishes downsection to roughly 55% at temperatures ranging from 64° to 100°C. At both sections, the onset of illitization occurs at roughly 40°C. From this information, variations in the ratios of smectite:illite abundance likely are due to depositional clay distributions, rather than a response to diagenetic transformation of smectite.

At Acadia and Triumph, diagenetic immaturity is suggested by complete absence of increasing illitization, despite burial depths of approximately 2000 meters and maximum downhole temperatures as high as 68°C.

Illitization patterns permit additional speculation about the diagenetic style of outer shelf and slope sequences. Considering the illitization mechanism discussed in Chapter 3, a source of K^+ and Al^{3+} is required to fuel the reaction. Although these sections do not contain abundant detrital K-feldspar, at Glenelg K-feldspar dissolution and leaching of very fine (<0.05 μm) 10 Å clay may have contributed a portion of those cations required for the transformation. However, the advanced degree of compaction evident at Glenelg may also have generated pore-fluid flux, stimulating illitization of smectite.

At Shubenacadie, absence of both K-feldspar dissolution and 10 Å clay leaching suggests that K^+ and Al^{3+} were provided mainly by flushing with pore-fluids bearing sufficient concentrations of appropriate cations. However, recognition of: (i) undercompacted lenses capable of inhibiting upward fluid mobility and (ii) a lack of elemental evidence supporting addition of K^+ to whole rock samples (from deeply buried sources), suggests that K^+ and Al^{3+} derived from fluid flux, in response to progressive compaction of more deeply buried, fine-grained rocks, are not abundant.

A mechanism of illitization requiring K^+ and Al^{3+} from expelled pore-fluids, possibly from depth, provides an explanation for inhibition of 17 Å clay illitization at Acadia and

Triumph. As these sections are suspected of being poorly compacted, possibly these units were not exposed to sufficient fluid flux to permit illitization. The compaction character of these sequences may have exercised more influence over their diagenetic styles than chemical or temperature considerations. Apparently Triumph has not undergone extensive clay diagenesis, despite maximum burial depths in excess of 2000 meters at temperatures of approximately 67°C.

C. DIAGENESIS OF FINE-GRAINED CLASTIC ROCKS IN OTHER BASINS

Studies of the diagenesis of fine-grained rocks have been conducted in diverse geologic settings. In this section, highlights of investigations from several basins are presented and compared with the model outlined previously for the Nova Scotia shelf and slope. From this comparison, it is possible to assess: (i) whether the Nova Scotia diagenetic model is reasonable given its geological setting and (ii) whether any important differences exist which may provide additional insights into diagenetic mechanisms in fine-grained rocks.

The diagenesis of mudrocks has been investigated in detail along the U.S. Gulf Coast. Models developed from this basin emphasize *chemical diagenesis*, specifically the transformation of smectite minerals to illitic phases in response to burial.

A physical approach to burial-related collapse of expandable clays was taken by Burst (1969). Considering changes in smectite expandability as an important diagenetic reaction in mudrocks, smectite collapse was attributed to loading affects resulting from overburden pressure. From observations, expandable clay collapse and dewatering become more complete with increasing burial depth.

During a *geochemical* examination of deeply buried mudrocks (14,000 ft., 4267 m thickness), Perry and Hower (1970) described the transformation of smectite to illite reaching 20% expandable layers in <1.0 μm clay. The lowest degree of expandability was measured at 3292 meters (10,518 ft.) below which no further collapse was observed. Perry and Hower (1970) attributed smectite collapse to fixation of K^+ into smectite-interlayer sites in response to increasing, negative layer charge. A concomitant decrease in the abundance of detrital illite suggested to Perry and Hower (1970) that 10 Å clay might be a source of K^+. As the degree of illitization measured from offshore-Louisiana was less than at equivalent depths from on-land wells from Texas, Perry and Hower (1970) suggested that temperature (i.e., geothermal gradient) was the greatest control on smectite illitization.

A more comprehensive, geochemical model of mudrock diagenesis was proposed by Hower et al. (1976). From examination of very fine clay-fractions, a trend of illitization was described reaching 20% interstratified expandable layers at a maximum temperature of 95°C. Coupled with belief of temperature dependence of the transformation, Hower et al. (1976) observed changes in the mineralogical and chemical character of whole rock, deeply buried samples. Very fine fractions are observed to become enriched in K_2O and Al_2O_3, and depleted in SiO_2 with progressive burial. As well, whole rock XRD indicates that K-feldspar and calcite disappear over the depth range at which illitization ceases.

Hower et al. (1976) proposed that smectite illitization, resulting from isomorphous substitution of Al^{3+} for Si^{4+}, proceeded by increased 2:1 layer-charge density so that K^+ was fixed into interlayer sites. Cations required for illitization likely were derived from K-feldspar dissolution. Acidity required to leach detrital, aluminosilicate grains resulted in calcite dissolution. A sink for Mg^{2+} and Fe^{2+}, thought to be released from smectite octahedral layers, was assigned to chlorite formation in deeper parts of the burial sequence. However a specific mechanism of chlorite formation was not discussed.

Possibly, pore-fluid flux was an important aspect of mudrock diagenesis because SiO_2, from feldspar dissolution and isomorphous substitution, could have been emitted into mudrock pore-fluids. Hower et al.'s (1976) model required sufficient pore-fluid mobility to supply necessary cations for the reaction and to remove reaction products (i.e., SiO_2). Unlike previous studies, this investigation proposed a comprehensive model integrating temperature and whole rock influences on mudrock diagenesis to create the image of an active, but closed, geochemical system operative during deep burial.

Yeh and Savin (1977) examined light stable isotopic properties of various mudrock constituents. Their study corroborated the model cited previously by suggesting that illitization is a real process which may have been active during burial along the Gulf Coast. The $\delta^{18}O$ ratios of various clay size-fractions were measured and converged to uniform and lighter values upon deeper burial. As well, Yeh and Savin (1977) measured the isotopic signature of very fine-grained quartz and quartz rims, and its enrichment in ^{18}O relative to detrital phases. By determining that a quartz-smectite/illite isotopic geothermometer could estimate present burial temperatures above 85°C, they *suggested* that very fine quartz was authigenic and had formed near equilibrium with illitized smectite (Yeh and Savin, 1977; Eslinger et al., 1979). This

suggestion supports a model of illitization through cation fixation in response to K-feldspar dissolution and SiO_2 emission into pore-fluids (Hower et al., 1976).

An alternative model of progessive illitization was proposed by Boles and Franks (1979) for Gulf Coast diagenesis. To account for large amounts of authigenic cement in particular sandstone units, they devised a model which would conserve Al^{3+} in 2:1 layer phases by consuming smectite layers during illitization. Regardless of whether this or Hower et al.'s (1976) model is correct, apparently both reactions consume K^+ and emit cations and SiO_2 into ambient pore-fluids.

Previously cited studies considered mudrock diagenesis to be an ongoing process with burial. However, Morton (1985) has offered a model of *punctuated illitization* as an alternative to classic models of progressive illitization. From a Gulf Coast burial sequence exhibiting an irregular illitization trend, Rb-Sr age dating of mixed-layer clay indicated that all phases equilibrated at roughly the same time along that trend, shortly after initial burial. Morton (1985) suggested that illitization occurred at shallower depths with maximum burial of <1200 meters (i.e., low temperature), prior to deep burial. Possibly, illitization was initiated at shallow depths in response to flushing by meteoric water during sub-aerial exposure. Meteoric fluids encouraged illitization because of increased acidity and higher feldspar solubility. During subsequent marine transgression, seawater influx inhibited further smectite transformation resulting in preservation of an ancient trend of decreasing smectitic interstratification. Morton (1985) considered recognition of mixed-layer clays containing 50% smectite interstratification at temperatures in excess of 100°C as evidence of possible inhibition of illitization.

As well, significant variations in the style of diagenesis can be recognised between depositional basins. In a general evaluation of the effects of smectite dehydration upon structural development, Bruce (1984) discussed the variability of temperatures over which illitization apparently was initiated. Even within certain basins, onset temperatures of smectite illitization are widely variable. At the Louisiana Gulf Coast, the onset of illitization occurs at temperatures ranging from 71°C to 163°C. In contrast, temperatures for the onset of illitization from in Brazos River area, Texas have a narrower, but higher, range from 93° to 138°C. Louisiana smectite contains an appreciable beidellitic component, in contrast to a predominantly montmorillonitic mineralogy at Texas (Bruce,1984). If illitization proceeds by tetrahedral substitution, as suggested by Hower et al. (1976), the localized occurrence of

beidellite may assist illitization.

An extreme temperature for initial illitization of 150°C was measured at the Niger Delta. This delta is characterized by: (i) an abundance of kaolinite relative to smectite and (ii) a brackish to marine pore-fluid composition.

The wide variability of temperatures assigned to the initiation of illitization was attributed by Bruce (1984) to the diversity of whole rock mineralogy and the specific type of smectite present. Close correlation was observed between the disappearence of K-feldspar with burial and the termination of illitization. Although Bruce (1984) recognised that undercompaction occurs in certain fine-grained sequences, consideration was not given to the influence of variations of pore-fluid chemistry and pressure upon diagenesis.

Smectite diagenesis from on-land wells in the Rhinegraben was considered by Heling (1974). Rhinegraben mudrocks of Tertiary age were deposited in brackish to marine environments to present burial thicknesses reaching 2800 m. Significant amounts of evaporitic material is associated with these mudrocks. In these sequences, smectite apparently was not observed at burial temperatures exceeding 70° to 80°C in mudrocks of marine character. In mudrocks of brackish origin, smectite only was observed at temperatures below 40°C. The absence of smectite at higher temperatures was attributed to diagenesis. Heling (1974) considered the greater degree of illitization observed at lower temperatures in brackishly derived mudrocks to be a response to higher permeabilities. Higher permeabilities may have permitted a greater degree of K^+ influx, facilitating illitization.

Although Heling (1974) did not measure significant variations in the major ion concentrations of certain species in pore-fluids, illitization may have been encouraged by pore-fluid composition, when compared to other geological settings of greater marine character. On land sequences may have experienced greater concentrations of specific cations required for illitization through: (i) association with evaporitic facies, (ii) higher fluid acidity and lower total dissolved solids resulting in mineral dissolution and (iii) higher ambient permeabilities than in predominantly marine mudrocks.

In a comparison of diagenetic styles between various on-land sequences, van Moort (1971) considered the diagenesis of deltaic mudrocks from Louisiana and marine, shelf-derived mudrocks from Papua, New Guinea. From the two Papuan wells, 60% smectite interstratification was measured in $<2.0\ \mu m$ clay down to 3100 to 3300 meters (10,200 - 10,800

ft.). Below this depth, a constant level of 10%-20% expandability was measured to TD. At Louisiana, similar trends of smectite interstratification were recognised below 3061 meters (10,045 ft.). Generally, highly smectitic phases are absent below 2740 meters (9,000 ft.). As well, lower K_2O and MgO contents were measured in clays from Papua than at Louisiana. Chemical discrepancies and the appearance of chlorite were attributed to detrital influences. However van Moort (1971) did suggest that higher K/Mg ratios (100/1) in initial pore-fluids (versus seawater) encouraged illitization. Yet, a specific mechanism for generating very early variations in pore-fluid composition was not offered.

Studies cited previously have considered primarily on-land sequences of either marine or brackish origin. Dypvik (1983) presented results of diagenetic studies of mudrocks from offshore wells from the North Sea. Sediments considered in Dypvik's (1983) study are hemipelagic and of Cretaceous to Tertiary age. Illitization was considered to be strongly controlled by temperature, so that specific levels of interstratification are recognised at certain temperatures. At 60° to 75°C, smectite interstratification was thought to have dropped to <50%. From 80° to 100°C, mixed-layer clay was characterized by <30% smectite and the absence of a discrete 17 Å phase. According to Dypvik (1983), the level of diagenesis recognised in the most deeply buried mudrocks corresponds to the first stage of dehydration associated with expulsion of interlayer water (Perry and Hower, 1970).

Diagenesis of mudrocks from a present deep-sea environment was addressed by Dilli and Rao (1982). A 770 meter-thick section, cored off the Bengal Fan from 3759 meters water depth, was examined for mineralogical and geochemical changes with burial. Despite estimates that maximum burial temperatures never exceeded 50°C, Dilli and Rao (1982) claimed that <2.0 μm size clay underwent an unspecified degree of illitization suggested by: (i) depletion of smectite and enrichment in illite with burial and (ii) an increase in K_2O content downsection. However, Dilli and Rao (1982) did not adequately demonstrate how their observations were uniquely explained by burial diagenesis, rather than depositional influences.

D. EVALUATION OF NOVA SCOTIA MODEL

Upper Cretaceous and Tertiary sequences lying along the Nova Scotia shelf and slope are characterized by a low degree of compaction and chemical diagenesis. This is apparent, despite maximum burial depths ranging from 1800 to 2800 meters and burial temperatures from

42° to 100°C. The character of compaction and chemical diagenesis is markedly different from diagenetic studies of fine-grained clastic sequences on land. Possibly, the environment in which fine-grained sediments off Nova Scotia have resided has influenced their diagenesis (Burst, 1957).

In fine-grained Nova Scotia sequences, chemical diagenesis has proceeded in pore-fluids characterized by moderate pH and high total dissolved solids. However, despite the presence of K^+-bearing phases and appreciable 17 Å clay, pore-fluid composition did not establish a strong environment for detrital mineral instability. As a result, most mineral reactions did not proceed rapidly. Further, a low level of compaction inhibited widespread fluid influx so that pore-fluid composition did not change appreciably from its marine precursor.

Most studies of diagenesis in fine-grained rocks have considered chemical and mineralogical changes in mudrocks of marine or brackish origin which are presently on land. In general, these studies suggested that diagenesis has been so active as to have altered a large portion of each rock sample upon deep burial. However, although Glenelg and Shubenacadie may have undergone illitization associated with: (i) increased compaction and (ii) local K-feldspar and 10 Å clay degradation, observations do not permit a ***detailed description*** of an illitization mechanism. A model of illitization through tetrahedral substitution is favoured (Hower et al., 1976); it is not possible to determine conclusively whether cations were supplied by pore-fluid influx from outside sequences examined (Weaver and Beck, 1971). The degree of diagenesis observed is so minimal that XRD, isotopic and elemental analyses could not detect whole rock trends attributable to diagenesis, regardless of external pore-fluid influx.

The Nova Scotia model suggests that the diagenesis of fine-grained rocks is ongoing, but is only at a very early stage. This is a response to weak compaction (i.e., poor fluid circulation, low burial temperatures); the composition of pore-fluids has not changed significantly. According to Hurst and Irwin (1982), diagenesis is apparently controlled by pore-fluid character. However, unlike Morton (1985) who required termination of illitization after marine influx, diagenesis may be ongoing in fine-grained rocks of wholly marine character, but at a reduced level.

Examining literature from other basins, most on-land sequences are characterized presently by a more mature state of diagenesis. In general, lower levels of smectite expandability and greater alteration of detrital grains are recognised (Perry and Hower, 1970;

Heling, 1974; Hower et al., 1976). Advanced diagenetic maturity may be related to: (i) initial pore-fluid chemistry (i.e., brackish) or (ii) subsequent circulation of more corrosive pore-fluids in response to exposure (i.e., meteoric fluid).

In contrast to on-land studies, a preliminary examination of illitization described by Dypvik (1983) proposed a level of smectite interstratification similar to the Nova Scotia model. Although this North Sea model indicated a slightly greater degree maturity for most temperatures, the similarity of geological conditions for both North Sea and Nova Scotia sequences apparently has resulted in a similar style of diagenesis.

In conclusion, the diagenetic style described for offshore-Nova Scotia may be typical of fine-grained sediments which have always resided in a marine environment. Relative to on-land sections of greater stratigraphic thickness (burial temperature), compaction and chemical diagenesis are significantly different. Classic models for the diagenesis of fine-grained sediments do not satisfactorally describe post-depositional changes in fine-grained Upper Cretaceous and Tertiary rocks from offshore-Nova Scotia.

E. BIBLIOGRAPHY

Bruce, C.H., 1984, Smectite dehydration - its relation to structural development and hydrocarbon accumulation in northern Gulf of Mexico Basin: Am. Assoc. Petroleum Geologists Bull., v. 68, p. 673-683.

Boles, J.R. and Franks, S.G., 1979, Clay diagenesis in Wilcox Sandstones of southwest Texas: implications of smectite diagenesis on sandstone cementation: Jour. Sedimentary Petrology, v. 49, p. 55-70.

Burst, J.F., Jr., 1959, Postdiagenetic clay mineral environmental relationships in the Gulf Coast Eocene: *in* The 6th National Conference on Clays and Clay Minerals, p. 327-341.

Burst, J.F., 1969, Diagenesis of Gulf Coast clayey sediments and its possible relation to petroleum migration: Am. Assoc. Petroleum Geologists Bull., v. 53, p. 73-93.

Coleman, M.L. and Raiswell, R., 1981, Carbon, sulphur and oxygen isotope variations in concretions from the Upper Lias of N.E. England: Geochimica et Cosmochimica Acta, v. 45, p. 329-340.

Dilli, K. and Rao, C.N., 1982, A note on the burial diagenesis of clay minerals in the Bengal Fan: Jour. Geol. Soc. India, v. 23, p. 561-566.

Dypvik, H., 1983, Clay mineral transformations in Tertiary and Mesozoic sediments from North Sea: Am. Assoc. Petroleum Geologists Bull., v. 67, p. 160-165.

Eslinger, E.V., Savin, S.M. and Yeh, H.W., 1979, Oxygen isotope geothermometry of diagenetically altered shales: Soc. of Economic Palentologists and Mineralogists Special Publication No. 26, p. 113-124.

Heling, D., 1974, Diagenetic alteration of smectite in argillaceous sediments of the Rhinegraben (SW Germany): Sedimentology, v. 21, p. 463-472.

Hower, J., Eslinger, E.V., Hower, M.E. and Perry, E.A., 1976, Mechanism of burial metamorphism of argillaceous sediment: 1. mineralogical and chemical evidence: Geol. Soc. America Bull., v. 87, p. 725-737.

Hurst, A. and Irwin, H., 1982, Geological modelling of clay diagenesis in sandstones: Clay Minerals, v. 17, p. 5-22.

Morton, J.P., 1985, Rb-Sr evidence for punctuated illite/smectite diagenesis in the Oligocene Frio Formation, Texas Gulf Coast: Geol. Soc. America Bull., v. 96, p. 114-122.

Perry, E. and Hower, J., 1970, Burial diagenesis in Gulf Coast pelitic sediments: Clays and Clay Minerals, v. 18, p. 165-177.

van Moort, J.C., 1971, A comparative study of the diagenetic alteration of clay minerals in Mesozoic shales from Papua, New Guinea, and in Tertiary shales from Louisiana, U.S.A.: Clays and Clay Minerals, v. 19, p. 1-20.

Weaver, C.E. and Beck, K.C., 1971, Clay water diagenesis during burial; how mud becomes gneiss: Geol. Soc. America Special Paper 134, 96 pp.

Yeh, H.W. and Savin, S.M., 1977, Mechanism of burial metamorphism of argillaceous sediments: 3. O-isotope evidence: Geol. Soc. America Bull., v. 88, p. 1321-1330.